Title of thesis	THERMODYNAMIC PROPERTIES MODELING OF AQUEOUS CARBONATE ELECTROLYTE SYSTEM FOR CO_2 SEPARATION FROM NATURAL GAS

I OMER EISA BABIKER ABDELGADIR, hereby allow my thesis to be placed at the information Resource Center (IRC) of Universiti Teknologi PETRONAS (UTP) with the following conditions:

1. The thesis becomes the property of UTP

2. The IRC of UTP may make copies of the thesis for academic purposes only.

3. This thesis is classified as

☐ Confidential

☑ Non-confidential

If the thesis is confidential, please state the reason:

_____
_____
_____

The contents of the thesis will remain confidential for _____ years.

Remarks on disclosure:

_____
_____
_____

Endorsed by

_____   _____
Signature of Author   Signature of supervisor

Permanent address: Name of supervisor
Faculty of Engineering   *Dr.Shuhaimi B Mahadzir*
and Technology, University of
Gezira Wad Medani , Sudan

Date: Date:

UNIVERSITI TEKNOLOGI PETRONAS

THERMODYNAMIC PROPERTIES MODELING OF AQUEOUS CARBONATE
ELECTROLYTE SYSTEM FOR CO_2 SEPARATION FROM NATURAL GAS

By

OMER EISA BABIKER ABDELGADIR

The undersigned certify that they have read, and recommend to the Postgraduate
Studies Programme for acceptance this thesis for the fulfillment of the requirements
for the degree stated.

Signature: _____

Main Supervisor: *Dr.Shuhaimi B Mahadzir*

Signature: _____

Head of Department: _____

Date: _____

THERMODYNAMIC PROPERTIES MODELING OF AQUEOUS CARBONATE

ELECTROLYTE SYSTEM FOR CO_2 SEPARATION FROM NATURAL GAS

By

OMER EISA BABIKER ABDELGADIR

A Thesis

Submitted to the Postgraduate Studies Programme
as a Requirement for the Degree of

MASTERS OF SCIENCE

CHEMICAL ENGINEERING DEPARTMENT

UNIVERSITI TEKNOLOGI PETRONAS

BANDAR SRI ISKANDAR

PERAK

JUNE 2010

Title of thesis	THERMODYNAMIC PROPERTIES MODELING OF AQUEOUS CARBONATE ELECTROLYTE SYSTEM FOR CO$_2$ SEPARATION FROM NATURAL GAS

I OMER EISA BABIKER ABDELGADIR, hereby declare that the thesis is based on my original work except for quotations and citations which have been duly acknowledged. I also declare that it has not been previously or concurrently submitted for any other degree at UTP or other institutions.

Witnessed by

Signature of Author

Signature of supervisor

Permanent address:
Faculty of Engineering
and Technology, University of
Gezira, Wad Medani , Sudan

Name of supervisor
Dr.Shuhaimi B Mahadzir

Date:

Date:

Abstract

Hot potassium carbonate (HPC) electrolyte solution is used in gas processing and fertilizer plant to chemically absorb CO_2 and H_2S gases. The HPC solvent usually contains K_2CO_3, $KHCO_3$, and H_2O, beside small quantities of the diethanolamine (DEA) activator and V_2O_5 corrosion inhibitor. The solution solubility is controlled by the concentrations of carbonate, bicarbonate and CO_2 in the mixture. The problem in this study is the saturation of the potassium carbonate and potassium bicarbonate into a solid crystal state at certain conditions during the process. Consequently, the phenomena lead to accumulation of solid particles inside the units, mainly the pipelines and heat exchangers. The crystallization problem typically leads to reduction of the heat transfer rate, stripper unit temperature, and the overall process efficiency. In order to remove the solid accumulations, the process has to be shut down which lead to further production loss. The electrolyte nonrandom two liquids (ELECNRTL) model is selected for HPC thermodynamic and physical properties calculation using ASPEN PLUS simulator. The ELECNRTL model was conducted on the basis of the relationship between the solutes ion species and solvent molecules. In this study, the effective thermodynamic factors are investigated to determine the critical condition of the electrolyte crystallization in HPC solution. Furthermore, it was desired to develop these characteristics within the industrial process conditions of pressure, temperature and concentration. The observation of solution solubility detects saturation points at temperatures higher than solution boiling point for 30 wt% K_2CO_3 standard solution. The stable temperature simulated in this study was at temperature range between 287.15 K and 362.15 K with the error of ± 4 K, respectively based on the given literature data of carbonate system. For carbonate/bicarbonate mixture system, increasing of the operation pressure from 1 bar to 2 bar increase the mixture solution boiling temperature with $\Delta T_{mean} = 18$ K. This gives a wider range of solvent

stability in liquid phase and was also affected on the solvent transport thermodynamics. Furthermore, for binary systems of carbonate, it was found that the possibilities of solution crystallization may happen at temperatures lower than 313.15 K, pressure 1 bar for concentrations higher than 3 mole K_2CO_3/Kg H_2O.

Abstrak

Sebatian electrolit kalium karbonat panas (*HPC*) digunakan dalam pemprosesan gas dan baja untuk menyerap gas CO_2 dan H_2S. Sebatian HPC umumnya terdiri daripada K_2CO_3, $KHCO_3$, dan H_2O, serta sedikit kuanti pengaktif diethanolamine (DEA) dan V_2O_5, penghalang karat. Kosentrasi sebatian dikawal oleh kepekatan karbonat, bikarbonat dan CO_2 dalam campuran tersebut. Masalah yang dikaji ialah tahap keterlarutan kalium karbonat dan kalium bikarbonat dalam penghasilan fenomena pepejal kristal pada situasi tertentu semasa proses dijalankan. Fenomena ini akan menjurus kepada penghasilkan pepejal kristal di dalam unit, khasnya *pipeline* dan *heat exchanger*. Oleh yang demikian, masalah ini akan menyebabkan kadar pemindahan haba, suhu dan seluruh efisien proses berkurangan, Bagi memindahkan pepejal kristal tersebut, proses terpaksa diberhentikan dan ini akan menjurus kepada kerugian produksi. Model *electrolyte nonrandom two liquids (ELECNRTL)* digunakan untuk mengira termodinamik dan sifat fizikal HPC dengan menggunakan *ASPEN PLUS simulator*. Model ELECNRTL digunakan berdasarkan hubungan ion zat larut dan molekul pelarut. Di dalam kajian ini, faktor keefektifan termodinamik dikaji untuk menentukan keadaan tahap kritikal elektrolit kristal dalam sebatian HPC. Ini adalah untuk menghasilkan karakter yang sesuai digunakan dalam proses industri yang melibatkan tekanan, suhu dan kosentrasi. Permerhatian ke atas keterlarutan sebatian mendapati tahap keterlarutan pada suhu yang tinggi berbanding tahap didih bagi 30 wt% sebatian standard K_2CO_3. Suhu stabil yang digunakan dalam kajian ialah di antara 287.15 K dan 362.15 K dengan *error* ± 4 K, berdasarkan sistem karbonat dalam data literasi yang diberikan. Untuk sistem campuran karbonat/ bikarbonat, penambahan operasi tekanan dari 1 bar kepada 2 bar menyebabkan kenaikan pada suhu tahap didih sebatian dengan $\Delta T_{men}= 18$ K. Ini memberikan ruang yang luas bagi stabiliti pelarut dalam fasa cecair dan memberi kesan kepada termodinamik pelarut.

Bagi sistem binari karbonat, kemungkinan untuk penghasilan sebatian kristal berlaku pada suhu yang rendah dari 313.15 K, tekanan 1 bar untuk kosentrasi tinggi dari 3 mol K_2CO_3/Kg H_2O.

Acknowledgement

For First and for most, I thank ALLAH for the strength that keeps me standing and for the hope that keeps me believing that this affiliation would be possible and more interesting.

I also wanted to thank my family who inspired, encouraged and fully supported me for every trial that come to my way, in giving me not only financial support, but also moral and spiritual support.

I would like to express my most sincere gratitude to my supervisor, Dr. Shuhaimi Mahadzir for his guidance and supervision of this research work.

Many thanks to my teacher and brother, Ir/ Mohammed Osman Hussein, for giving me his advice and experience in the simulation work. And many thanks to my friends, Eng. Mr/ Altahir Abd-Allah Altahir for his help in MATLAB coding, and Eng. Mr/ Biruh.

Finally, a very special tribute to the Universiti Teknologi PETRONAS for giving me the opportunity of study, and I wish to progress and development.

All other colleagues are thanked for providing an inspiring and relaxed working atmosphere.

Dedication

To my father's soul

x

Table of content

List of figures

xvi

List of tables

Nomenclature

ACES   Aqueous carbonate electrolyte system

API   Standard API gravity

CHARGE   Ionic charge

CHI   Stiel polar factor

DGAQFM   Aqueous free energy of formation at infinite dilution

DGAQHG   Standard Gibbs free energy of formation of aqueous species

DGFORM   Standard free energy of formation

DGFVK   Parameter for free energy formation

DGSFRM   Solids free energy of formation at 25ºC

DHAQFM   Aqueous heat of formation at infinite dilution

DHAQHG   The standard enthalpy of formation of aqueous species

DHFORM   Standard heat of formation

DHFVK   Parameter for enthalpy of formation, mass based version

DHSFRM   Solid enthalpy of formation

DHVLB   Heat of vaporization at TB

DLWC   Vector indicating Diffusion or non diffusion components for Wilke-Chang model

DVBLNC   Vector indicating Diffusion or non diffusion components for Chapman- Enskog-Wilke-Lee model

HCOM   Standard enthalpy of combustion at 298.2 K

IONRDL	Riedel ionic coefficient for correction to the liquid mixture thermal conductivity of a mixture due to the presence of electrolyte
IONTYP	Criss-Cobble ion type
MUP	Dipole moment
MW	Molecular weight
NG	Natural gas
OMEGA	Pitzer a centric factor
OMEGHG	Born coefficient
OMGPR	A centric factor for the Peng-Robinson equation of state
OMGRKS	A centric factor for the Redlich-Wong equation of state
PC	Critical pressure
PCPR	Critical pressure for Peng-Robinson equation of state
PCRKS	Critical pressure for the Redlich-Wong equation of state
RADIUS	Born radius of ionic species
RHOM	Density
RKTZRA	Rstaactekett liquid density parameter
S025C	Criss-Cobble absolute entropy at 25°C
S025E	Sum of element entropy at 25^0C
S25HG	Absolute entropy of aqueous species for the Helgeson electrolyte model
SG	Specific gravity
TB	Norma boiling point
TC	Critical temperature
TCPR	Critical temperature for Peng-Robinson equation of state

TCRKS	Critical temperature for the Redlich-Wong equation of state
TFP	Normal freezing point
TREFHS	Reference temperature
VB	Liquid molar volume at TB
VC	Critical volume
VCRKT	Critical volume for Rachett liquid molar volume model
VLSTD	Standard liquid volume at 60°F
ZC	Critical compressibility factor
GMELCC-1	Electrolyte-molecule and electrolyte-electrolyte pair parameters required by the electrolyte NRTL model
GMELCD-1	Electrolyte-molecule and electrolyte-electrolyte pair parameters required by the electrolyte NRTL model, parameter D
GMELCE-1	Electrolyte-molecule and electrolyte-electrolyte pair parameters required by the electrolyte NRTL model, parameter E
GMELCN-1	Electrolyte-molecule and electrolyte-electrolyte pair parameters required by the electrolyte NRTL model, parameter N

Chapter 1

Introduction

1.1   Background

1.1.1   Natural gas

Natural gas is directly obtained from gas fields or it is found as a co-product of crude oil refining processes. The composition of natural gas contains mixture of organic compounds mainly methane, ethane, propane, butane and pentane. Beside organics, natural gas normally contains minor amount of inorganic compounds such as carbon dioxide (CO_2), sulfur dioxide (SO_2), oxygen (O_2), nitrogen (N_2) and small amount of inert gases (He, Xe, and Ne). Table 1.1 shows a typical composition of natural gas composition (Ikoku, 1992).

Table 1-1 Natural gas composition (Ikoku, 1992)

Component	Chemical formula	Volume %
Methane	CH_4	>85
Ethane	C_2H_6	3-8
Propane	C_3H_8	1-2
Butane	C_4H_{10}	<1
Pentane	C_5H_{12}	<1
Carbon dioxide	CO_2	1-2
Hydrogen sulfide	H_2S	<1
Nitrogen	N_2	1-5
Helium	He	<0.5

1.1.2 Natural gas purification

The process of natural gas purification involves the removal of vapor phase impurities and liquids from gas streams. Natural gas that contains significant amount of acid gases such as CO_2 and H_2S is called sour gas. The processes used for sour gas purification are classified into five types, namely absorption, adsorption, permeation, chemical conversion, and condensation.

The absorption technology mainly comprises physical and chemical absorption. A physical absorption is defined as the process that employs non-reactive organic as the treating agents (Kohl, 1997). On the other hand, chemical absorption can be defined as mass transfer from gas phase into liquid phase based on chemical reaction when the liquid phase components react with the absorbents (Aresta, 2003).

1.1.3 Benfield's process

One of the most important and useful technology for acid gas removal is the hot potassium carbonate process. The process was developed back in the 1970s by Benson and Field in Pennsylvania. It is commercially well known as the Benfield's process. Benfield's process is classified into the chemical absorption processes using hot potassium carbonate as reactive chemical solvent. The flow sheet shown in Figure (1.1) illustrates an absorber where the solvent contacts with the sour gas in a counter current flow, hence removing the acid gases from the natural gas. The rich solvent is regenerated in the stripping unit at high temperature for liberating the acid gases, mainly CO_2 and H_2S. The treated or sweet gas normally contains less than 1 ppmv H_2S and 50 ppmv CO_2 (Kohl, 1997).

The composition of hot potassium carbonate is typically made-up of 20-40 wt% potassium carbonates (K_2CO_3), 1-3 wt% diethanolamine (DEA), 0.4-0.7 wt% V_2O_5 and the balance is water. DEA acts as an activator while V_2O_5 is a corrosion inhibitor.

2

The standard operating condition for CO_2 absorption and stripping requires the pressure to be in the range between 1 and 2 atm and the temperature ranges between 70 and 130 ^{0}C. The absorption process normally occurred at low temperatures in the range between 25^0C and 75^0C and the CO_2 liberation process occurred at high temperatures between 80^0C and 130^0C (Kohl, 1997). Table (1-2) represents a typical operation condition for Benfield's system including the chemical component composition during the process. The data present different cases of Benfield's system for hot potassium solution concentration between 21 and 31.6 wt%.
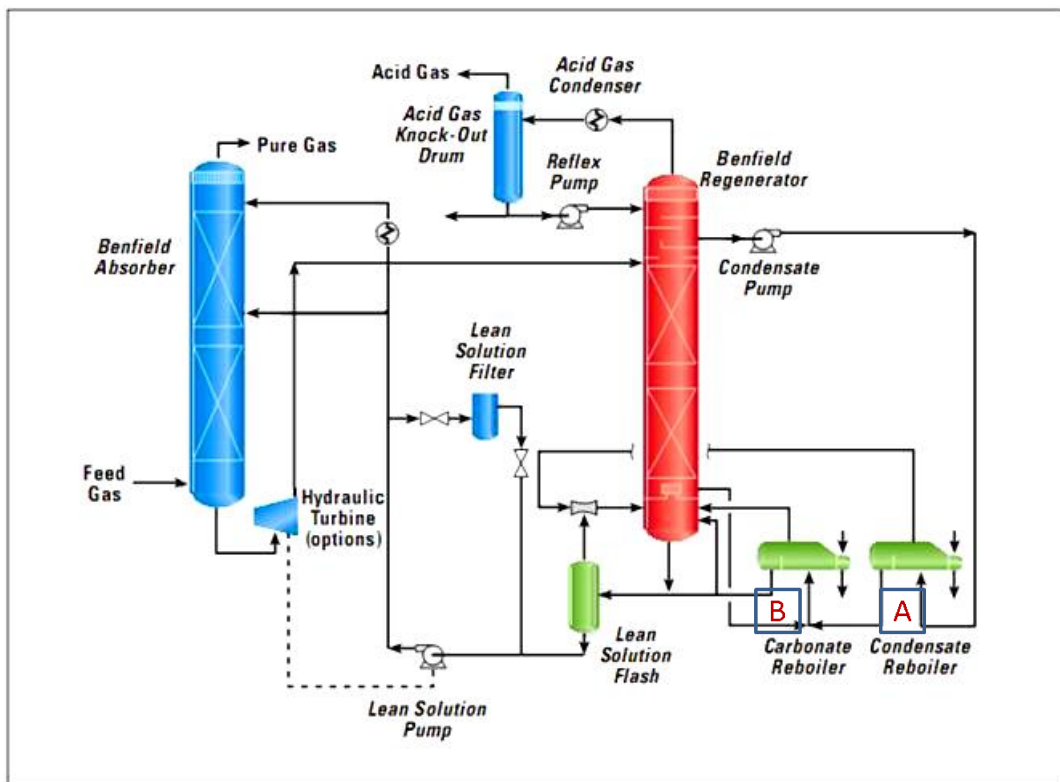
Figure 1-1 Benfield's Process flow diagram (UOP)

Table 1-2 Operation data of Benfield's system

Location	Case[1]	Case[2]	Case[3]	Case[4]
Absorber top temperature (^{0}C)	72.2	71.7	73.2	75.1
Absorber bottom temperature (^{0}C)	128.6	129.4	130.0	127.9
Absorber pressure drop (atm)	0.17	0.17	0.17	0.16
Stripper top temperature (^{0}C)	108.6	109.4	109.1	107.3
Stripper bottom temperature (^{0}C)	129.6	130	134	140
Stripper bottom pressure (atm)	1.3	1.3	1.5	2
Stripper pressure drop (atm)	0.2	0.3	0.38	Over scale

The designed operation pressure for absorber and stripper is 1 atm

Benlfield's solvent composition (wt %)				
H_2O	67.86	69.21	66.56	71.06
K_2CO_3	30.2	29.9	31.6	27
KVO_3	0.9	0.88	0.94	0.9
DEA	1.04	0.01	0.9	1.04

Data collected from (Benfield system Users' Forum (Penang, January 2001)

1.2   Chemical solvent classification

The chemical solvents that are used for CO_2 capture processes can be classified in two types. These are the amine system and hot potassium carbonate system.

1.2.1   Amine system

This system includes four organic chemical solvents based on amine compound. These solvents are; Monoethanolamine (MEA), Diethanolamine (DEA), Diglycolamine (DGA) and Methylediethanolamine (MDEA). Table (1-3) shows some

4

common parameters for amine system. The amine system was designed into two types of units, the single process unit and the multiple process units. The multiple process units are used within industrial plants such as oil refineries as shown in Figure (1.2). In the amine process, the absorber temperature is designed to be at the range of 35 to 50 ^{0}C and the pressure range of 5 to 205 atm. The concept of CO_2 absorption by such amines is obtained by controlling the molecular structure. Furthermore, the amine solution can be synthesized to form either stable carbonate ion, unstable carbonate ion, or no carbonate ion. The amine system has such an operation difficulties including foaming, failure to meet the sweet gas specification standard, high solvent losses due to volatility, entrainment and degradation, corrosion, fouling of equipment and contamination of amine solution (Kohl, 1997).

Table 1-3 Representative parameters for amine systems (Kidnay, 2006)

Component	MEA	DEA	DGA	MDE
(wt%) amine	15- 25	25- 35	50 -70	40- 50
Rich amine acid gas loading (mole acid gas/mole amine)	0.45- 0.52	0.43-0.73	0.35-0.40	0.4-0.55
Acid gas pick up (Mole acid gas/mole amine)	0.33- 0.40	0.35- 0.65	0.25- 0.3	0.2- 0.55
Lean solution residual acid gas (Mole acid gas/mole amine)	±0.12	±0.08	±0.1	0.005-0.01
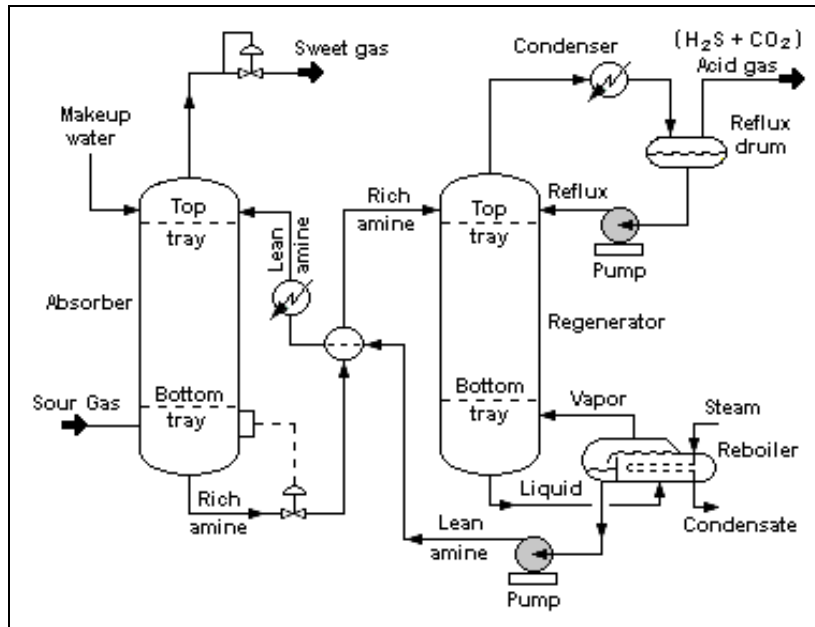
Figure 1-2 Amine system process flow diagram (Kidnay, 2006)

1.2.2 Hot potassium carbonate system

Hot potassium carbonate system is used to remove CO_2 and H_2S from gas streams. This process requires relatively high partial pressures of CO_2. The chemical reactions are very complex but the basic reaction chemistry of aqueous carbonate and CO_2 is specifically represented by the following reversible reactions (Robert, 1982):

$$K_2CO_3 + H_2O + CO_2 \leftrightarrow 2KHCO_3 \tag{1.1}$$

$$K_2CO_3 + H_2S \leftrightarrow KHS + KHCO_3 \tag{1.2}$$

The first reaction shows the reaction between potassium carbonate in aqueous solution with carbon dioxide to form potassium bicarbonate. The second reaction shows the reaction between potassium carbonate and hydrogen sulfide to form potassium hydrosulfide and potassium bicarbonate. Both reactions are reversible reactions.

6

The chemical reactions between the gas phase and the liquid phase generally enhance the rate of absorption and increase the capacity of the liquid solution to dissolve the solute. Therefore, the efficiency of acid gases capture in the chemical absorption is greater than the physical absorption (Perry,1999).

The equilibrium vapor pressure of CO_2 for the solution containing 20 wt% and 30 wt% potassium carbonate is a function of the reversible reaction mechanism when the carbonate converts to bicarbonate during the absorption process. Table 1.4 shows the experimental reaction rate constant (K) values based on equation (1.3):

$$K = \frac{[KHCO_3]^2}{[K_2CO_3]P_{CO_2}}$$
(1.3)

In the above equation [KHCO$_3$] and [K$_2$CO$_3$] are concentrations in mole/L while P_{CO_2} is the partial pressure in mmHg (Kohl, 1997)

Table 1-4 Average values of equilibrium constant for 20 wt% and 30 wt% K$_2$CO$_3$

Temperature ^{0}C	K, 20 wt% solution	K, 30 wt% solution
70	0.042	0.058
90	0.022	0.030
110	0.013	0.017
130	0.0086	0.011

The reaction kinetics can be interpreted based on the forward and reverse reactions, which are occurring in the absorber and the stripper, respectively. The basis of kinetics is built on the main reaction (1.1) and the equilibrium reactions between CO_2 and H_2O. The mechanism is explained by Rahimpor (2004) and Yi (2009) as follows:

$$r_{OH} = K_{OH}[OH^-][CO_2] - K_{OH^-}[HCO_3^-]$$
(1.4)

At equilibrium conditions;

$$r_{OH^-} = K_{OH^-}[HCO_3^-] = K_{OH^-}[OH^-][CO_2]_e \qquad (1.5)$$

Substituting (1.4) into (1.3)

$$r_{OH^-} = (K_{OH^-}[OH^-])([CO_2] - [CO_2]_e) \qquad (1.6)$$

The concentration of OH^- in the carbonate/bicarbonate buffer solution is not significantly near the surface. Therefore, equation (1.6) can be written as:

$$r_{OH^-} = (K_1([CO_2] - [CO_2]_e) \qquad (1.7)$$

In equation (1.7), K_1 denotes apparent first order rate constant.

When a small amount of amine is added to the system, the rate of CO_2 absorption will be enhanced according to the following reactions:

$$CO_2 + RR'NH \leftrightarrow RR'NCOOH \qquad (1.8)$$

$$CO_2 + RR'NH \leftrightarrow HCO_3^- + RR'NCOOH \qquad (1.9)$$

The amine acts as a promoter used to increase the reaction rate at high temperatures. By using the same approach of reaction (1.7), the amine reaction rate r_{Am} can be determined by the following relations:

$$\begin{aligned} r_{Am} &= (k_{Am}[Am])([CO_2] - [CO_2]_e \\ &= k_2([CO_2] - [CO_2]_e) \end{aligned} \qquad (1.10)$$

where k_2 is the apparent first-order rate constant.

$$\begin{aligned} r &= (k_{OH}[OH^-] + k_{Am}[Am])([CO_2] - [CO_2]_e) \\ &= k([CO_2] - [CO_2]_e) \end{aligned} \qquad (1.11)$$

In equation (1.11), k is overall apparent first order rate constant which can be explained as:

$$k = (k_{OH}[OH^-] + k_{Am}[Am]) \qquad (1.12)$$

1.3 Electrolyte thermodynamics

Electrolyte thermodynamics are properties which can be affected directly or indirectly by thermodynamic influences such as pressure and temperature. For an aqueous electrolyte system, the thermodynamics are dependent on the chemical potential factor. This refers to the change of internal energy with the number of parameters such as chemical potential, fugacity, ionic activity, activity coefficient, osmotic coefficient and Gibbs free energy.

1.3.1 Chemical potential

Chemical potential (μ_i) of a thermodynamic system is the amount by which the energy of the system would change if an addition particle was introduced with entropy and volume held constant. Mathematically, chemical potential of species i can be defined as (Job, 2006):

$$\mu_i = \left(\frac{\partial U}{\partial N_i} \right)_{(S,V,Nj \neq i)} \tag{1.13}$$

where:

U = the internal energy

N = number of species

S = entropy

V = volume

1.3.2 Fugacity

Fugacity (f) is a measure of chemical potential in form of adjusted pressure. It reflects the tendency of substance to prefer one phase (liquid, solid or gas). The definition of fugacity based on the Boltzmann constant (k_B), temperature (T) and chemical potential (μ) can be represented by the following equation (Maurer, 2004):

$$f = \exp\left(\mu \Big/ k_B T \right) \tag{1.14}$$

1.3.3 Activity

Activity (a) in chemical thermodynamics is a dimensionless quantity. Activity is a measure of the effective concentration of species in a mixture. Activity quantity depends on the system effective parameters such as temperature, pressure, concentration and composition of the mixture. The activity based on the chemical potential of species i is defined by:

$$a_i = \exp\left(\frac{\mu_i - \mu_i^{\Theta}}{RT}\right)$$

(1.15)

where

μ_i^{Θ} = the chemical potential at the standard state

R = gas constant

1.3.4 Activity coefficient

Activity coefficient (γ) is a factor used in thermodynamics to account for deviation from ideal behavior in a mixture of chemical substances. Activity coefficient relates to the activity to measure the amount fraction (x_i), molality (m_i) or concentration (c_i) as follows (Mills, 2007):

$$a_i = \gamma_{x,i.} x_i$$

(1.16)

$$a_i = \gamma_{m,i.} \cdot \frac{m_i}{m_{\Theta}}$$

(1.17)

$$a_i = \gamma_{c,i.} \cdot \frac{c_i}{c_{\Theta}}$$

(1.18)

In equations (1.7) and (1.8), Θ refers to the standard amount.

Equation (1.19) shows a general dissociation reaction for an ionic solution. Considering a given solute AB undergoing ionic dissociation in solution, the system

10

becomes directly non-ideal and the activity is defined for anions (A^+) and cations (B^-) as shown in the equation below.

$$AB \Leftrightarrow A^+ + B^- \tag{1.19}$$

The ions activity and molality are defined as equations (1.20) and (1.21), respectively.

$$a_\pm^{\ v} = a_+^{\ v+} . a_-^{\ v-} \tag{1.20}$$

$$m_\pm^{\ v} = m_+^{\ v+} . m_-^{\ v-} \tag{1.21}$$

a is the activity of ionic component.

m is the molality concentration of the ionic component.

Furthermore, the mean ionic activity coefficient of solute can be defined as (Barthel, 1998):

$$\gamma_\pm^{\ v} = \gamma_+^{\ v+} . \gamma_-^{\ v-} \tag{1.22}$$

where:

v is the summation of the ionic charges.

v^+ is the number of cations ionic charges.

v^- is the number of anions ionic charges.

1.3.5 Osmotic coefficient

Osmotic coefficient (φ) is also known as rational osmotic coefficient. The coefficient φ is the quantity that characterizes the deviation of solvent A from its ideal behavior with reference to Raoult's law. It can be defined based on molality or an amount of fraction as shown in equation (1.23) and (1.24) respectively.

$$\varphi = \frac{\mu_A^* - \mu_A}{RTM_A \sum_i m_i} \tag{1.23}$$

$$\varphi = \frac{\mu_A{}^* - \mu_A}{RTM_A \ln x_A} \qquad (1.24)$$

In the equation above,

$\mu_A{}^*$ is chemical potential of pure solvent.

μ_A is chemical potential of solvent.

M_A is molar mass of solvent.

1.3.6 Gibbs free energy

The Gibbs free energy (G) is defined as the maximum amount of non-expansion work that can be extracted from a closed system. For chemical reactions, Gibbs free energy represents the driving force of reaction and it is equals to the difference between products' and reactants' free energy.

The Gibbs free energy for substances undertaking the chemical reactions or phase changes in aqueous electrolyte systems depends on temperature, pressure and the amount of each substance i, present as n_i. At constant temperature and pressure with small changes in the amount of substance dni, the Gibbs free energy can be written as (Margaret, 2007):

$$(dG)_{T,P,n_1,n_2,....} \alpha dn_i \qquad (1.25)$$

The Gibbs free energy change can be defined as bases of chemical potential μ_i :

$$dG = \mu_i \times dn_i \qquad (1.26)$$

Then the chemical potential:

$$\mu_i = \left(\frac{\partial G}{\partial n_i} \right)_{T,P,n2,n3,.....} \qquad (1.27)$$

The Gibbs free energy changes for each substance according to:

$$dG = \sum_i \mu_i dn_i \qquad (1.28)$$

12

If both of pressure and temperature are allowed to vary as well, then the change in Gibbs free energy may be written as:

$$dG = vdp - sdT + \sum_i \mu_i dn_i$$
(1.29)

where, v is the molar volume and s is the entropy.

A general chemical reaction at constant pressure and temperature can be written as:

$$aA + bB \leftrightarrow cC + dD$$
(1.30)

where a, b, c and d equals to the quantities of each species. The change in Gibbs free energy of this reaction is given as:

$$\Delta G = +\mu_C + \mu_D - \mu_A - \mu_B$$
(1.31)

1.4   Problem statement

Hot potassium carbonate is an important class of electrolyte solution in CO_2 absorption processes. The main advantages include higher capacity to capture CO_2 even in presence of other compounds like SO_2, more efficient separation because the absorption occurs at high temperature, lower toxicity and lower tendency to degrade. However, the main disadvantage of the hot potassium carbonate solvent system is the precipitation of the potassium carbonate and bicarbonate salts, which forms of fouling through accumulation of the salt crystals in the reboilers system due to the evaporation of water from the aqueous solution. The normality of the solution is strong electrolyte and the electrolytes react with the metallic materials such as steel and ferrite compounds. The reaction between the potassium carbonate solution and the metallic materials makes the packed corrosive.

The main problem that will be dealt in this study is the precipitation of the potassium carbonate into a solid state which is caused by the saturation of hot potassium carbonate solution under process operation condition. Consequently, the phenomena would lead to accumulation of solid particles inside the units, mainly the pipelines and reboilers labeled (A) and (B) in Figure (1.1) respectively. The formation

of these particles reduces the heat transfer rate, stripper temperature and the process efficiency. In order to remove the solid accumulations, the process has to be shut down causing unnecessary loss of production.

The studies of industrial processes problems contribute to the development of a scientific basis that can directly lead to understand the causes of problems beside the ability to solve or avoid the problems. The study of the crystallization problem of Benfield's solution aimed to predict the solvent properties including the chemical, physical and thermodynamic properties.

1.5 Objectives

The objectives of this research are as follows:

- ➢ To study the saturation behavior of potassium carbonate solution at different operating conditions and different concentrations.
- ➢ To determine the effective parameters on solution thermodynamic and its chemical and physical properties.
- ➢ To predict the saturation conditions of the potassium carbonate at the low and high operation temperature.
- ➢ To validate the simulation results with the experimental data.

1.6 Scope of study

This study focuses on the thermodynamic properties of the Benfield's system for acid gas removal. The Benfield's solvent contains potassium carbonate/bicarbonate in aqueous system with varying carbonate conversion ratio for different operating conditions. The study also focuses on the analysis of complex solution based on varying concentrations, temperatures and pressures to establish the thermodynamics as well as the chemical and physical properties of the solution.

The electrolyte data properties used in this work are generated using Aspen Plus process simulator based on the default model used for vapor liquid equilibrium of

14

electrolyte system and the electrolyte nonrandom two liquids (ENRTL) activity coefficient model (AspenTech, 1989).

The Benfield's process data is collected from a local fertilizer plant. The data includes the operation conditions, solution composition and solution analysis for different cases at the time of operations.

Chapter 2

Literature review

2.1 Benfield solution

Benfield's solution is designed based on the equilibrium of the absorption reaction and the conversion of potassium carbonate to potassium bicarbonate. The empirical studies of the process used many equivalent concentrations of potassium carbonate which are ranged from 20 to 60 wt% aqueous solution (Kidnay, 2006).

At 115.6 0C, the 60 wt% potassium carbonate solution can be converted to only about 30% bicarbonate without the formation of precipitate. A 50 wt% solution can achieve up to 50% conversion and a 40 wt% solution can theoretically reach a 100% conversion as it shown in appendix B, Figure B5. The literature study concluded that a 40 wt% equivalent concentration of potassium carbonate is the maximum concentration that can be used for the acid gas treating operation without the occurrence of precipitation, and a 30 wt% solution is considered a reasonable design value for most applications. The operation under this range should be accurate in the optimum operation conditions, but if cooling of the solution should occur at even a 30 wt% potassium carbonate solution, it may even result in higher precipitation. On the basis of commercial plant experience with natural gas treating, the 30 wt% potassium carbonate equivalent has been recommended as a maximum solution concentration for Benfield process (Kohl, 1997).

2.2 Activated CO_2 absorption

Due to the importance of hot potassium carbonate system in the purification of natural

gas, many studies have been conducted to develop solvent activators that would increase the efficiency of acid gases absorption. The piperazine promoter was developed by Hilliard (2005; 2008) in Texas University and the study included thermodynamic properties estimation for the potassium carbonate solution. The study employed the method of regression of experimental data using Aspen Plus data analysis tools for electrolyte system (AspenTech, 1989). The research also focused on studying the interactions between molecules-molecules, molecules-electrolytes, for example between water and ion species, and the interactions between electrolytes or two different salts. The electrolyte NRTL model was used to estimate and predict the thermodynamic quantities, CO_2 pressure, and the other thermal quantities such as heat capacity, enthalpy and Gibbs energy. The experimental data used in this study was collected from the pilot plant study in Austin Texas, for binary electrolyte systems of potassium carbonate, potassium bicarbonate, CO_2, and water properties in aqueous systems (Zaytsev and Aseyev, 1992). In addition, the comparison has been adopted in the real data of Benfield's process that were collected from Field (1960) and Kohl (1997).

Cullinane (2004) compared the advantages and disadvantages of amine and potassium carbonate systems. The study indicated that carbonate system has low heat of regeneration. However, its rate of reaction was slower compared to amines system. This research also included the study of thermodynamics and kinetics data of potassium carbonate promoted by piperazine. Cullinane (2004) investigated the promoted solvent at 20-30 wt% K_2CO_3 system in wetted-wall column by using concentrations of 0.6 molality basis piperazine at range between 40 and 80 0C. The rate of CO_2 absorption in promoted solvent compared favorably to that of 5.0 molality bases MEA and the heat of absorption increased from 3.7 to 10 kcal/mole. The capacity ranged from 0.4 to 0.8) mole CO_2/kg H_2O.

2.3 Electrolyte thermodynamics

Thomsen (1997) studied the thermodynamics of electrolyte system at low and high concentrations. The main goal of the study was to estimate the phase diagrams of

17

binary, ternary and quaternary systems for several salts in electrolyte system. The extended UNIQUAC model has been used for excess Gibbs energy for such aqueous solutions. The experimental parameters was estimated for the ten ions of Na^+, K^+, H^+, Cl^-, NO_3^-, SO_4^{2-}, OH^-, CO_3^{2-}, HCO_3^-, and $S_2O_8^{2-}$. The study also focused on the design, simulation, and optimization of the fractional crystallization processes using a steady state computer program simulator. In addition, the study also estimated the electrolyte solutions thermodynamics such as the excess enthalpy, heat capacity, activity coefficient and osmotic coefficient beside the salt saturation for the presented phases. The phase diagrams have been predicted by the extended UNIQUAC model and it was compared with experimental data from IVC-SEP electrolyte databank. The results of the study gave a satisfactory agreement with the collected experimental data. Moreover, the significant improvements in the design of crystallization process proved that the fractional crystallization process is theoretically possible.

Other thermodynamic study presented by Liang-Sun et.al (2008) to predict the enthalpies of vaporization, freezing point depression and boiling point evaluations for aqueous electrolyte solution. The presented thermodynamic properties was predicted with the two-ionic parameters model involving the activity coefficients of two electrolyte-specific approaching and solution parameters of individual ions of electrolyte in aqueous solution. The results of this work showed a 60% relative deviation for enthalpy of vaporization and 70% for freezing point and boiling point evaporations. The relative deviation values accepted for some solutions of high concentration and also for that non-completely dissociated week electrolytes.

Abovsky (1998) modified the electrolyte NRTL model based on concentration dependence parameters to enhance the model capability in representing the non-ideality of concentrated electrolyte solutions. The concentration was assumed to be dependence on the activity coefficient expression for anions, cation, and molecular species which are derived from excess Gibbs free energy expression. The calculated values and the experimental data were reported in excellent agreement. The results showed that the derivations within experimental uncertainty were significantly smaller than those using the original model.

18

Haghtalab (1988) studied the molal mean activity coefficient of several electrolytes consisting of long-range forces that were represented by the Debye-Huckel theory and short-range forces represented by local compositions through nonrandom factors. The model is valid for whole range of electrolytes concentrations. The mean activity coefficient results were compared to the models which were obtained from two parameters and one parameter such as Meissner (1972), Bromley (1972), Pitzer (1975) and Chen et.al (1981). The model presented the experimental values from dilute region up to saturation concentrations.

Haghtalab and Kiana (2009) are obtained a new electrolyte-UNIQUAQ-NRF excess Gibbs function for activity coefficient calculation of short-range contribution. The new model limited for binary electrolyte systems at temperature of 25^0C. The model applied to calculate the activity coefficient for more than 130 binary electrolyte solutions based on the two adjustable parameters per electrolyte. Further, the model also used for the prediction of osmotic coefficients for the same electrolyte. The results of the new model compared with the excised models of electrolyte-NRTL-NRF, N-Wilson-NRF and electrolyte-NRTL. The comparison demonstrated that the new model can correlate the activity coefficient from experimental data beside the prediction of osmotic coefficient.

Speideh et.al (2007) are approached the Ion Pair Ghotbi-Verg Mean Spherical Approximation (IP-MGV-MSA) model for the ionic activity coefficient correlation. The model calculations based on MGV-MSA model which is correlate the mean ionic activity coefficient (MIAC) to a number of symmetric and non-symmetric aqueous electrolyte solutions at 25^0C. The results of the new model of IP-MGV-MSA compared with those obtained from GV-MSA and MGV-MSA models. The comparison showed that the model can give more superior results than those obtained from MGV-MSA and GV-MSA models.

Moggia (2007) estimated the electrolyte mean activity coefficient using the Pitzer specific ion interaction model. The study observed the disadvantage of Pitzer model of the dependence on semi-empirical parameters. These parameters are not directly

acceptable from experimental measurement but can only be estimated using numerical techniques.

2.4 Solubility and saturation index

Kohl (1997) presented the results of an experimental estimation for the transport thermodynamic properties, mainly the specific gravity and viscosity for 20, 30 and 40 wt% potassium carbonate solutions. For 30 wt% equivalent K_2CO_3 standard solution, the solution freezing temperature was observed at 50^0F (10^0C) and the boiling temperature was at 200^0F (93.3^0C). These points represented the critical temperatures of crystallization and evaporation of Benfield's solution as minimum and maximum limits of operation.

More recently, the solid-liquid equilibrium of K_2CO_3-K_2CrO_4-H_2O has been studied by Du et al. (2006). The research was focused to study the solubility of the system at temperatures of 40, 60, 80 and 100 0C in order to determine the crystallization area in solid-liquid phase diagram. The experiment took ratios of components at fixed temperature and pressure. The results showed that the system does not form solid solution, and the salting-out (adding more of K_2CO_3 to precipitate K_2CrO_4) effect of K_2CO_3 on K_2CrO_4 was very strong which led to the decreased solubility of K_2CrO_4 in the solution. Furthermore, it was found that the evaporating crystallization was preferential and highly efficient way to separate most of K_2CrO_4 from the system.

Larson (1942) determined the saturation index and alkalinity of $CaCO_3$ based on the ionic strength, second ionization constant for HCO_3^- dissociation, ionization constant of water dissociation, solubility product, and solution pH. The experimental work showed that the activity concepts gave more nearly correct results for water having values greater than 500 ppm. The results also discussed the correlations in form of alkalinity and saturation index. In addition, the correction values of the calculated solubility product of $CaCO_3$ were presented at temperature range between

20

0 ^{0}C and 80 ^{0}C. Furthermore, the method was used to calculate the solution pH and indicated the relation between active CO_2 and the saturation index.

2.5 Vapor liquid equilibrium

Chen (1980) simulated the electrolyte system vapor-liquid equilibrium of industrial electrolytes. The study used several methods to calculate the electrolytes thermodynamic properties. Pitzer equation was selected to calculate the excess Gibbs free energy. The results of excess Gibbs free energy found good agreement with the industrial data of vapor-liquid equilibrium under limiting conditions.

Instead of the non applicability of Pitzer equation for mixed solvent, the local composition model was developed. The assumption of the developed model was that the excess Gibbs free energy is equal to the summation of long-range and short-range contribution forces. The concepts of local contribution model are similar to the electrolyte NRTL model.

The results of the simulation data with the experimental data of hot carbonate system for water activity coefficient, water pressure, CO_2 pressure, heat capacity and heat enthalpy at different temperatures and concentrations was compared. The results also included the Pitzer parameters of electrolytes and salt activity coefficients at different molar concentrations (Chen, 1980).

Chapter 3

Modeling electrolyte system

3.1 Introduction

Aqueous electrolyte system can be defined simply as the composition uniform basis. The system consists of water in the form of solvent and ions in the form of solutes. The electrolyte system often behaves in complex and counter intuitive ways. This behavior may introduce a great risk into the plant design and operations if not properly understood and accounted for. The electrolyte system chemistry is also particularly complex and challenging to understand and predict. This statement is especially true for real industrial systems containing many compounds and operating under broad range of pressures, temperatures and concentrations. Some examples of these operations include aqueous chemical and separation process, solution crystallization, pharmaceuticals and specialty chemical manufacturing, reactive separation including the acid gas treatment, waste water process, corrosion and scaling of equipments (Abdel-Aal, 2003).

This chapter describes the development of models which are used to predict the thermodynamic properties of hot potassium carbonate system using Aspen Plus simulator (AspenTech, 1989). The study focuses on the analysis of carbonate/ bicarbonate solution at different operation conditions which are out of the common standard conditions to determine the critical operating conditions leading to the electrolyte crystallization.

3.2   Research methodology

The research methodology included two main sections; modeling and simulation. These sections involve the process of data collection, software selection, model descriptions and selection of solubility index model.

3.2.1   Data collection

The research focuses on an acid gas removal unit, specifically the Benfield's system. Benfield's system is actually using different types of operation conditions based on the process design and the natural gas composition. These differences lead to an expansion of the data collection sources. The data were eventually collected from two different plants, namely a fertilizer plant and a natural gas processing plant.

The collected data comprises the process flow diagram beside the operation conditions and Benfield's solvent composition. The process flow diagram consists of the absorption unit, the stripper unit, reboilers system and other utilities. The operation condition data considered in the study are temperatures, pressures, mass flows, chemical reactions and material conversion rate. The Benfield's solvent composition comprises the standard solvent composition, rich solvent composition and lean solvent composition.

The natural gas uses as a feed material to produce granular urea from ammonia and carbon dioxide in the fertilizer plant. The production involves series of chemical processes that ends with the synthesis of urea accordingly. The synthesis of urea also results in excess ammonia which can be sold. The co-product of methanol will provide feedstock for the production of formaldehyde required in granular urea production. The fertilizer plant operation capacity designed to be 2100 metric ton per day of granular urea.

The main unit which is involves in this study called Benfield's process. This unit used for natural gas purification or CO_2 production. The CO_2 absorption process designed to operate at low pressure process of 1 bar and temperature range between

(25 and 75) ^{0}C and the regeneration (CO$_2$ liberation) at temperature range between (80 and 120) ^{0}C. The K$_2$CO$_3$ concentration designed to be 30 wt% beside a (1-3) wt% of DEA activator and (0.4-0.7) wt% of V$_2$O$_5$ corrosion inhibitor as shown in Table 1-2 for four cases included the deviations of actual operation conditions from the designed conditions.

In the natural gas processing and liquefy natural gas (LNG) plants, Benfield's system use in gas purification section for CO$_2$ and SO$_2$ absorption. The natural gas process unit was presented in the current study as a high pressure operation process. The unit designed in tow typical stages with treating capacity of 18.705 Kgmol/hr, pressure from 2 bar up to 6 bar. The losses of Benfield's solution composition presented to be (14,000 Kg/year) K$_2$CO$_3$, (1,400 Kg/year) DEA, (400 Kg/year) V$_2$O$_5$ and the circulation of the lean solution contained (694 to 1017) m3/hr. the treated gas composition contained 2 ppmv CO$_2$ and 2.5 ppmv SO$_2$ as a maximum amounts.

3.2.2   Software selection

Aspen plus electrolyte system is found to be the most appropriate electrolyte system simulator. It is capable of computing many electrolytes properties such as physical, chemical and thermodynamic properties. The software offers a comprehensive collection of built-in binary parameters for activity coefficient models based on the WILSON, NRTL and UNIQUAC property methods. The data bank is available for vapor-liquid (VLE) and liquid-liquid (LLE) equilibrium and also contains a large collection of Henry's law constants (AspenTech, 1989).

In Aspen plus electrolyte system, the vapor-liquid equilibrium application consists of databanks of VLE_IG, VLE_RK, VLE_HOC, and VLE-LIT. These databanks developed by Aspen Technology using VLE data from the Dortmund databank. Additional data of pressures and temperatures are also built for limited components. Table (3.1) shows the built-in binary parameters for vapor liquid systems (Aspen Tech, 1989).

24

Table 3-1 The Built Binary parameters for liquid system

Databanks	Property methods	Vapor phase model	Number of component pairs
VLE-IG	WISON,NRTL, UNIQUAC	Ideal gas	3600
VLE-RK	WILS-RK, NRTL-RK, UNIQ-RK	Redlich-Kwong	3600
VLE-HOC	WILS-HOC, NRTL-HOC, UNIQ-HOC	Hayden-O'Connell	3600
VLE-LIT	WILSON, NRTL, UNIQUAC	Ideal gas	1200

The generation of solution chemistry in Aspen Plus is based on the components that make-up the solution's composition. The carbonate system selected components are H_2O, CO_2, K_2CO_3 and $KHCO_3$. The component CO_2 is defined as Henry component for vapor-liquid equilibrium between CO_2 and water. The aqueous phase reactions that are considered in this system are shown in the following equations:

$$K_2CO_3 \leftrightarrow 2K^+ + CO_3^{2-} \tag{3.1}$$

$$KHCO_3 \leftrightarrow K^+ + HCO_3^- \tag{3.2}$$

$$CO_2 + 2H_2O \leftrightarrow HO^- + HCO_3^- \tag{3.3}$$

$$HCO_3^- + H_2O \leftrightarrow H_3O^+ + CO_3^{2-} \tag{3.4}$$

$$2H_2O \leftrightarrow H_3O^+ + OH^- \tag{3.5}$$

$$K_2CO_{3(S)} \leftrightarrow 2K^+ + CO_3^{2-} \tag{3.6}$$

$$KHCO_{3(S)} \leftrightarrow K^+ + HCO_3^- \tag{3.7}$$

The reactions above comprise the dissociation, vapor liquid equilibrium reaction between water -CO_2 and the solid liquid equilibrium for carbonate and bicarbonate.

Reactions (3.1) and (3.2) describe the dissociation of potassium carbonate and bicarbonate in water to produce (K^+), (CO_3^{2-}) for potassium carbonate and (K^+), (HCO_3^-) for bicarbonate. Reaction (3.3) describes the hydrolysis and ionization of dissolved CO_2 to H_3O^+ and bicarbonate (HCO_3^-) ions. Reaction (3.4) describes the dissociation of (HCO_3^-) to (H_3O^+) and (CO_3^{2-}) ions. Reaction (3.5) describes the water dissociation to (H_3O^+) and (OH^-) ions. Reactions (3.6) and (3.7) describe the dissociation of solid carbonate and bicarbonate to (K^+), (CO_3^{2-}) for carbonate and (K^+), (HCO_3^-) for bicarbonate (Hilliard, 2005; Hilliard, 2008).

3.2.3   Simulation flow diagram description

The installation of Aspen Plus property analysis starts with the collection of the operation conditions and the chemical composition of carbonate/bicarbonate aqueous electrolyte solution. The input data includes the components' concentrations, temperatures, and pressures. The electrolyte chemistry has been generated using the format of the chemical reaction equations and electrolyte ionic species composition. The valid phase of the absorption process selected to be a vapor-liquid phase. The electrolyte NRTL model has been selected as a property method and Redlich-Kwong (RK) model selected for the vapor-liquid equilibrium (VLE) calculations. Furthermore, CO_2 was defined as Henry component to validate Henry's law. The input data needed for property analysis manipulated in order to calculate the selected thermodynamic properties. The input conditions of property analysis engine can be separated (optionally) from the main flow sheet. The success of the simulation run associated to the estimated degree of freedom (DOF) of the process parameters. The generated results can be only accepted if the DOF=0. The DOF values which are less or greater than zero are only point to a wrong or mistaken results. In addition, the input data can be modified after the simulation runs to fix the errors. Figure 3.1 summarizes the flow of the simulation process and the simulation steps shown in appendix (A) with Aspen Plus simulator interface.

The simulation outputs generation depends on the selected property data for the valid phase. Table 3-2 shows the selected property data for K_2CO_3-H_2O, $KHCO_3$-H_2O, and K_2CO_3-$KHCO_3$-H_2O-CO_2 systems.

Table 3-2 Property sets as data analysis outputs

| Property symbol	Property details
SOLINDEX	Salt Solubility index
THERMAL	Enthalpy, heat capacity and thermal conductivity
TXPORT	Density, viscosity and surface tension
VLE	Fugacity, activity and vapor pressure
pH	pH at current temperature
FTRUE	True component mole flow in liquid phase
XTRUE	True component mole fraction in liquid phase
FAPP	Apparent component mole flow in liquid phase
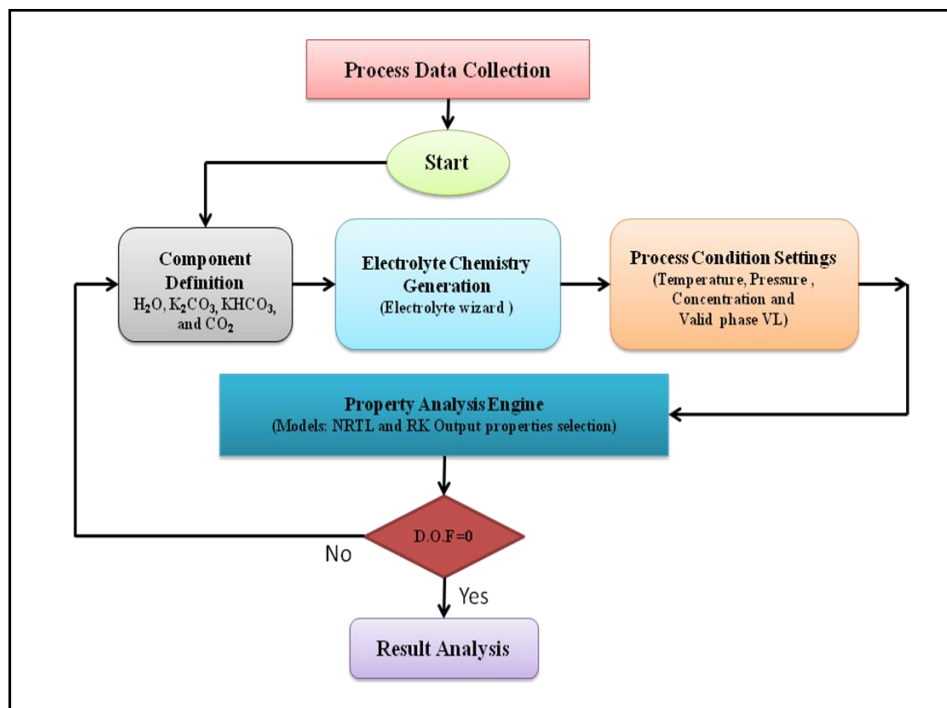
Figure 3-1 Simulation flow diagram

3.2.4 Model descriptions

Aspen Plus electrolyte database contains 300 electrolyte components defined with chemical and physical properties. It can be used for very low and high concentrations of electrolytes. For vapor liquid equilibrium, the ELECNRTL property method is fully supported with the Redlich-Kwong equation of state. This property method is defined as NRTL-RK (Park, 1997).

Aspen Plus property data includes many binary and pair parameters. It also accounts the chemical equilibrium constants which are generated from regression of experimental data.

3.2.4.1 Vapor phase model

The modified Soave-Redlich-Kwong equation of state is given by the following expression (Hilliard, 2005; Hilliard, 2008; and AspenTech, 1989):

$$P = \frac{RT}{Vm - b} - \frac{a}{Vm(Vm - b)} \tag{3.8}$$

In the equation above, the parameters are further defined as follows:

$$a = \sum_i \sum_j (a_i a_j)^{0.5} (1 - k_{ij}) \tag{3.9}$$

$$k_{ij} = k_{ji} \tag{3.10}$$

$$b_i = 0.08664 \frac{RTc,i}{Pc,i} \tag{3.11}$$

$$a_i = \alpha_i 0.42747 \frac{R^2 T^2 c,i}{Pc,i} \tag{3.12}$$

$$\alpha_i = \left[1 + m_i (1 - T_{ri}^{0.5})\right]^2 \tag{3.13}$$

$$m_i = 0.48 + 1.57\omega_i - 0.176\omega_i^2 \tag{3.14}$$

where:

$p =$ The equilibrium total pressure of the system in (Pa)

$R = 8.3144$ J/K.mole

$T =$ Temperature in K

$\alpha =$ Nonrandom less parameter (0.2)

$a_i =$ Activity of component i

$V_m =$ Molar volume

$\omega =$ A centric factor $= \log(P_r^{sat}) - 1$ at (T$_r$=0.7)

3.2.4.2 Activity coefficient model

The electrolyte nonrandom two liquid (NRTL) is a versatile model for activity coefficient using binary and pair parameters. The model can represent aqueous electrolyte system as well as mixed solvent. Furthermore, it can calculate the activity coefficient ($\gamma+, \gamma-$) and mean ionic activity coefficient ($\gamma\pm$) for ionic species and molecular species in aqueous electrolyte system. The calculation of mean ionic activity coefficient is given by the following expression (AspenTech, 1989):

$$\gamma\pm = (\gamma_+^x \gamma_-^y)^{\frac{1}{(x+y)}}$$

(3.15)

where x, y are the number of cations and anions, respectively.

The electrolyte NRTL activity coefficient model is based on two fundamental assumptions. The first assumption is the like-ion repulsion. This assumption states that the local composition of cations around anions is zero (and likewise for anions around cations). This is due to the repulsive force between the same charged ions is extremely large and is also very strong for the neighboring species. The second assumption is based on the local electroneutrality, which states that the contribution of cations and anions around a central molecular species is such that the net local ionic charge is zero. Local electroneutrality has been observed for interstitial molecules in salt crystals (AspenTech, 1989; and Hilliard, 2004).

Aspen plus electrolyte NRTL is also used to calculate enthalpies and Gibbs free energy of electrolyte system. The adjustable parameters of electrolyte include the pure

component dielectric constant coefficient of non-aqueous solvent, Born radius of ionic species and the NRTL parameters for molecule-molecule, molecule-electrolyte, and electrolyte- electrolyte pairs (Orbey, 1998).

3.2.4.3 Energy parameters

Electrolyte NRTL database contains the norandomness factors GMELCN along with the energy parameters of GMELCC, GMELCD and GMELCE for many molecule-electrolyte and electrolyte-electrolyte pairs. Temperature dependency of the dielectric constant of solvent is defined by (AspenTech, 1989):

$$\varepsilon_B(T) = A_B + B_B\left(\frac{1}{T} - \frac{1}{C_B}\right) \tag{3.16}$$

The temperature dependency relations of electrolyte NRTL parameters are:

    (a)   Molecule-molecule Binary parameters

$$\tau_{BB'} = A_{BB'} + \frac{B_{BB'}}{T} + F_{BB'}\ln(T) + G_{BB'}T \tag{3.17}$$

    (b)   Electrolyte-molecule Pair parameters

$$\tau_{ca,B} = C_{ca,B} + \frac{D_{ca,B}}{T} + E_{ca,B'}\left[\frac{\left(T^{ref}-T\right)}{T} + \ln\left(\frac{T}{T^{ref}}\right)\right] \tag{3.18}$$

$$\tau_{B,ca} = C_{B,ca} + \frac{D_{B,ca}}{T} + E_{B,ca}\left[\frac{\left(T^{ref}-T\right)}{T} + \ln\left(\frac{T}{T^{ref}}\right)\right] \tag{3.19}$$

    (c)   Electrolyte-electrolyte Pair parameters

$$\tau_{c'a,c''a} = C_{c'a,c''a} + \frac{D_{c'a,c''a}}{T} + E_{c'a,c''a}\left[\frac{\left(T^{ref}-T\right)}{T} + \ln\left(\frac{T}{T^{ref}}\right)\right] \tag{3.20}$$

$$\tau_{ca',ca''} = C_{ca',ca''} + \frac{D_{ca',ca''}}{T} + E_{ca',ca''}\left[\frac{\left(T^{ref}-T\right)}{T} + \ln\left(\frac{T}{T^{ref}}\right)\right] \tag{3.21}$$

In the above equations;

τ = the NRTL energy parameter

B = solvent

c = cation

a = anion

T^{ref} = 298.15 K

T = the actual temperature

3.2.4.4 Excess Gibbs free energy model

The excess Gibbs free energy expression which contains two contributions was proposed by Chen et.al (1982). The first contribution is for the long range ion-ion interaction and the second is related to the local interactions that exist around the species. The unsymmetrical Pitzer-Debije-Huchel (PDH) model and the Born equation are used to represent the contribution of the long range ion-ion interactions while the NRTL method is used to represent the local interaction (lc). The local interaction model was developed as a symmetric model with a reference state based on pure solvent and pure completely dissociated liquid electrolyte. In infinite dilution, activities are then normalized by the model to obtain an unsymmetrical model. The NRTL expression for the local interactions, the Pitzer-Debije-Huchel expression and the Born equation are added to give the following for excess Gibbs free energy equation;

$$\frac{G_m^{*E}}{RT} = \frac{G_m^{*E,PDH}}{RT} \frac{G_m^{*E,Born}}{RT} \frac{G_m^{*E,lc}}{RT} \tag{3.22}$$

$$\ln \gamma_i = \frac{G_m^{*E}}{RT} = \left[\delta(\frac{n G_m^{*E}/RT}{\delta n_i}) \right] \tag{3.23}$$

This leads to:

$$\ln \gamma_i^{*E} = \ln \gamma_i^{*E,PDH} + \ln \gamma_i^{*E,Born} + \ln \gamma_i^{*E,lc} \tag{3.24}$$

The Pitzer-Debije-Huchel equation is presented as follows:

$$\frac{G_m^{*E,PDH}}{RT} = \sum_k x_k \left(\frac{1000}{M_s} \right)^{0.5} \left(\frac{4A_\phi I_x}{\rho} \right) \ln\left(1 + \rho I_x^{0.5}\right) \tag{3.25}$$

31

$$I_x = 0.5 \sum_i x_i z_i^2 \tag{3.26}$$

$$A_\phi = \frac{1}{3} \left(\frac{2\pi N_0 d}{1000} \right) 0.5 \left(\frac{e^2}{D_w kT} \right)^{1.5} \tag{3.27}$$

where:

M_s = the molecular weight of the solvent

ρ = the (closest approached) parameter

I_x = the ionic strength on the mole fraction base

A_ϕ = Debjie Huckel Parameter

x_i = mole fraction of the component i

z_i = the ionic charge of component i

N_0 = Avogadro's number

d = is the solvent density

e = the charge of an electron

Dw = the dielectric constant of water

T = the temperature in Kelvin

k = the Boltzmann constant

The Born correlation for Gibbs energy calculation is based on the change in reference state given by the difference in the dielectric constant.

$$\frac{G_m^{*E,Born}}{RT} = \left(\frac{e2}{2kT} \right) \left(\frac{1}{D_m} \frac{1}{D_w} \right) \frac{\sum_i x_i z_i^2}{r_i} \tag{3.28}$$

In equation (3.28), r_i is the Born radius, D_m is the dielectric of mixed solvent and

D_w is the dielectric of water.

The equation for NRTL Gibbs energy model is given by:

$$G_m^* = x_w \mu_w^* + \sum_k x_k \mu_k^\infty + \sum_j x_j \ln x_j + G_m^{*E} \tag{3.29}$$

where:

G_m^* =Molar Gibbs energy

G_m^{*E} =Molar excess Gibbs free energy and * refers to a symmetrical reference state

μ_w^* =Thermodynamic potential

$$\mu_w^* = \mu_w^{*,ig} + \left(\mu_w^* - \mu_w^{*,ig} \right) \tag{3.30}$$

$$\mu_k^\infty = fcn + \left(\Delta_f G_k^{\infty,aq}, G_{pk}^{\infty,aq} \right) \tag{3.31}$$

The electrolyte NRTL model can be extended to handle multicomponent systems. The excess Gibbs free energy expression is:

$$\frac{G_m^{*E,lc}}{RT} = \sum_B X_B \frac{\sum_j X_j G_{jB} \tau_{jB}}{\sum_k X_k G_{kB}} +$$

$$\sum_c X_c \sum_{a'} \left(\frac{Xa}{\sum_{a''} X_{a''}} \right) \frac{\sum_j X_j G_{jc,a'c} \tau_{jc,a'c}}{\sum_k X_k G_{kc,a'c}} + \tag{3.32}$$

$$\sum_a X_a \sum_{c'} \left(\frac{Xc'}{\sum_{c''} X_{c''}} \right) \frac{\sum_j X_j G_{ja,c'a} \tau_{ja,c'a}}{\sum_k X_k G_{ka,c'a}}$$

j and k can be any species (a, c, or B).

The activity coefficient equation for molecular component is given by:

$$\ln \gamma_B^{lc} = \frac{\sum_j X_j G_{jB} \tau_{jB}}{\sum_k X_k G_{kB}} + \sum_{B'} \left(\frac{X_{B'} G_{BB'}}{\sum_k X_k G_{kB'}} \right) \left(\tau_{BB'} - \frac{\sum_k X_k G_{kB'} \tau_{kB'}}{\sum_k X_k G_{kB'}} \right) +$$

$$\sum_c \sum_{a'} \frac{X_a}{\sum_{a''} X_{a''}} \frac{X_c G_{Bc,a'c}}{\sum_k X_k G_{kc,a'c'}} \left(\tau_{Bc,a'c} - \frac{\sum_k X_k G_{kc,a'c} \tau_{kc,a'c}}{\sum_k X_k G_{kc,a'c}} \right) + \qquad (3.33)$$

$$\sum_c \sum_{a'} \frac{X_{c'}}{\sum_{c''} X_{c''}} \frac{X_a G_{Ba,c'a}}{\sum_k X_k G_{ka,c'a}} \left(\tau_{Bc,c'a} - \frac{\sum_k X_k G_{ka,c'a} \tau_{ka,c'a}}{\sum_k X_k G_{ka,c'a}} \right)$$

For cations, the activity coefficient equation is given by (AspenTech, 1989):

$$\frac{1}{z_c} \ln \gamma_c^{lc} = \sum_{a'} \frac{X_{a'}}{\sum_{a''} X_{a''}} \frac{\sum_k X_k G_{kc,a'c} \tau_{kc,a'c}}{\sum_k X_k G_{kc,a'c'}} +$$

$$\sum_{B'} \left(\frac{X_B G_{cB}}{\sum_k X_k G_{kB}} \right) \left(\tau_{cB} \frac{\sum_k X_k G_{kB} \tau_{kB}}{\sum_k X_k G_{kB}} \right) + \qquad (3.34)$$

$$\sum_a \sum_{c'} \frac{X_{c'}}{\sum_{c''} X_{c''}} \frac{X_c G_{ca,a'c}}{\sum_k X_k G_{ka,c'a}} \left(\tau_{ca,c'a} - \frac{\sum_k X_k G_{ka,c'a} \tau_{ka,c'a}}{\sum_k X_k G_{ka,c'a}} \right)$$

For anions, the activity coefficient equation is given by (Aspen Tech, 1989):

$$\frac{1}{z_a} \ln \gamma_a^{lc} = \sum_{c'} \frac{X_{c'}}{\sum_{c''} X_{c''}} \frac{\sum_k X_k G_{ka,c'a} \tau_{ka,c'a}}{\sum_k X_k G_{ka,c'a}} + \sum_B \left(\frac{X_B G_{cB}}{\sum_k X_k G_{kB}} \right) \left(\tau_{cB} \frac{\sum_k X_k G_{kB} \tau_{kB}}{\sum_k X_k G_{kB}} \right) +$$

$$\sum_a \sum_{c'} \frac{X_{c'}}{\sum_{c''} X_{c''}} \frac{X_c G_{ca,a'c}}{\sum_k X_k G_{ka,c'a}} \left(\tau_{ca,c'a} - \frac{\sum_k X_k G_{ka,c'a} \tau_{ka,c'a}}{\sum_k X_k G_{ka,c'a}} \right) \qquad (3.35)$$

where:

$$G_{cB} = \frac{\sum_a X_a G_{ca,B}}{\sum_{a'} X_{a'}} \qquad (3.36)$$

34

$$G_{aB} = \frac{\sum_c X_c G_{ca,B}}{\sum_{a'} X_{c'}} \tag{3.37}$$

$$\alpha_{Bc} = \alpha_{cB} \frac{\sum_a X_a \alpha_{B,ca}}{\sum_{a'} X_{a'}} \tag{3.38}$$

$$\alpha_{Ba} = \alpha_{aB} \frac{\sum_c X_c \alpha_{B,ca}}{\sum_{c'} X_{c'}} \tag{3.39}$$

$$\tau_{cB} = -\frac{\ln G_{cB}}{\alpha_{cB}} \tag{3.40}$$

$$\tau_{aB} = -\frac{\ln G_{aB}}{\alpha_{aB}} \tag{3.41}$$

$$\tau_{Ba,ca} = \tau_{aB} - \tau_{ca,B} + \tau_{B,ca} \tag{3.42}$$

$$\tau_{Bc,ac} = \tau_{cB} - \tau_{ca,B} + \tau_{B,ca} \tag{3.43}$$

where:

$X_j = x_j\, C_j$ ($C_j = Z_j$ for ions; C_j = unity of molecule).

z_c = charge number of cation

z_a = charge number of anion

τ = binary energy interaction parameter

3.2.4.5 Electrolyte NRTL enthalpy model

The enthalpy of electrolyte nonrandom two liquids defined by the following relation;

$$H_m^* = x_w H_m^* + \sum_k x_k H_k^\infty + H_m^{*E} \tag{3.44}$$

where:

H_m^* is the molar enthalpy.

H_m^{*E} is the molar excess enthalpy calculated from NRTL activity coefficient model.

H_w^* the pure water molar enthalpy.

The subscript * refers to pure component.

$$Hw* = \Delta H_f^{*,ig}{}_{(T=298.15)} + \int_{298.15}^{T} C_{p,k}{}^{ig} dT + \left(H_w(T,P) - H_w{}^{ig}(T,P) \right) \tag{3.45}$$

The subscript k can refer to molecular solute *(i)*, to a cation *(c)*, or an anion *(a)*:

$$H_k^{\infty} = \Delta_f H_k^{\infty,aq} + \int_{298.15}^{T} C_{p,k}{}^{\infty,aq} \tag{3.46}$$

The property H_k^{∞} can be calculated from infinite dilution aqueous phase heat capacity polynomial model based on the Criss-Cobble model for ions and from Henry's law for molecular solutes (AspenTech, 1989).

3.2.5   Solubility index model

The solubility index (*SI*) is a useful property for analyzing the solutions solid-liquid phase equilibrium. For electrolyte solutions, an *SI* value of greater than 1 indicates that the salt exists as a solid. On the other hand, an *SI* value of less than 1 means the salt has not reached the saturation point and will be in the aqueous phase. The solubility index is defined as activity product of the salt divided by the solubility product (Thomsen, 1997; Thomsen, 2008; and Kontogeorgis, 2004):

$$SI = \frac{\sum_{i=1}^{NC} a_i{}^{v_{ij}}}{K_j} \tag{3.47}$$

$$SI = \frac{a_k{}^k a_A{}^{\infty} a_w{}^n}{K_{k_k} A_a H_2 O} \tag{3.48}$$

$$K = e^{[-\frac{\Delta G^0}{RT}]} = e^{[\sum \ln a_i{}^{v_i}]} \tag{3.49}$$

where:

NC= number of the chemical species

a = activity

A = Debjie Huckel parameter

n = mole number

w = water

36

K = solubility product

k = stoichiometric coefficient for cation

α = degree of dissociation

ΔG^0 = Gibbs energy at standard conditions

Chapter 4

Results and discussion

4.1   Introduction

This chapter presents the results of the HPC thermodynamic study and discusses the reality and deviation of the results from the experimental data. Most of the results of electrolyte system were verified with the experimental of certain studies of certain electrolyte system. These experimental studies are; properties of aqueous solutions of electrolytes (Zaytsey, 1992), experimental studies of Benfield system (Kohl, 1997) and thermodynamics of hot potassium carbonate system using Aspen Plus (Hilliard, 2004; Hilliard, 2008).

The implementation of the simulation was based on the real data for the Benfield's system. These data were introduced into the simulation in order to determine the effects of process conditions electrolyte properties such as solubility index, pH, thermal, VLE, and transport properties using Aspen electrolyte property analysis tools.

4.2   Case study details

The case study contains the primary findings of the crystallized solvent and the analysis of the dry bases found in several positions of reboilers shell side and pipelines in the Benfield's system. In addition, the case study also includes the history report of the reboilers' blockage and the operation monitors in the cause of reboilers' blockage due to crystal formation.

Three different studies were simulated, each of which is based on specific consideration of several distributed concentrations that depend on the chemical conversion and solution composition. The three studies are:

(i)   30 wt% equivalent K_2CO_3 standard solution

(ii) $K_2CO_3+KHCO_3+H_2O+CO_2$ mixture solution

(iii) $K_2CO_3+ H_2O$ and $K_2CO_3+ H_2O$ binary system

4.2.1   Reboilers blockage of Benfield system

Benfield's system at a local fertilizer plant has two units of Reboilers A and B. The two reboilers are of the shell and tube type with two tube passes. Both units are scheduled for tube bundle inspection during the operation time.   Aqueous carbonate solution was drained after shut down via the bottom reboilers drain valves. Reboiler A was completely drained. Further, an internal inspection showed few locations in the shell side with black solid layer. However the draining of reboiler B was incomplete. This was because of some aqueous solution still remained in the system. Upon inspection, it was found that about 60% of the unit was immersed in crystallized solution and the tube bundle could not be removed for inspection.
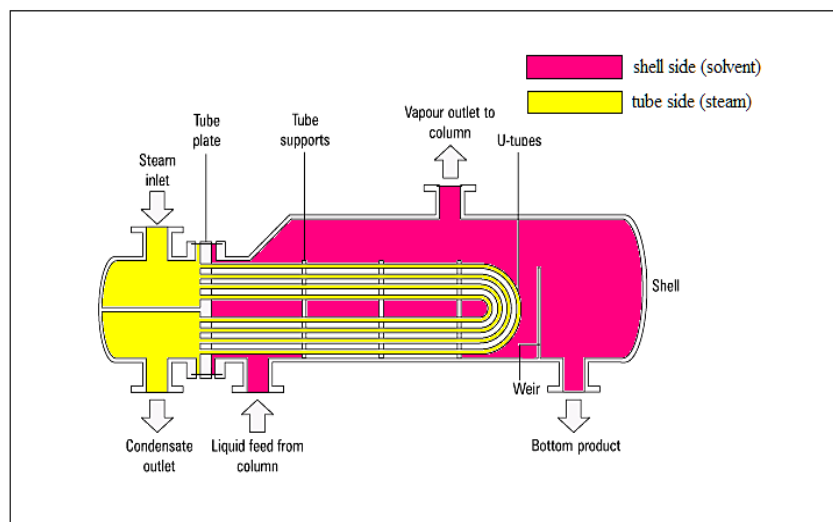

Figure 4-1 shell-tube Reboiler design with two tube passes

4.2.2 Operation monitors on the cause of reboilers blockage

The Benfield's plant already had several unplanned shut downs before the time for scheduled shutdown of the total plant. Most of the incidents were due to boilers tripping, lost of circulation from the reboilers to the regenerator, or blockage of drain valves. From observation, it was found that insufficient regeneration and lack of steam supply during these occasions has led to the drop of temperature in the system. The accumulated carbonate solution then started to crystallize as the temperature cools. The crystallization problem was further aggravated by the repeated unplanned shut downs that led to the accumulation of crystallized Benfield's solution. The level transmitters of both of Reboilers A and B gave a zero reading after draining activity, while the solution was not completely drain.

4.2.3 The reported analysis for Benfield's reboilers system crystallization

The solid content of Benfield solution collected from the bundle pipes of reboilers A and B after process shutdown in fertilizer plant was sent for laboratory analysis. In reboiler A the crystals was found to be containing 30.6 wt% K_2CO_3 dry bases. In addition, brown mud was found in reboiler B. The mud was found to be containing 63 wt% K_2CO_3 dry bases along with suspected bicarbonate crystals. These results collected form Benfield system Users' Forum Book (Penang, January 2001).

4.2.4 Chemical data inputs

The input data for electrolyte thermodynamic analysis of each of the case studies include the solution composition (Table 4-1), the equilibrium and dissociation reactions of the electrolyte solution (Table 4-2), the basic thermodynamic properties of components (Tables 4-3 to 4-6) and the NRTL pair parameters values (Table 4-7 to 4-10). The solution concentration and the components distribution are selected discretely for three different cases. Firstly for 30 wt% equivalent K_2CO_3 standard solution, the concentration of K_2CO_3 is constant. Secondly for mixture solution of ($K_2CO_3+KHCO_3+H_2O+CO_2$) system, the variable values represent the concentrations

of carbonate and bicarbonate based on the chemical conversion as shown in Table 4-11. The table describes ten carbonate/bicarbonate ratios commencing from (2.1706/ 0.0000) molality bases, which is equals to 30% K_2CO_3 standard solution to (0.0000/2.9953). The aim of this case focuses to determine the effect of the appearance of bicarbonate species on the solution properties in the case of the ideal operational process. The third case is the binary systems of ($K_2CO_3+H_2O$) and ($KHCO_3+H_2O$), the concentrations changes from (1 to 7.0) mole/KgH_2O. These distributions can cover all the composition and concentration possibilities that could be going through the solution stream from the absorption unit to the regeneration unit.

Table 4-1 Carbonate solution composition

Chemical formula	Type	Scientific name
H_2O	CONV	WATER
K_2CO_3	CONV	POTASSIUM-CARBONATE
$KHCO_3$	CONV	POTASSIUM-BICARBONATE
H_3O^+	CONV	H_3O^+
K^+	CONV	K^+
CO_2	CONV	CARBON-DIOXIDE
$KHCO_{3(S)}$	SOLID	POTASSIUM-BICARBONATE
$K_2CO_{3(S)}$	SOLID	POTASSIUM-CARBONATE
HCO_3^-	CONV	HCO_3^-
CO_3^{-2}	CONV	$CO3^{--}$
OH^-	CONV	OH^-

Table 4-2 Equilibrium and dissociation reactions

Reaction	Type	Reaction equation
1	Equilibrium	$2\ H_2O \longleftrightarrow H_3O^+ + OH^-$
2	Equilibrium	$CO_2 + 2\ H_2O \longleftrightarrow H_3O^+ + HCO_3^-$
3	Equilibrium	$HCO_3^- + H_2O \longleftrightarrow H_3O^+ + CO_3^{--}$
$K_2CO_{3(S)}$	Salt	$K_2CO_3(S) \longleftrightarrow 2\ K^+ + CO_3^{--}$
$KHCO_{3(S)}$	Salt	$KHCO_3(S) \longleftrightarrow K^+ + HCO_3^-$
K_2CO_3	Dissociation	$K_2CO_3 \longrightarrow 2\ K^+ + CO_3^{--}$
$KHCO_3$	Dissociation	$KHCO_3 \longrightarrow K^+ + HCO_3^-$

Table 4-3 Components basic thermodynamic properties

Property	Units	H_2O	K_2CO_3	$KHCO_3$	H_3O^+	K^+	CO_2	$KHCO_{3(S)}$	$K_2CO_{3(S)}$	HCO_3^-	CO_3^{--}	OH^-
API	-	10	-	-	-	-	340	-	-	-	-	-
CHARGE	-	0	0	0	1	1	0	0	0	-1	-2	-1
CHI	-	0	0	0	0	0	0	0	0	0	0	0
DGAQFM	J/KMOL	0	0	0	-237129000	-283270000	-385980000	0	0	-586770000	-527810000	-157244000
DGAQHG	J/KMOL	0	0	0	-237129000	-282650868	-386232300	0	0	-587332678	-528336479	-157402746
DGFORM	J/KMOL	-228766750	0	0	0	481200000	-394647770	0	0	0	0	0
DGFVK	J/KMOL	0	0	0	0	0	0	0	0	0	0	0
DGSFRM	J/KMOL	-236760000	$-10635*10^5$	-863500000	0	0	0	-863500000	$-10635*10^5$	0	0	0
DHAQFM	J/KMOL	0	0	0	-285830000	-252380000	-413800000	0	0	-691990000	-677140000	-229994000
DHAQHG	J/KMOL	0	0	0	-285830000	-252338436	-414074520	0	0	-690394946	-675686718	-230177704
DHFORM	J/KMOL	-241997040	0	0	0	514260000	-393768540	0	0	0	0	-143510000
DHFVK	J/KMOL	0	0	0	0	0	0	0	0	0	0	0

Table 4-4 Continues components basic thermodynamic properties

Property	Units	H_2O	K_2CO_3	$KHCO_3$	H_3O^+	K^+	CO_2	$KHCO_{3(S)}$	$K_2CO_{3(S)}$	HCO_3^-	CO_3^{--}	OH^-
DHSFRM	J/KMOL	-292920000	-1151020000	-963200000	0	0	0	-963200000	-1151020000	0	0	0
DHVLB	J/KMOL	40683136	-	-	-	-	17165880	-	-	-	-	-
DLWC	-	1	1	1	1	1	1	1	1	1	1	1
DVBLNC	-	1	1	1	1	1	1	1	1	1	1	1
HCOM	J/KMOL	0	0	0	0	0	0	0	0	0	0	0
IONRDL	WATT/M-K	-	-	-	-0.009071	-0.00756	-	-	-	-0.016631	-0.00756	0.020934
IONTYP	-	0	0	0	1	1	0	0	0	4	3	2
MUP	(J*CUM)**.5	5.69E-25	0	0	0	0	0	0	0	0	0	0
MW	-	18.01528	138.2058	100.11544	19.02267	39.09775	44.0098	100.11544	138.2058	61.01769	60.0103	17.00789
OMEGA	-	0.320965206	0	0	0.296	0.296	0.225	0	0	0.296	0.296	0.296
OMEGHG	J/KMOL	0	0	0	121945527	80679636	-8373600	0	0	533105244	1419911350	722055528
OMGPR	-	0.320965206	0	0	0	0	0.225	0	0	0	0	0
OMGRKS	-	0.320965206	0	0	0	0	0.225	0	0	0	0	0

Table 4-5 Continues components basic thermodynamic properties

Property	Units	H_2O	K_2CO_3	$KHCO_3$	H_3O^+	K^+	CO_2	$KHCO_{3(S)}$	$K_2CO_{3(S)}$	HCO_3^-	CO_3^{--}	OH^-
PC	N/SQM	22048320	5000000	5000000	2968820	2968820	7376460	5000000	5000000	2968820	2968820	2968820
PCPR	N/SQM	22048320	5000000	5000000	5000000	5000000	7376460	5000000	5000000	5000000	5000000	5000000
PCRKS	N/SQM	22048320	5000000	5000000	5000000	5000000	7376460	5000000	5000000	5000000	5000000	5000000
RADIUS	METER	-	3E-10	3E-10	3E-10	3E-10	-	3E-10	3E-10	3E-10	3E-10	3E-10
RHOM	KG/CUM	0	0	0	0	0	0	0	0	0	0	0
RKTZRA	-	0.259354595	0.29185962	0.29185962	0.25	0.25	0.2736149	0.29185962	0.29185962	0.25	0.25	0.25
S025C	J/KMOL-K	0	0	0	69910	102500	117600	0	0	91200	-56900	-10750
S025E	J/KMOL-K	0	0	0	233253.5	-670	210887.4	0	0	444140.9	444140.9	233253.5
S25HG	J/KMOL-K	0	0	0	69910	101111.22	117649.08	0	0	98515.404	-50032.26	-10718.208
SG	-	1	-	-	-	-	0.3	-	-	-	-	-

Table 4-6 Continues components basic thermodynamic properties

Property	Units	H_2O	K_2CO_3	$KHCO_3$	H_3O^+	K^+	CO_2	$KHCO_{3(S)}$	$K_2CO_{3(S)}$	HCO_3^-	CO_3^{--}	OH^-
TB	K	373.2	341.9	341.9	341.9	341.9	194.7	341.9	341.9	341.9	341.9	341.9
TC	K	647.3	2000	2000	507.4	507.4	304.2	2000	2000	507.4	507.4	507.4
TCPR	K	647.3	2000	2000	500	500	304.2	2000	2000	500	500	500
TCRKS	K	647.3	2000	2000	500	500	304.2	2000	2000	500	500	500
TFP	K	273.2	1174	177.8	177.8	177.8	216.6	177.8	1174	177.8	177.8	177.8
TREFHS	K	298.15	298.15	298.15	298.15	298.15	298.15	298.15	298.15	298.15	298.15	298.15
VB	CUM/KMOL	0.01963607	0.140903	0.140903	0.140903	0.140903	0.035637394	0.140903	0.140903	0.140903	0.140903	0.140903
VC	CUM/KMOL	0.05589534	0.1	0.1	0.369445	0.369445	0.093944596	0.1	0.1	0.369445	0.369445	0.369445
VCRKT	CUM/KMOL	0.05589534	0.369445	0.369445	0.25	0.25	0.093944596	0.369445	0.369445	0.25	0.25	0.25
VLSTD	CUM/KMOL	0.020246805	0.298906345	0.298906345	-	-	0.0535578	0.298906345	0.298906345	-	-	-
ZC	-	0.229	0.2	0.2	0.26	0.26	0.274	0.2	0.2	0.26	0.26	0.26

Table 4-7 NRTL pair parameter CC-1

Molecule i	Electrolyte i	Molecule j	Electrolyte j	VALUE
H_2O		H_3O^+	HCO_3^-	8.045
H_3O^+	HCO_3^-	H_2O		-4.072
H_2O		H_3O^+	CO_3^{--}	8.045
H_3O^+	CO_3^{--}	H_2O		-4.072
H_2O		K^+	HCO_3^-	8.75
K^+	HCO_3^-	H_2O		-4.489
H_2O		K^+	CO_3^{--}	0.7833727
K^+	CO_3^{--}	H_2O		0.602788
CO_2		H_3O^+	HCO_3^-	15
H_3O^+	HCO_3^-	CO_2		-8
CO_2		H_3O^+	CO_3^{--}	15
H_3O^+	CO_3^{--}	CO_2		-8
H_2O		H_3O^+	OH^-	8.045
H_3O^+	OH^-	H_2O		-4.072
H_2O		K^+	OH^-	7.840673
K^+	OH^-	H_2O		-4.258696
CO_2		H_3O^+	OH^-	15
H_3O^+	OH^-	CO_2		-8

Table 4-8 NRTL pair parameter CN-1

Molecule i	Electrolyte i	Molecule j	Electrolyte j	VALUE
CO_2		H_3O^+	HCO_3^-	0.1
CO_2		H_3O^+	CO_3^{--}	0.1
CO_2		H_3O^+	OH^-	0.1

Table 4-9 NRTL pair parameter CD-1

Molecule i	Electrolyte i	Molecule j	Electrolyte j	VALUE
H_2O		K^+	CO_3^{--}	0
K^+	CO_3^{--}	H_2O		-1173.117
CO_2		H_3O^+	HCO_3^-	0
H_3O^+	HCO_3^-	CO_2		0
CO_2		H_3O^+	CO_3^{--}	0
H_3O^+	CO_3^{--}	CO_2		0
H_2O		K^+	OH^-	773.3601
K^+	OH^-	H_2O		-305.6509
CO_2		H_3O^+	OH^-	0
H_3O^+	OH^-	CO_2		0

Table 4-10 NRTL pair parameter CE-1

Molecule i	Electrolyte i	Molecule j	Electrolyte j	VALUE
CO_2		H_3O^+	HCO_3^-	0
H_3O^+	HCO_3^-	CO_2		0
CO_2		H_3O^+	CO_3^{--}	0
H_3O^+	CO_3^{--}	CO_2		0
H_2O		K^+	OH^-	-5.852382
K^+	OH^-	H_2O		4.75413
CO_2		H_3O^+	OH^-	0
H_3O^+	OH^-	CO_2		0

Table 4- 11 Case study concentration ratios of (carbonate/bicarbonate) at pressures (1 and 2) bar and temperature range between (298.15 to 403.15) K

K_2CO_3 (mole)	$KHCO_3$ (mole)
2.1706	0.0000
1.9294	0.3328
1.6882	0.6657
1.4471	0.9985
1.2059	1.3313
0.9647	1.6641
0.7235	1.9970
0.4824	2.3298
0.2413	2.6627
0.0000	2.9953

4.2.5   30 wt% Potassium carbonate standard solution

The thermodynamic analysis of the present Benfield's system is based on potassium carbonate solution (30 wt%) and the solution of carbonate/bicarbonate mixture. The transport properties estimated for 30 wt% carbonate solution are solution viscosity, density and saturation index for a temperature range (280.15 and 370.15 K) based on the freezing and boiling temperatures at 283.15 K and 366.48 K respectively (Kohl, 1997) see appendix B, Figure B3. As shown in Figure 4.2, the viscosity decreased with temperature until it reaches the boiling temperature, then it increased at temperatures higher than the boiling temperature, which might be due to the evaporation of water and hence the change in the liquid solvent volume. The present estimated boiling temperature (362.15 K) satisfactorily agrees with the reported value of 366.15 K (Kohl, 1997) with an error of -1.1 %. Figure 4.3, shows the solubility index values at similar conditions. The estimated freezing temperature of 287.15 K

(for the solubility index 1) agrees well with the reported experimental data (Kohl, 1997). The error is only +1.4 %.

Figure 4.4, shows the estimated values of solution density whereas the estimated specific gravity values are compared with the reported values of Kohl (1997) as it shown in Table 4-12. The original graph of specific gravity shows in appendix B, Figure B4. Figure 4.5 shows the effect of temperature on the water activity coefficient and Table 4-13 shows the comparison of present estimated water activity coefficient values with that of Walker (1970). The literature data of water activity and density presented in appendix B, Figure B6 and the Tables from B1 to B8. Beside the presented properties, the heat capacity, enthalpy, and solution pH have been estimated and they are shown in Figures 4.6, 4.7 and 4.8 respectively. In Figure 4.6, the solution total heat capacity increased from 1831.4 J/kg.K to 2347.1 J/kg.K for temperatures 366.15K and 280.15 K, respectively that because of the changing of the K_2CO_3 system internal energy. On the other hand, the temperature was also used to increase quantity of total heat enthalpy by effecting on water and solute dissociation; these results shown in Figure 4.7. Figure 4.8 showed the solution (water) pH curve which is increase until the temperature of 304.75 K and then decreased to the temperature of 366.15 K. this behavior related to the water dissociation, solute dissociation and solute activity coefficient at temperatures lower than 304.75 K. Table 4-14 shows the values of water activity, density, enthalpy, heat capacity, solubility index, and solution pH at the critical point of freezing and boiling temperatures.
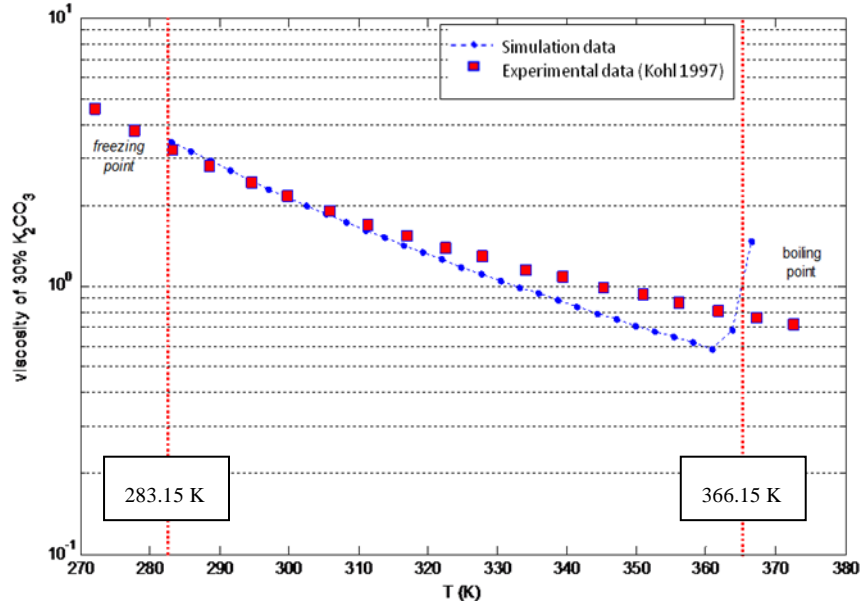
Figure 4-2 Viscosity of 30 wt% K_2CO_3 at 1 bar
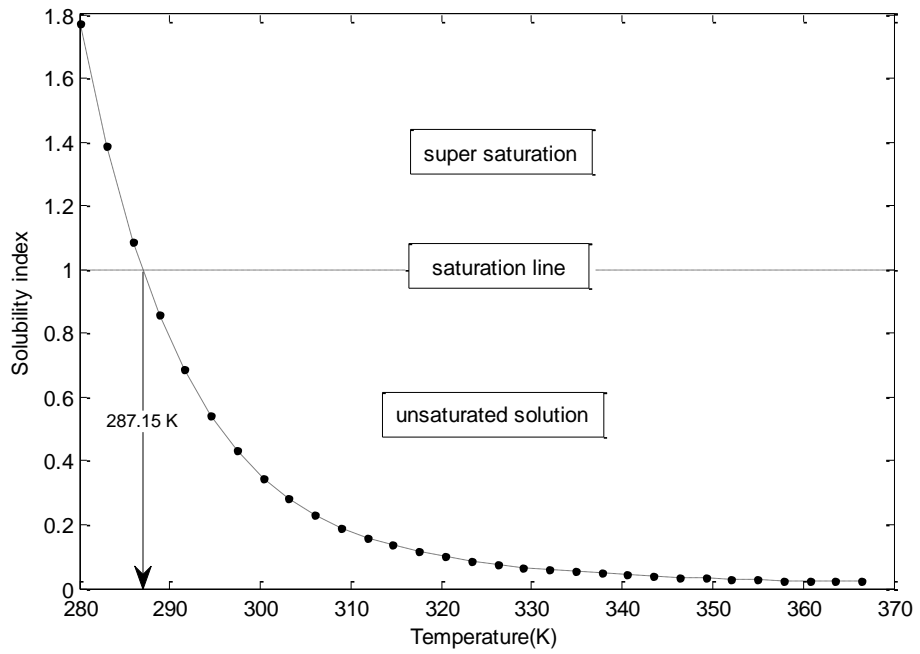
Figure 4-3 Solubility index of 30 wt% K_2CO_3 at pressure 1 bar

51
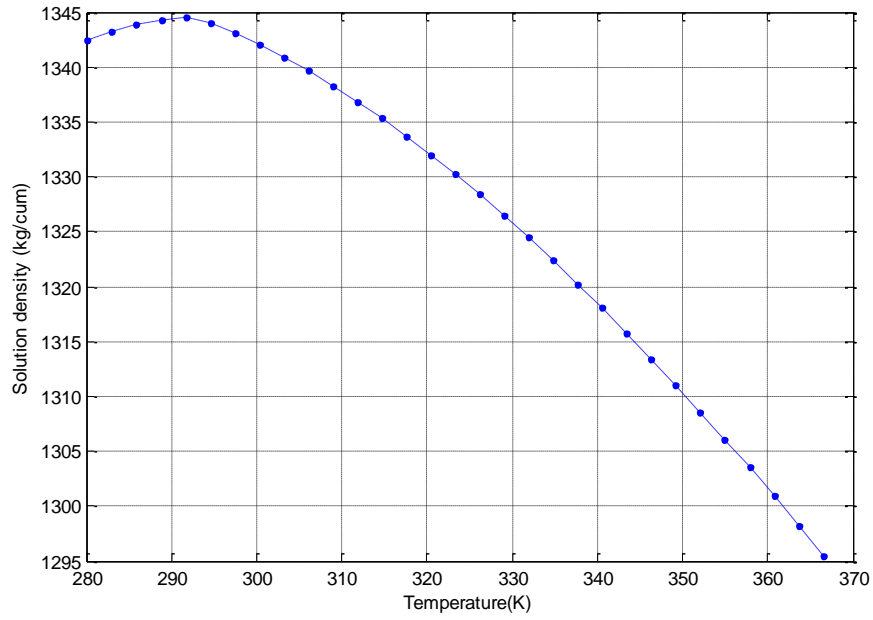
Figure 4-4 The solution density changes with temperature at pressure 1 bar
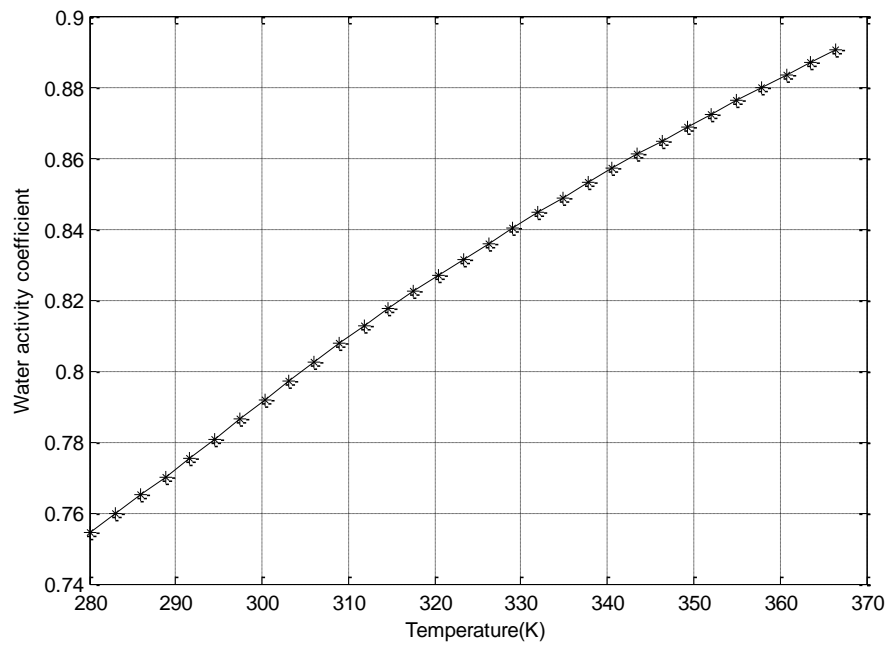
Figure 4-5 Water activity coefficient for 30 wt% K_2CO_3 at 1 bar
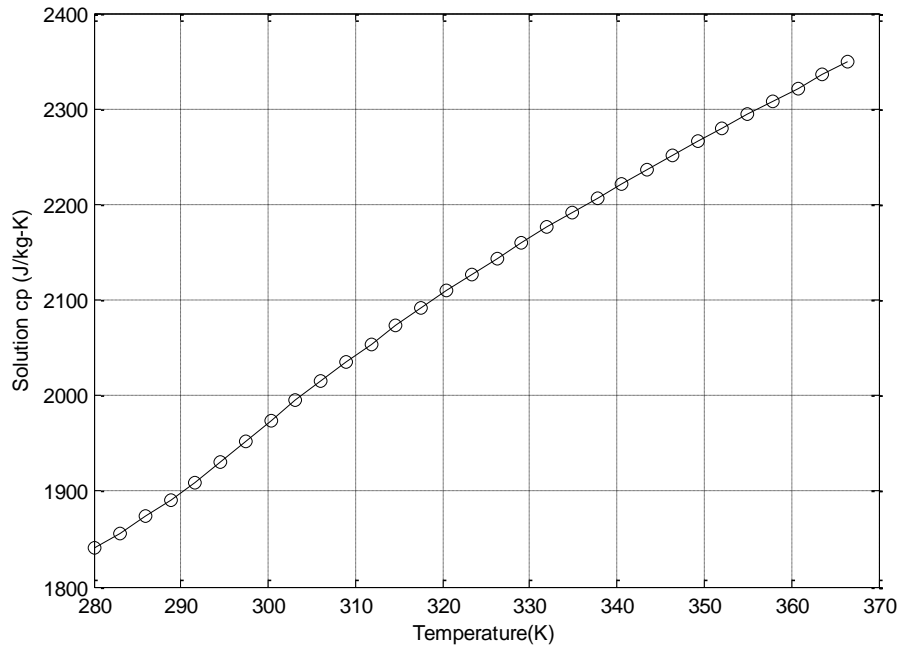
Figure 4-6 Solution heat capacity at constant pressure 1 bar
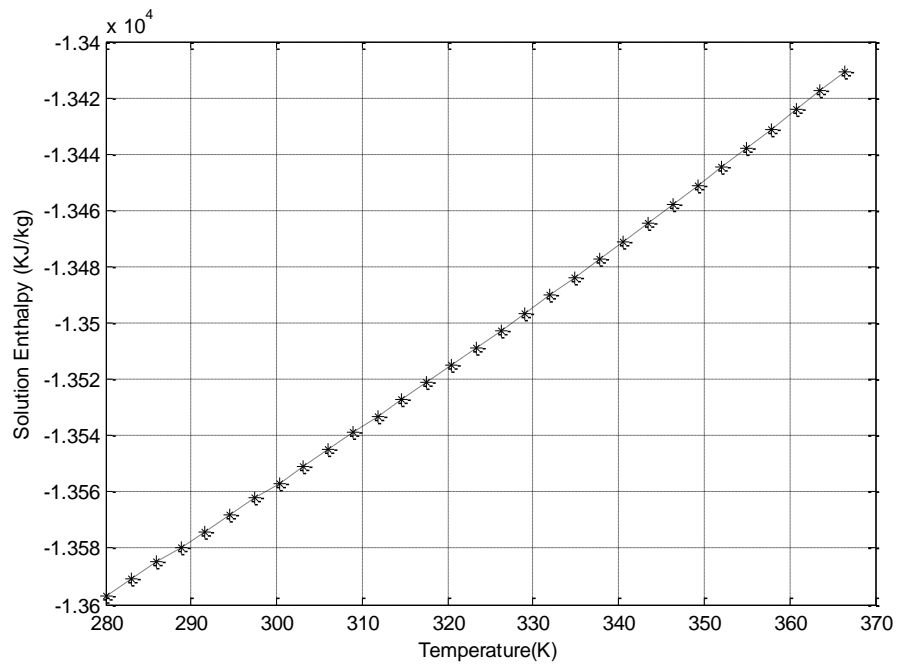
Figure 4-7 Solution heat enthalpy at constant pressure 1 bar
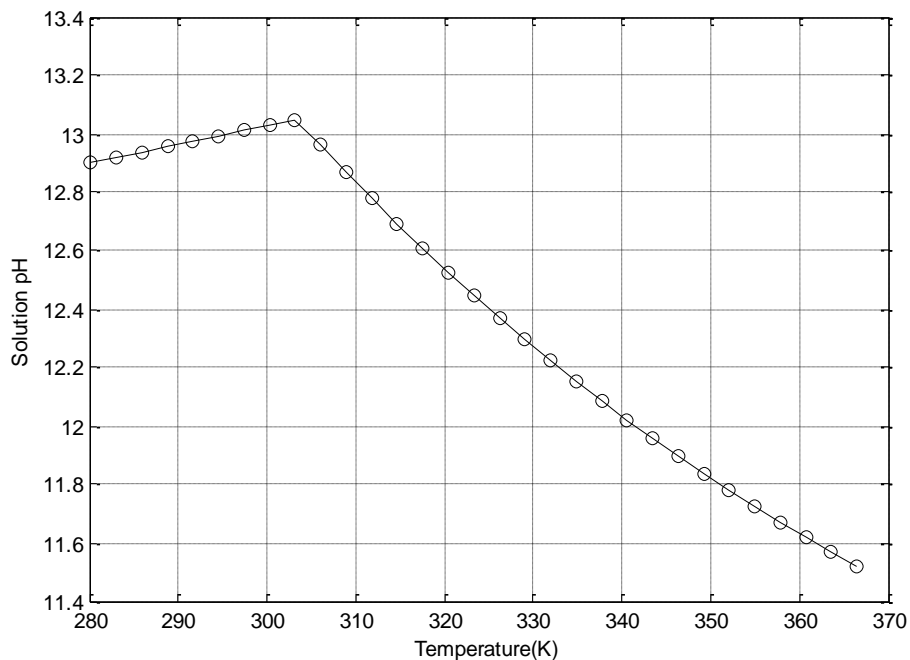
Figure 4-8 Solution pH at constant pressure 1 bar

Table 4-12 Specific gravity (SG) error

T^0C	Kohl (1997)	This study	Relative error%
70	1.3006	1.3158	1.17%
75	1.2948	1.3111	1.26%
80	1.2900	1.3086	1.44%
85	1.2842	1.3009	1.32%
90	1.2795	1.2982	1.49%
95	1.2736	1.2955	1.77%
100	1.2690	1.2907	1.71%
105	1.2642	1.2837	1.58%

Table 4-13 Water activity coefficient error

T ^{0}C	Walker (1970)	This study	Relative error %
30	0.8855	0.7970	-9.99
40	0.8864	0.8147	-8.09
50	0.8885	0.8310	-6.47
60	0.8910	0.8462	-5.03
70	0.8948	0.8604	-3.85
80	0.9001	0.8736	-2.94
90	0.9037	0.8861	-1.95
100	0.9043	0.8979	-0.70

Table 4- 14 Thermodynamic values of 30 wt% K_2CO_3 at the critical temperatures

Temperature (K)	Water activity	Enthalpy KJ/Kg	Cp J/Kg-K	Density Kg/cum	Solubility index	Solution pH
Min 287.15	0.76449	-13585	1873.37	1343.896	1	12.938
Max 362.15	0.887	-13417.52	2349.53	1298.913	0.02216	11.569

4.2.6 K_2CO_3+$KHCO_3$+H_2O+CO_2 mixture system

Since the present simulated results of K_2CO_3 solution in this study showed a fair degree of accuracy with the available literature, it is further decided to extend the simulation for of K_2CO_3+$KHCO_3$+H_2O+CO_2 mixture system. By following the similar procedure, the simulation was carried out by taking the possibilities of different carbonate/bicarbonate ratios in the solution based on the initial concentration of 2.1706 mole K_2CO_3. It was assumed that the carbonate was totally converted to bicarbonate during the CO_2 absorption process and all bicarbonate were assumed to be converted back into carbonate during the stripping process based on the absorption reaction (Equation 1.1). These assumptions were critical in evaluating the properties of mixed carbonate/bicarbonate solution at varying pressures and temperatures. In

addition, the assumptions gave an ability to perform the chemical conversion of the ideal process for all the possibilities of carbonate/bicarbonate concentration ratios.

The present analysis has been performed for different concentration ratios as shown in Table 4-11 at a temperature range of 298.15 to 403.15 K and at 1 and 2 bar pressures. In Table4-11, the initial ratio (carbonate/bicarbonate) for 30 wt% potassium carbonate was 2.1706:0.0000 at zero conversion. For 100% conversion, the final ratio was presented at 0.0000:2.9953.

Figure 4.9 shows the density changes with the carbonate/bicarbonate concentration. The estimated solution densities are higher for the higher concentrations of carbonate, and lower for the higher concentrations of bicarbonate. For the first ratio (2.1706/0.0000), the solution density decreases when the temperature increases until the boiling temperature of 378.65 K for 1 bar pressure and 396.15 K for 2 bar. For the other ratios from (1.9294/0.3328 to 0.0000/2.9954), the density shows a different behavior with the appearance of bicarbonate anion (HCO_3^-). The concentration of the bicarbonate anion (HCO_3^-) starts to increase as the CO_2 absorption into the liquid phase increases. Figures (4.10) and (4.11) show the relation between the mole rate of the CO_2 and all of the carbonate and bicarbonate anions under similar conditions.

The liquid density increases from 298.15 K to the range of 312.15 K- 322.15 K and then it starts to decrease until it reaches the boiling temperature. This increases of density usually occurred at the low temperatures when the bicarbonate anions give activity coefficient values that is higher than unity. The mixture solution densities were increased at temperatures higher than the estimated boiling point for all concentration ratios used in the present study. Figures 4.12 and 4.13 further showed the thermodynamic quantities of enthalpy and heat capacity at different concentration ratios.
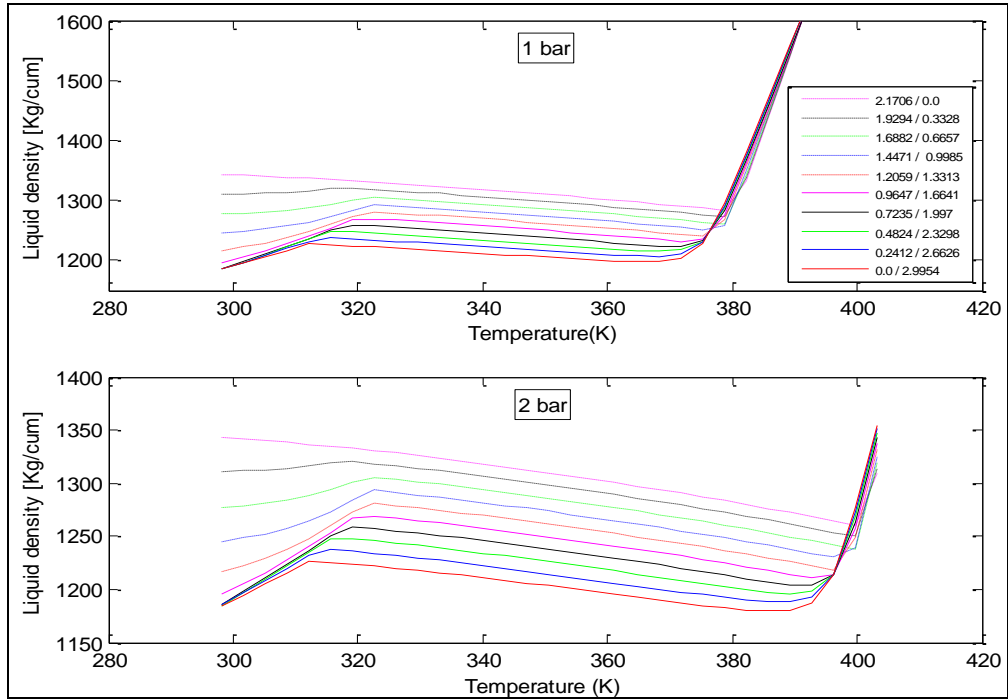
Figure 4-9 Effects of K_2CO_3 conversion and temperature on solution density
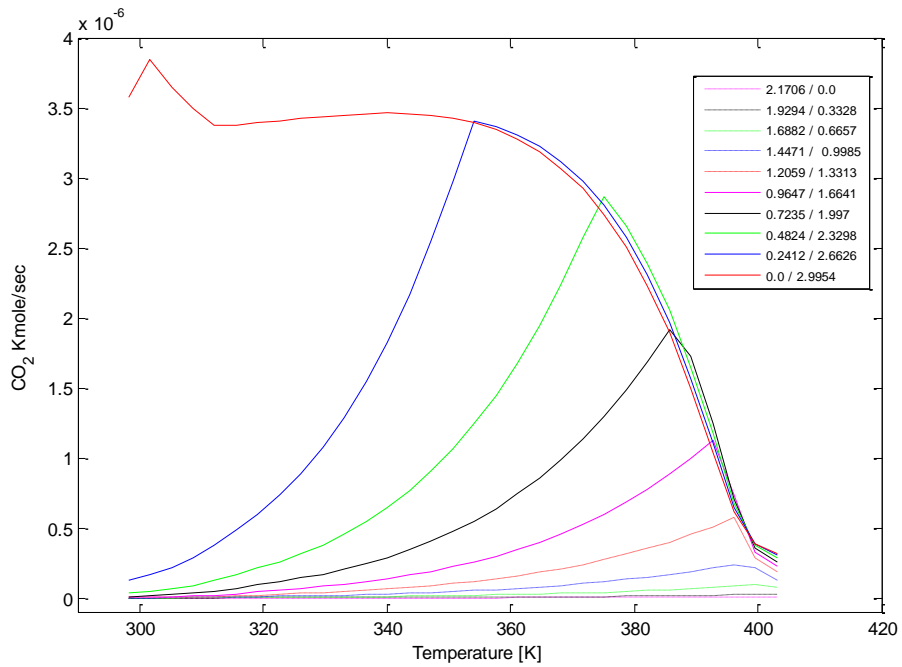
Figure 4-10 Temperature effects on CO_2 mole rate in the liquid phase
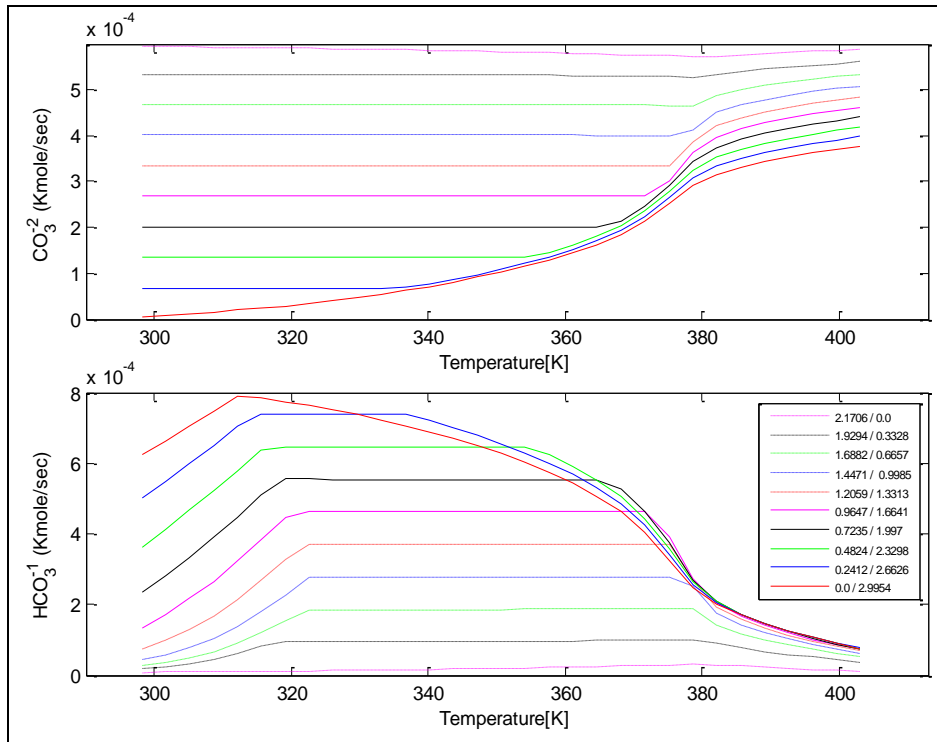
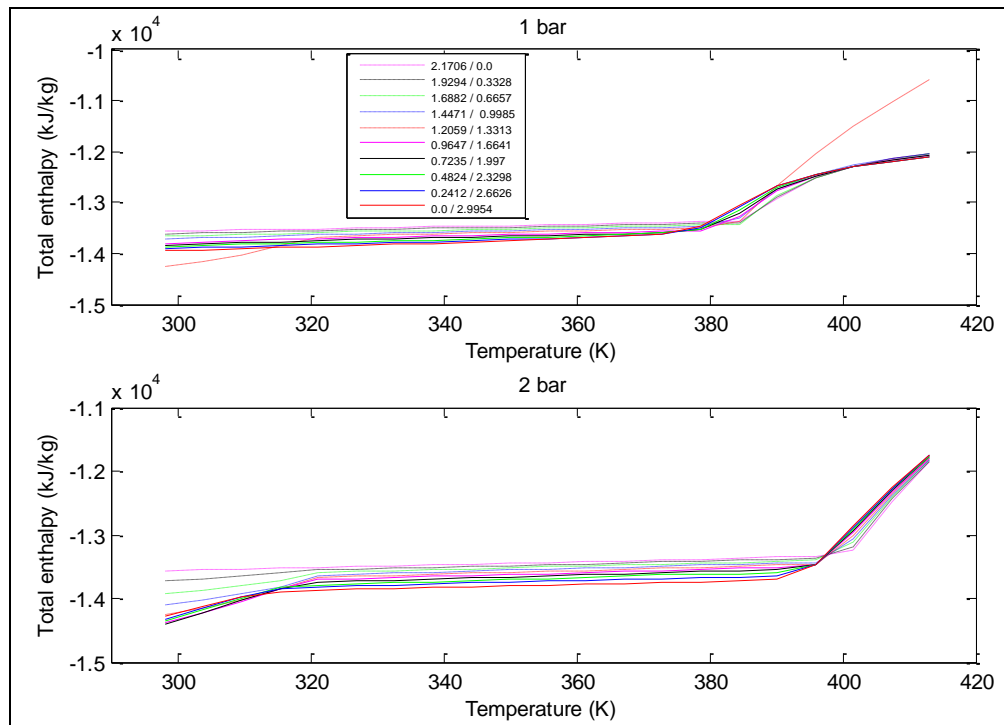Figure 4-11 The true component rate for CO_3^{2-} and HCO_3^- in mixture solution

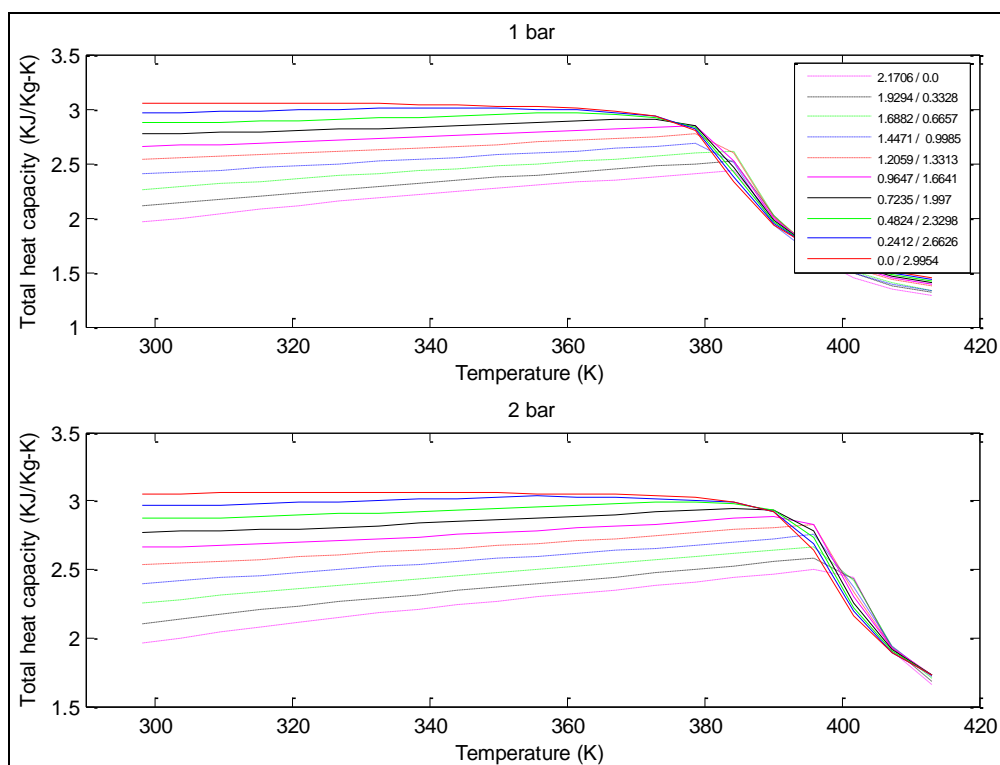Figure 4-12 Effects of K_2CO_3 conversion and temperature on solution enthalpy

Figure 4-13 Effects of K_2CO_3 conversion and temperature on solution heat capacity

The solvent thermodynamic activity can be measured by solubility, vapor pressure and electrochemical potential (Butler, 1998). The electrochemical potential of a solution is affected by the ions composition, types of ion, pressure and temperature. Most of the electrolyte data estimated at the standard conditions of 25^0C temperature and 1 atm pressure. Aspen Plus simulator has the capability to predict the electrolyte temperature dependence properties based on the equilibrium data of electrolytes (AspenTech, 1989). The water properties were determined as monitor properties and they can point to the solid-liquid equilibrium at a known carbonate/bicarbonate concentration, temperature and pressure.

The deviation of water fugacity coefficient records very small changes with the chemical conversions, but the boiling point increases from 385 K to 395 K at pressures 1 bar and 2 bar respectively. These results are shown in Figure 4.14.

59

The water activity coefficient values of mixed carbonate/bicarbonate solution are shown in Figure 4.15 for different temperatures and pressures. A decrease in the concentration of K_2CO_3 affected positively in the water activity coefficient due to the depression of K_2CO_3 concentration with the chemical conversion from (2.1706 to 0.0000) mole/KgH_2O. An increase in the temperature from 298.15 to 378.15 K increases the water activity coefficient due to the dissociation effect of water and the solubility of the carbonate and bicarbonate mixture. The water activity values decreases for the entire mixture solution ratios at temperatures greater than 378.15 K. This might be due to the effect of higher boiling temperature on the liquid volume as the pressure increases. The water pressure increased from 921.69 mmHg to 2023.01 mmHg, while the water mole fraction decreased slightly from 0.854 to 0.6013 for temperatures 378.65 K and 403.15 K, respectively, at pressure of 1 bar.

For pressure at 2 bar, the water pressure was increased from 1634.86 mmHg to 2023.91 mmHg and the liquid mole fraction was decreased from 0.8535 to 0.8316 for temperatures of 396.15 K and 403.15 K, respectively. Figure 4.16 shows direct relations between the water vapor pressure and the average mole fraction of water at pressures of 1 and 2 bar. In Figure 4.16, the presented values of water mole fraction in the liquid phase at pressures 1 bar and 2 bar proved that the operation performed at 2 bar pressure gave a wider range of liquid phase than the operation at 1 bar. The reason of this behavior is related to the changes of boiling temperature between operating pressures of 1 and 2 bar. It is further justified that the effects of operating pressure on the boiling temperature has also an effect on the liquid volume of the solution and this can explain the sudden drop of water mole fraction at vapor pressure of 1.5×107 mmHg at pressure 1bar. However, it slightly decreases from vapor pressure of 2.75×107 mmHg at pressure 2 bar. The change of the liquid mole fraction between pressures of 1 bar and 2 bar can be generalized for the other properties at the similar temperatures.
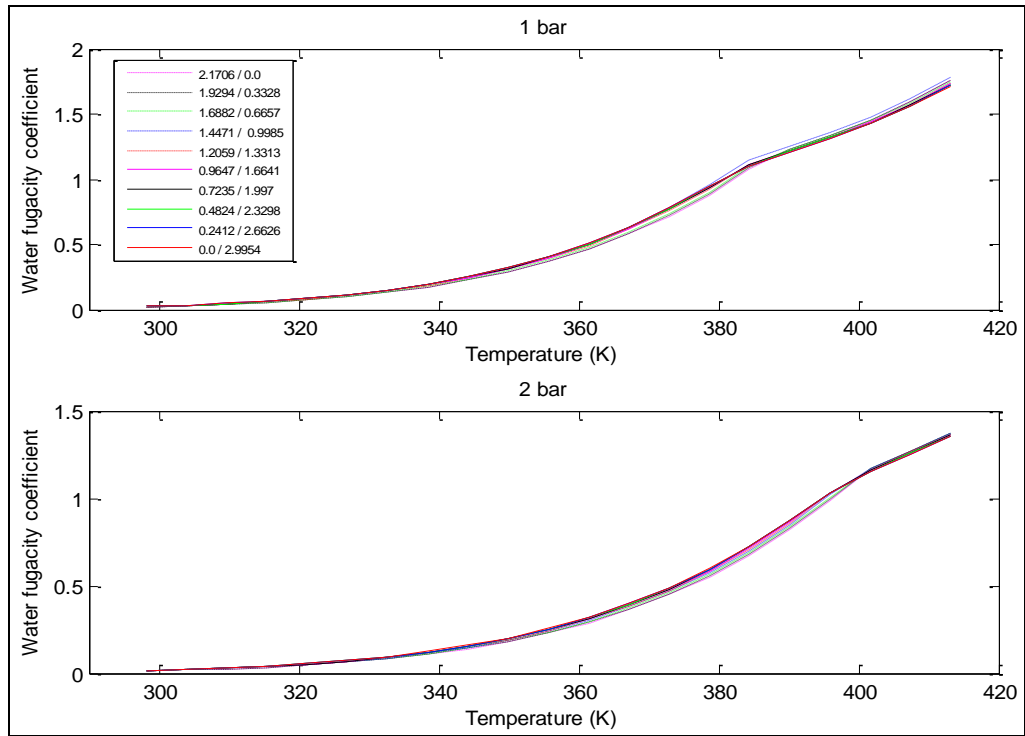
Figure 4-14 Effects of K_2CO_3 conversion and temperature on water fugacity

Figure 4.17 shows the solution pH estimation as a function of temperature and concentration. Based on Handeson-Hasselbalch equation, the change of temperature can affect pH by temperature-induced shift in the *pK* value (Grinstein, 1988). This relation given by:

$$pH = pK + \frac{[base]}{[acid]}$$

(4.1)

$$pK = \frac{[products]}{[react]}$$

(4.2)

The temperature always supports the water dissociation reaction and the water ionization constant (K_w) will increase proportionally with the increase in the pH value. The concentration factor strongly affects the solution pH vis-a-vis the temperature. In HPC solution, the pH value controlled is by the carbonate (CO_3^{--}) and bicarbonate

(HCO_3^-) ions. Therefore higher pH values are found at high concentrations of carbonate ions.
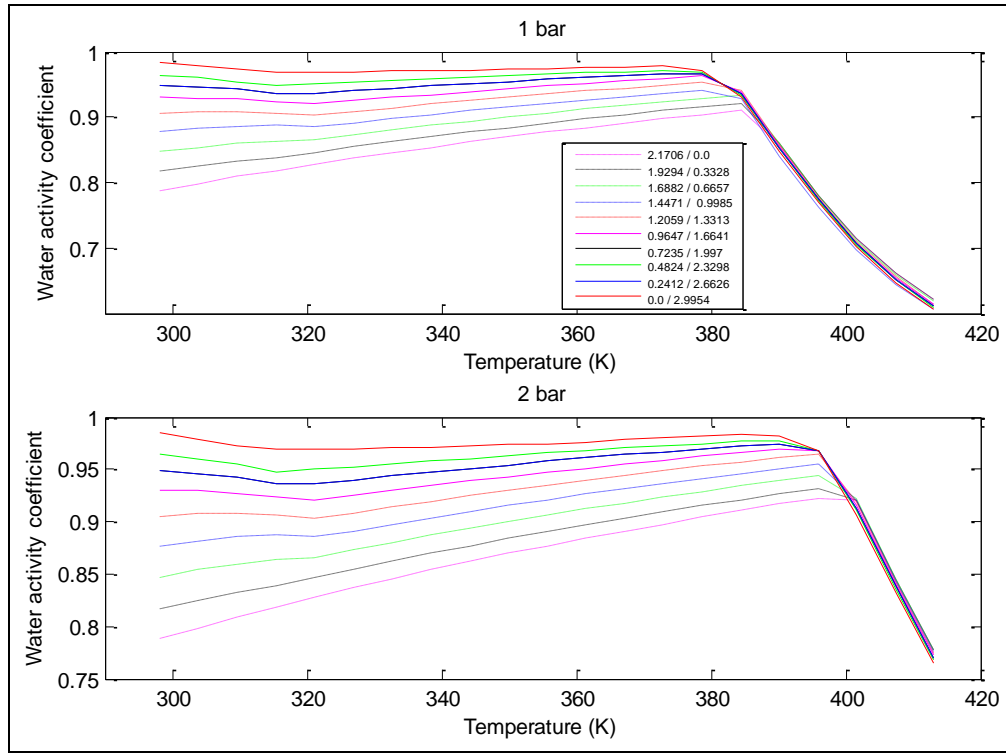
Figure 4-15 Effects of K_2CO_3 conversion and temperature water activity coefficient
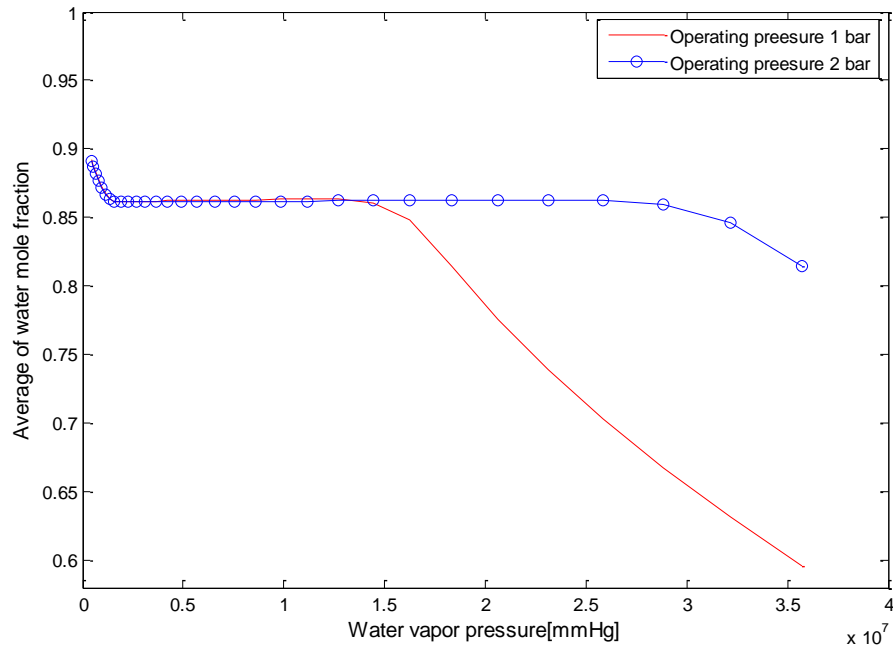
Figure 4-16 The relation between water pressure and the average of water mole fraction
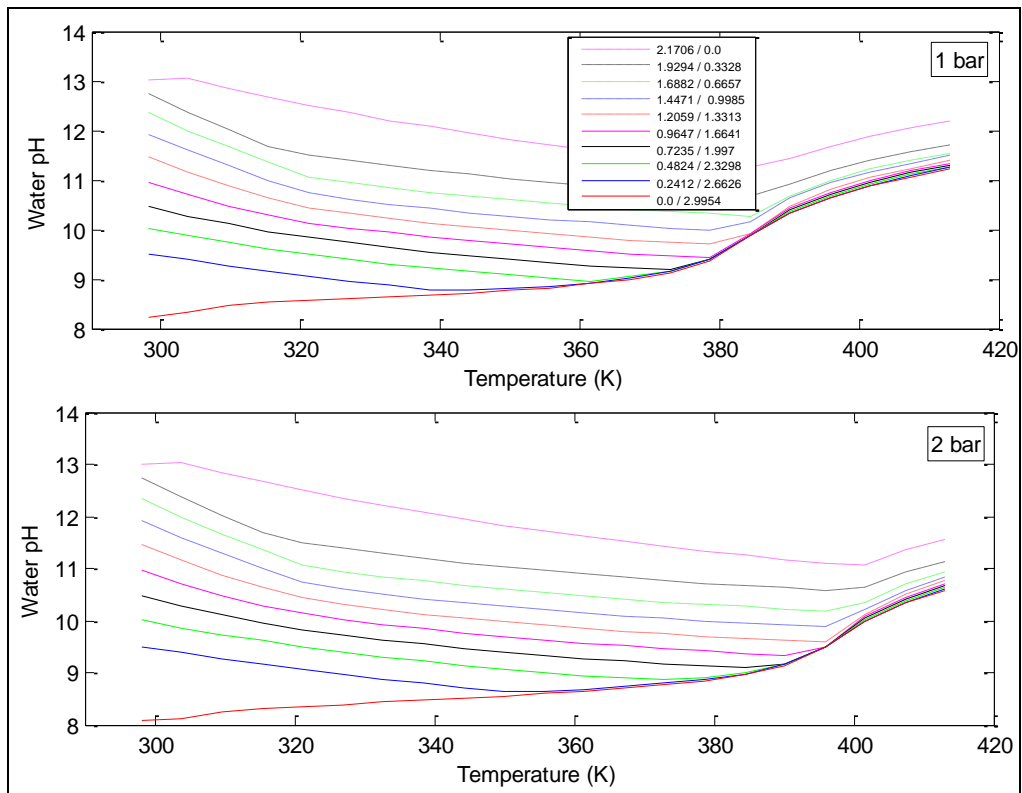
Figure 4-17 Effects of K_2CO_3 conversion and temperature on water pH

The mean activity coefficient of carbonate and bicarbonate are presented in Figures 4.18 and 4.19, respectively. The carbonate ions give value of mean activity coefficient values higher than the bicarbonate in references to the high alkalinity of carbonate ions in the solution.

The mathematical relation between solubility product and solubility given by:

$$\sqrt[n]{\frac{K_{sp}}{x^x \cdot y^y}} = \frac{S}{M_m}$$

(4.3)

where n is the total number of $(x + y)$ ions, x is moles of cations, y is moles of anions, K_{sp} is solubility product constant and S is the solubility of salt as mass fraction of solute in kg solvent (Butler, 1998). The solubility product constant is related directly to the salt concentration and at the same time the solubility product constant is a function of temperature.

The relation between concentration and solubility is inversely proportional. Furthermore, the temperature affects proportionally on the solubility up to the solution boiling point. Figures 4.20 and 4.21 showed the temperature effects on solution solubility in cases of carbonate and bicarbonate. The graphs clarified the critical temperature of the boiling points at different pressures. In this case, the study did not find any critical points for crystallization at lower temperatures for both carbonate and bicarbonate. The solubility index graph in Figure 4.20 explains the solid-liquid equilibrium points for carbonate at pressure 1 bar and temperature 396 K. For bicarbonate component as shown in Figure 4.21, all the estimated values of solubility index were found lower than the unity at pressures 1 bar and 2 bar.
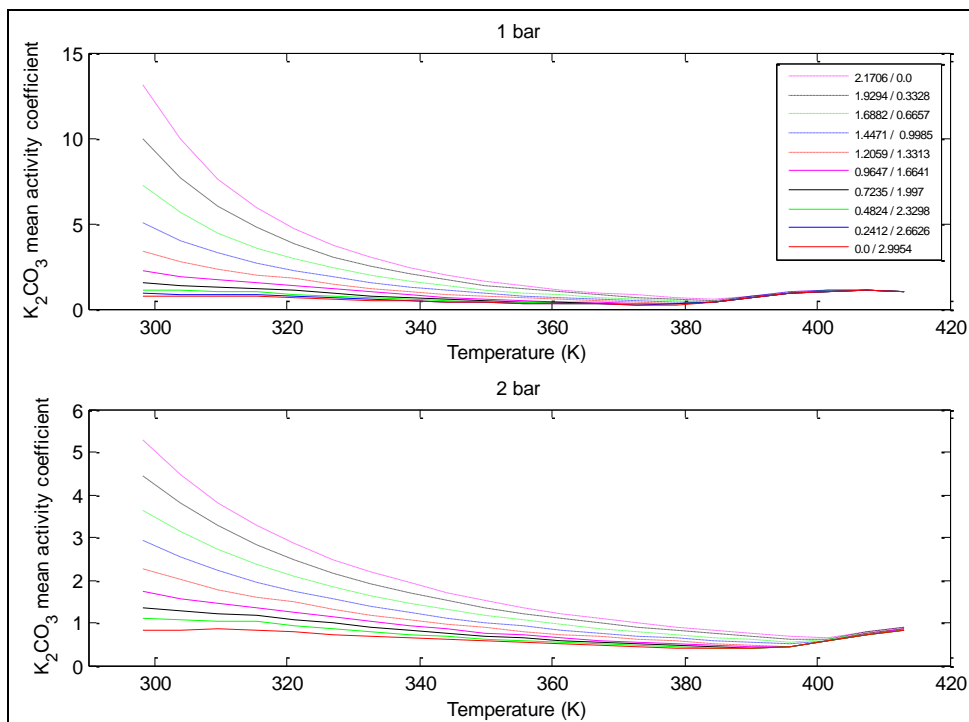
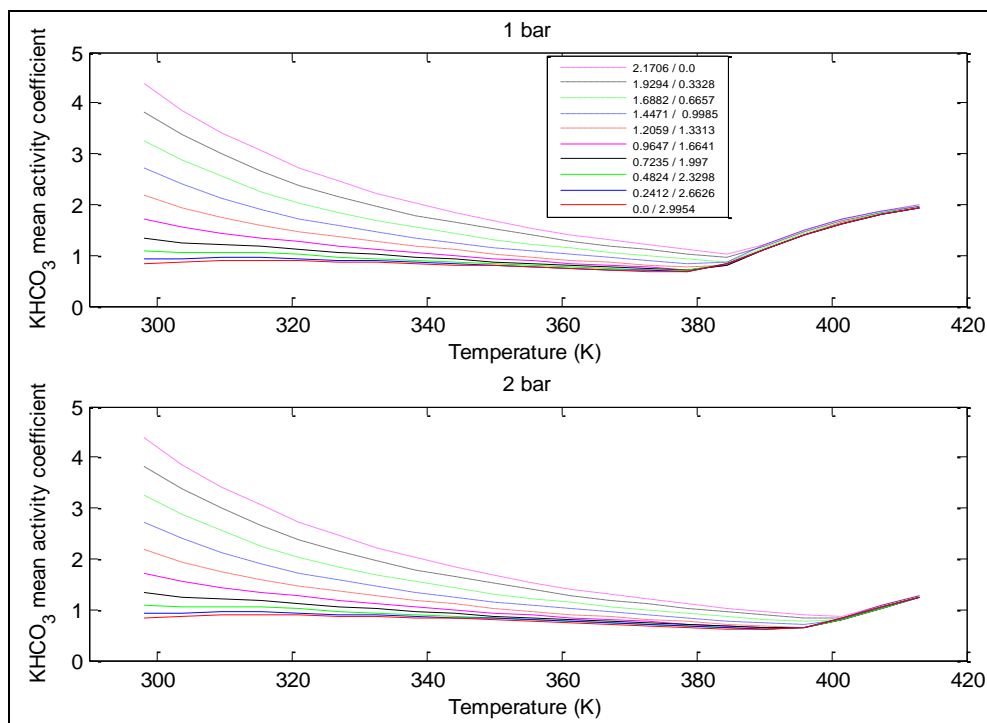Figure 4-18 Temperature effects on K_2CO_3 activity coefficient in mixture solution

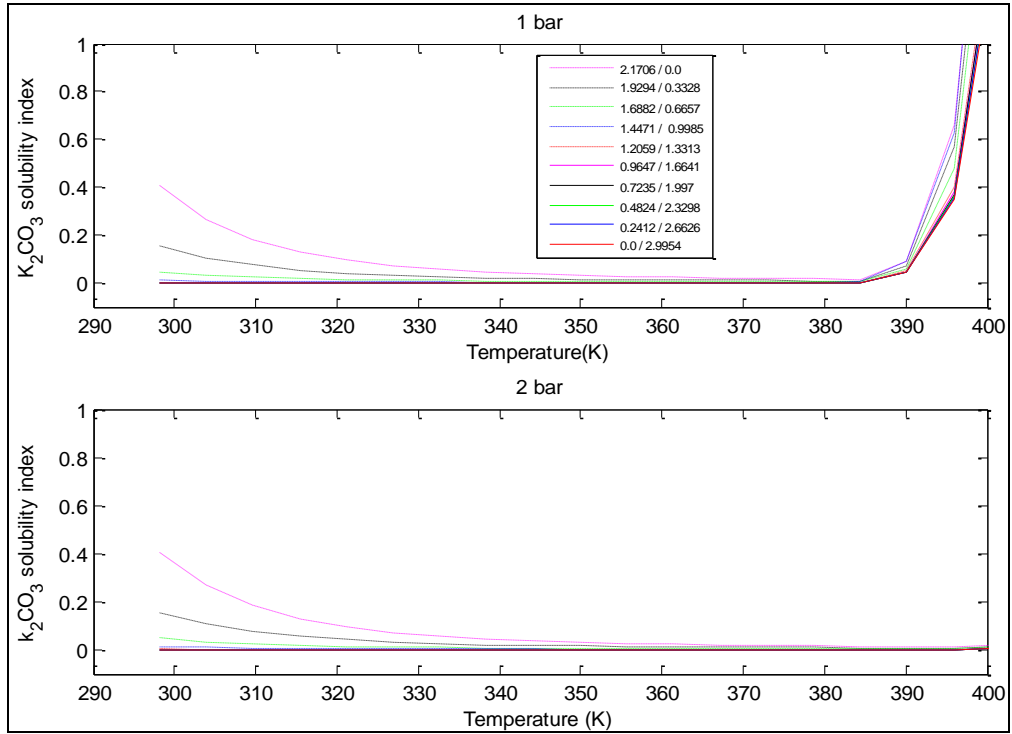Figure 4-19 Temperature effects on $KHCO_3$ activity coefficient in mixture solution

65

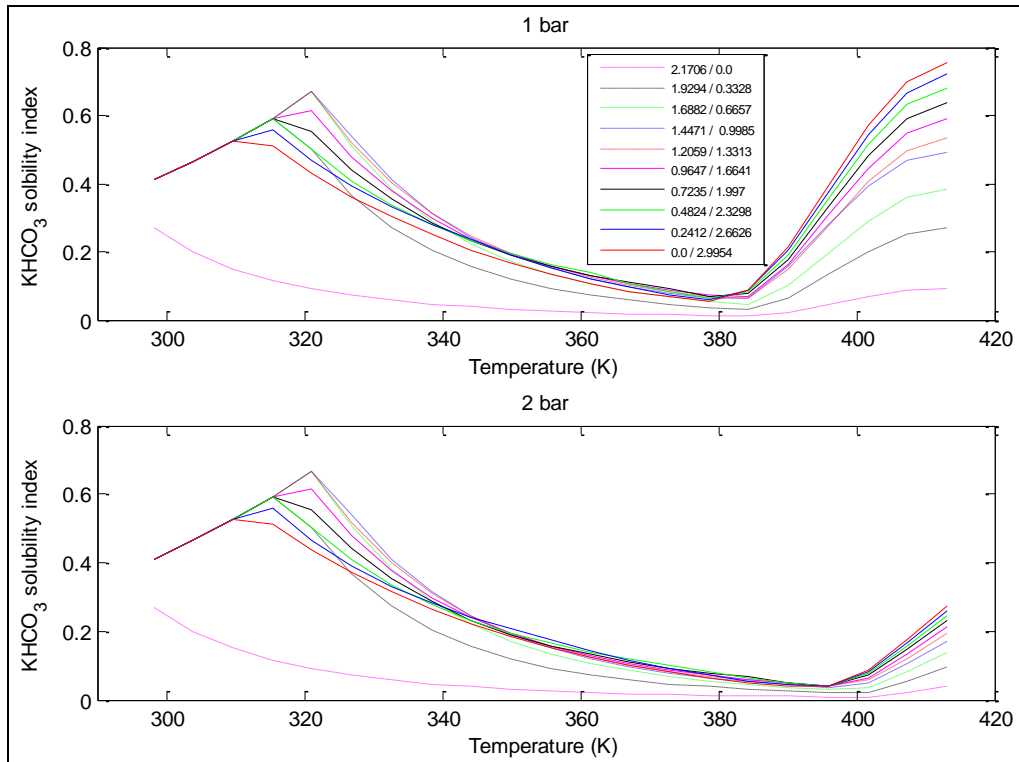Figure 4-20 Temperature effects on K_2CO_3 solubility index in mixture solution

Figure 4-21 Temperature effects on $KHCO_3$ solubility index in mixture solution

4.2.7 K₂CO₃+H₂O and KHCO₃+H₂O binary system analysis

In this part, the study simulates the binary system of carbonate and bicarbonate individually in order to investigate the solution solubility change with temperature at different concentrations. The input values comprise concentration range between 1 m and 7 m, temperature ranges from 298.15 K to 413.15 K, and pressures of 1 bar and 2 bar.

In the electrolyte systems, the quantity of solution liquid enthalpy is equals to the summation of three types of enthalpies: the molar enthalpy, the excess enthalpy which calculated with the NRTL activity coefficient and the molar enthalpy of pure water as it shown in equation (3.44). The excess NRTL enthalpy changed with the solution activity coefficient at the current temperature and constant pressure as show in the following expression;

$$H_m{}^E = -RT^2 \sum_i x_i \frac{\partial \ln \gamma_i}{\partial T} \tag{4.3}$$

Moreover, total heat capacity of the solution is given by the following thermodynamic relation;

$$C_p = \left(\frac{\partial H}{\partial T} \right)_p \tag{4.4}$$

For the carbonate binary system, Figure 4-22 showed the variation of heat enthalpy changing with temperature and solute concentration. The quantity of the solution heat enthalpy increased slightly with an increase in temperature for each concentration and it gave a wide change with the carbonate solute concentration. The increases of carbonate concentration from 1m to 7m used to increase the enthalpy. In the exothermic reactions of salt dissociation, the increase of salt concentration is used to increase the produced heat enthalpy. These explanations can be generalized for enthalpies of bicarbonate binary system in Figure 4-23 with a difference in the enthalpy quantities. On the other hand, the temperature that used to increase the heat

capacity of both carbonate and bicarbonate binary systems and concentrations decrease the heat capacity as it shown in figures 4-24 and 4-25, respectively.

The water activity coefficient of carbonate and bicarbonate are presented in the Figures 4.26 and 4.27, respectively. The concentration of both electrolytes affected negatively on water activity coefficients, while the temperature affected the activity coefficients positively. This is because of the temperature supported the dissociation reaction of carbonate and bicarbonate, which lead to increase in the reaction equilibrium constant. Figures 4.32 and 4.33 show the simulation heat capacity results compared with experimental data collected from Zaytsey and Aseyev (1992) .

The study of single component electrolyte solubility index for carbonate and bicarbonate are presented in Figures 4.28 and 4.29. For 1 m, 2 m, and 3 m carbonate solutions, these concentrations are unsaturated at the lower temperatures. The saturation starts from 4 m K_2CO_3 up to 7 m K_2CO_3. The prediction of potassium carbonate solute solubility index showed several saturation points at concentrations greater than 3m. At pressure of 1 bar, 4m potassium carbonate was saturated at temperature of 315.15 K, 5m was saturated at temperature of 344.15 K, 6m was saturated at temperature 373.15 K and 7m was supersaturated for all given temperatures. For operation at pressure of 2 bar, the saturation points didn't change for concentrations 4m, 5m and 6m. For 7m concentration, it has been saturated at temperature 413.15 as the highest operating temperature. Tables 4-15 and 4-16 showed the saturation points for K_2CO_3 binary system solution at pressures 1 bar and 2 bar in details. The results obtained for bicarbonate solubility index give values lower than unity at pressure of 2 bar. Moreover, at pressure of 1 bar, the results showed saturation points for concentrations at 5 m, 6 m, and 7 m $KHCO_3$. The solubility behavior gives positive results at pressure 2 bar compared with 1 bar that is due to the specific effects of operating pressure on the solution boiling temperature. The increases of operating pressure from 1 bar to 2 bar used to extend the boiling temperature with mean different of 18 Kelvin for both Carbonate and bicarbonate binary mixtures.

68

The operating temperature has a major effect on the water vapor pressure. Figure 4-30 shows the relation between the operating temperature and the water vapor pressure. In this figure, the increases of operating temperature from 298.16 K to 415.15 K was used to slightly evaporate the water from the solution and dependently increase the water vapor pressure in the system. On the other hand, Figure 4.31 shows relation between operating temperature and the CO_2 pressure in the system. Based on the equilibrium reaction of CO_2 absorption in equation (1.1) and CO_2 rate in the liquid phase (Figure 4-10), it can be concluded the significance of the effect of temperature on the CO_2 absorption and liberation due to the proportional relation between temperature and both of carbon dioxide activity in the liquid phase and vapor pressure. See also Appendix B, Figures B1 and B2 which presented the CO_2 and water pressure change with conversion rate of carbonate to bicarbonate in mixture system.
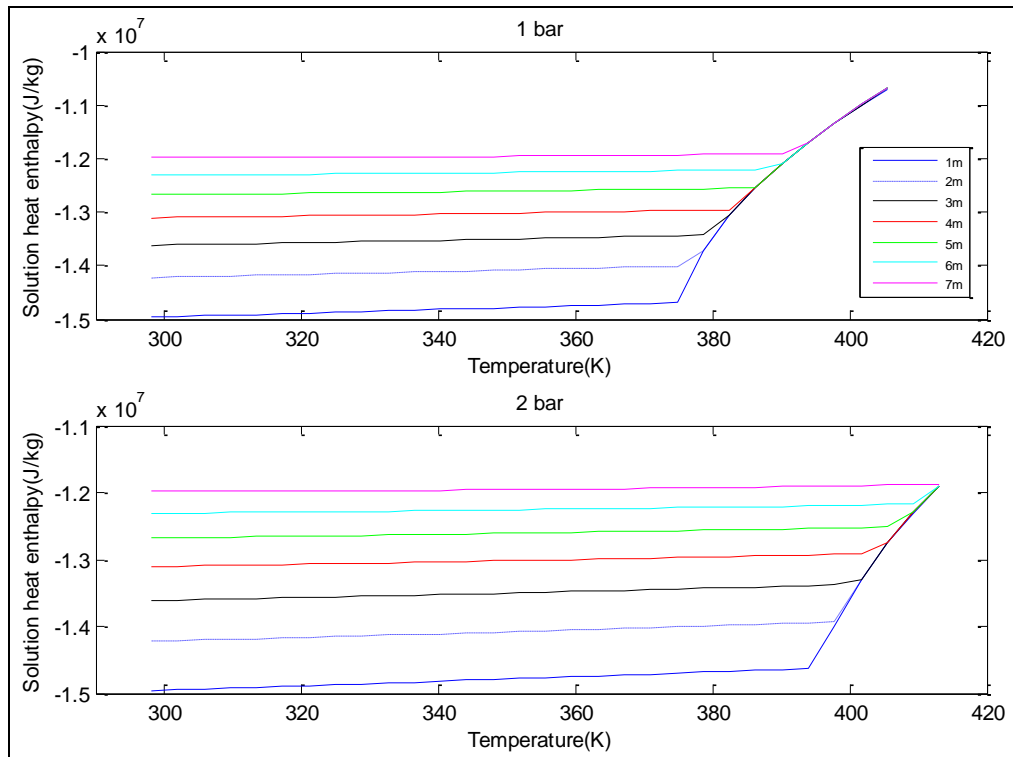
Figure 4-22 Temperature effects on K_2CO_3 solution enthalpy
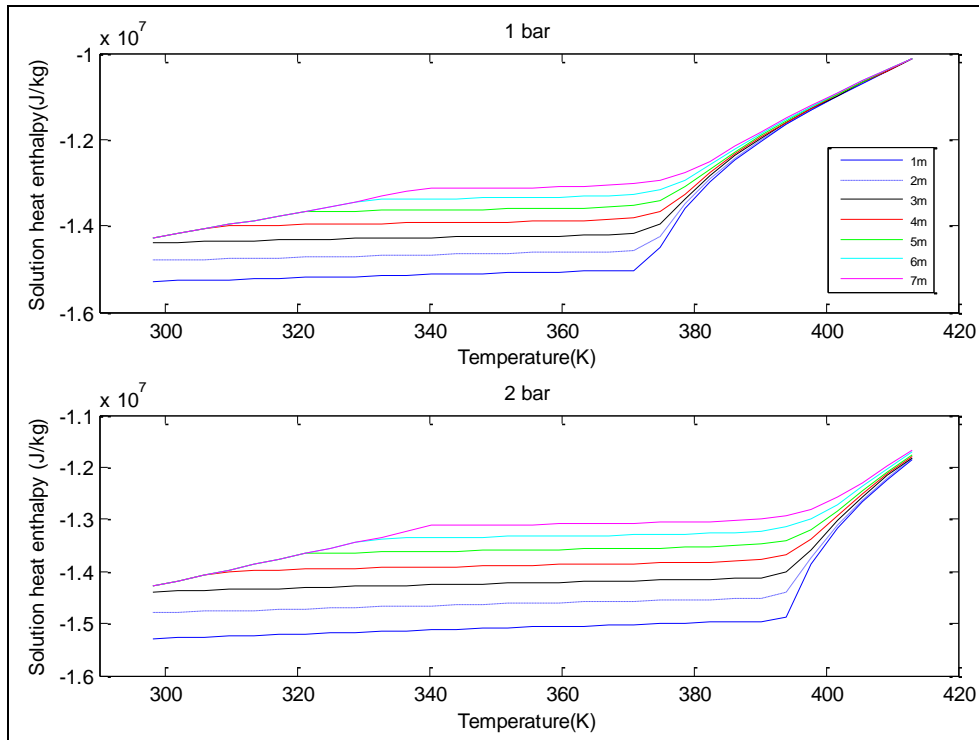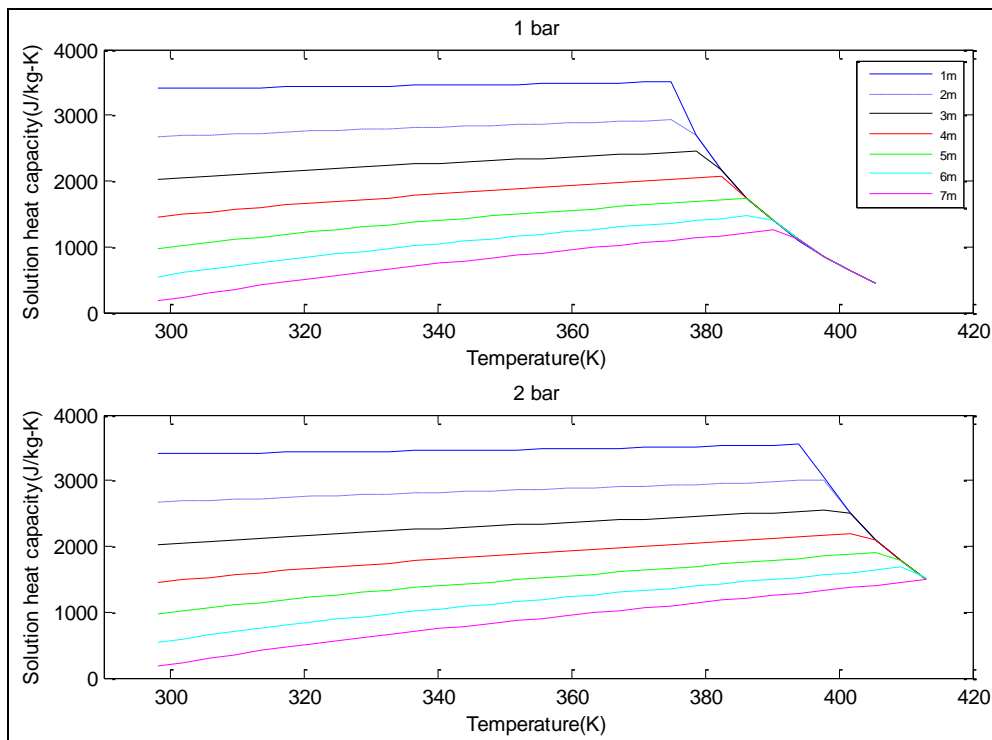
Figure 4-23 Temperature effects on KHCO$_3$ solution enthalpy

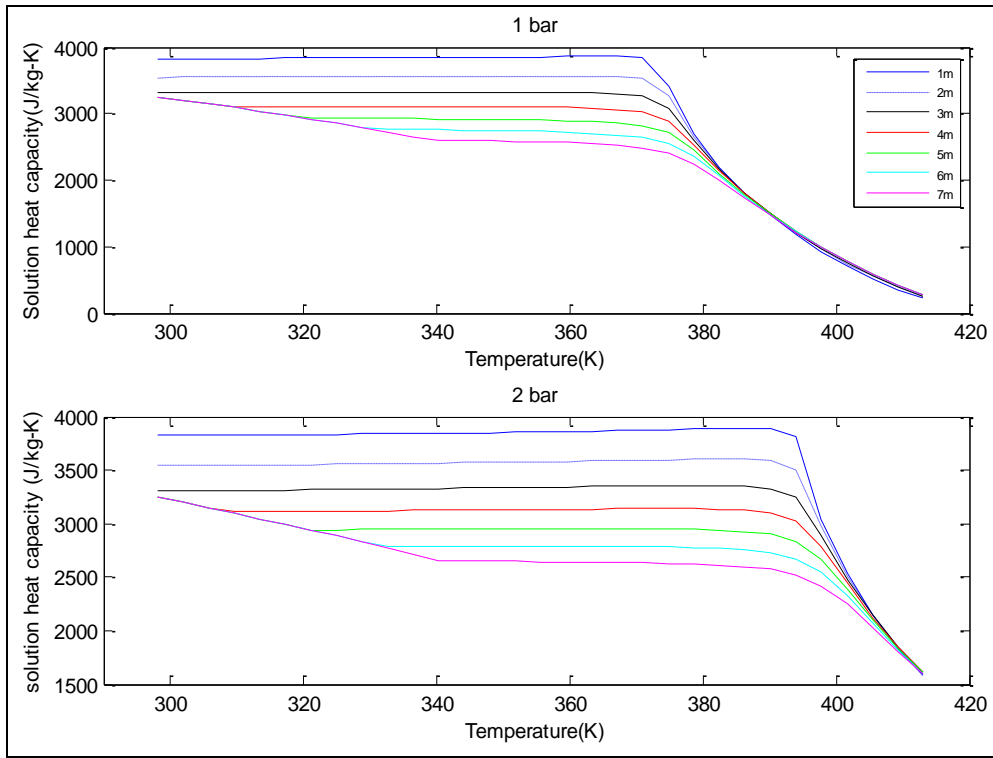Figure 4-24 Temperature effects on K$_2$CO$_3$ solution heat capacity

70

Figure 4-25 Temperature effects on KHCO$_3$ solution heat capacity
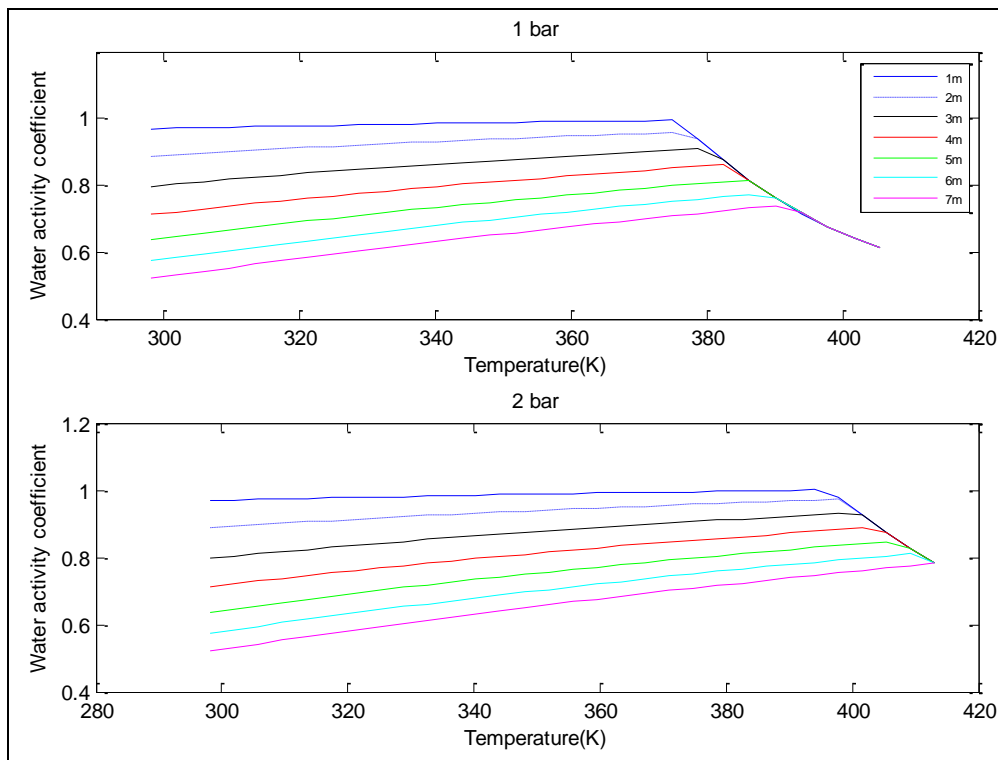

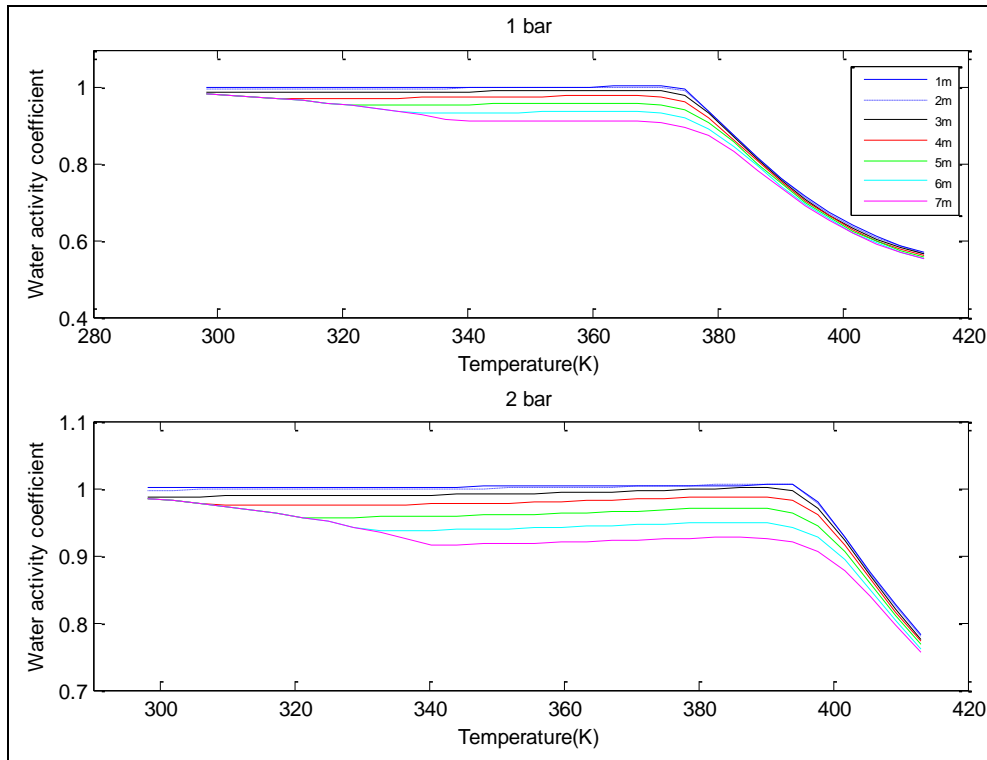Figure 4-26 Temperature effects on water activity in K$_2$CO$_3$ solution

71

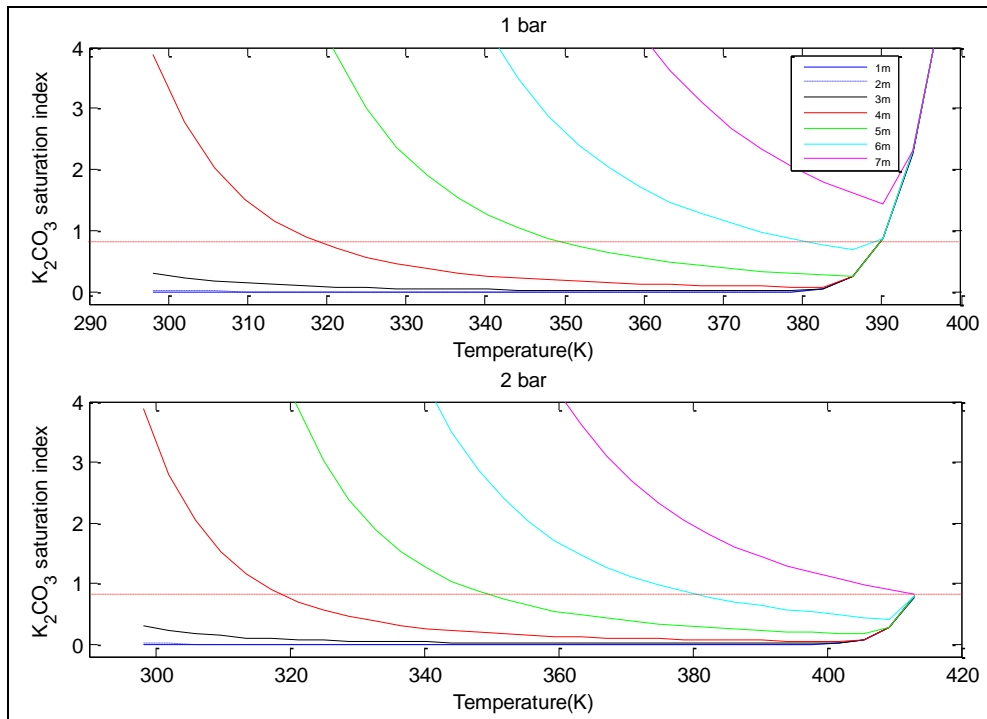Figure 4-27 Temperature effects on water activity in KHCO$_3$ solution

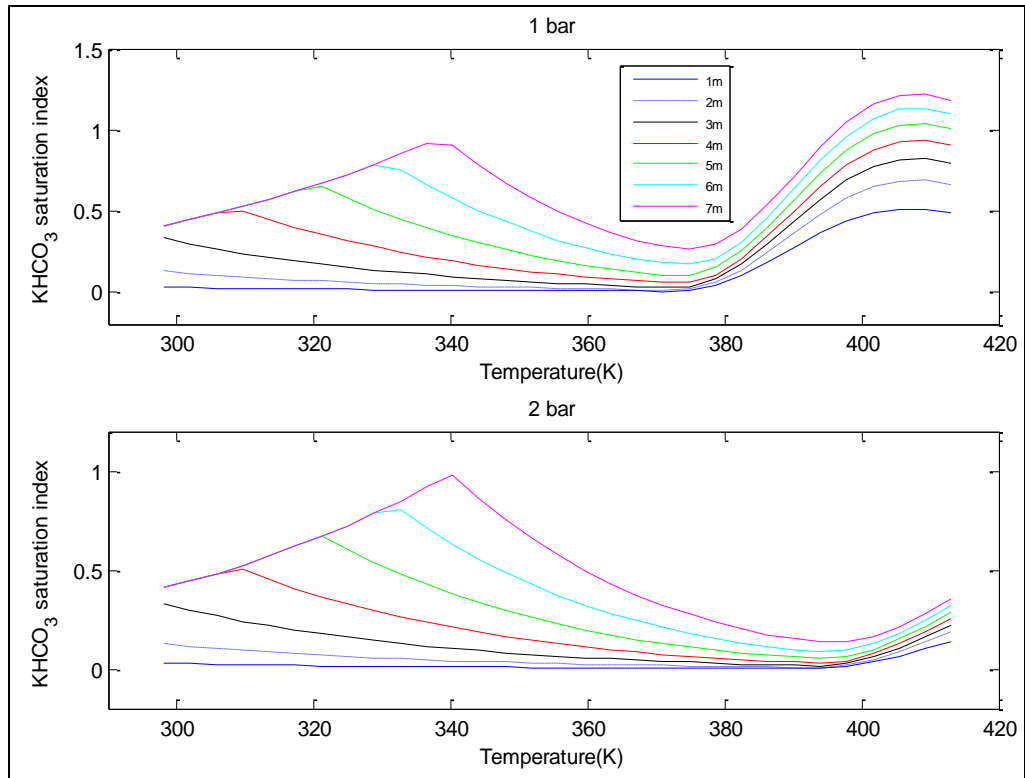Figure 4-28 Temperature effects on K$_2$CO$_3$ saturation index

Figure 4-29 Temperature effects on KHCO$_3$ solubility index

Table 4-15 The saturation points for K$_2$CO$_3$ binary system solution at pressure 1 bar

K$_2$CO$_3$ concentration mole/Kg H$_2$O	min T [K]	Saturation index (*SI*)	max T [K]	Saturation index (*SI*)
1	< 298.15	< 1	390.15-391.15	0.8-1.2
2	< 298.15	< 1	390.15-391.15	0.9-1.2
3	< 298.15	< 1	390.15-391.15	0.88-1.2
4	315.15	1.01	390.15-391.15	0.88-1.2
5	344.15	1.04	344.15	1.01
6	373.15	1.01	390.15-391.15	0.88-1.21
7	solution saturated at operation conditions			

Table 4-16 The saturation points for K_2CO_3 binary system solution at pressure 2 bar

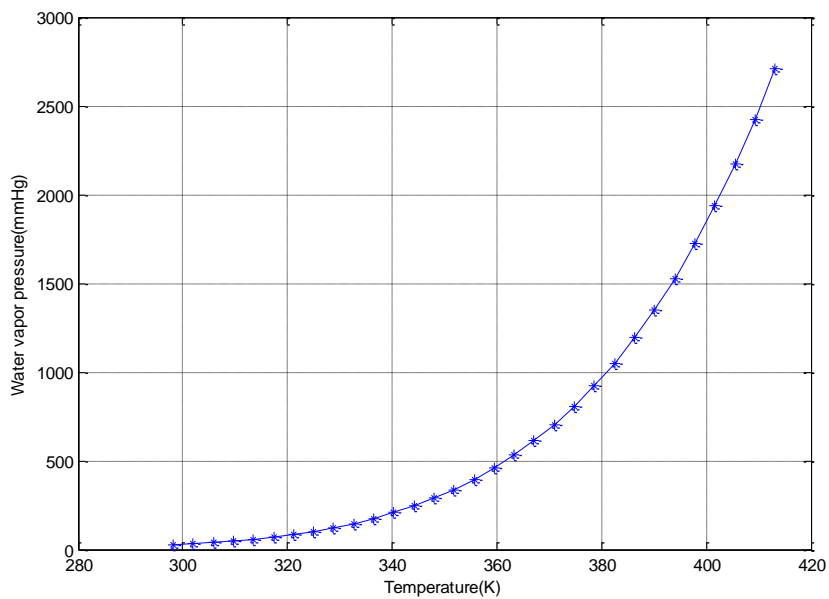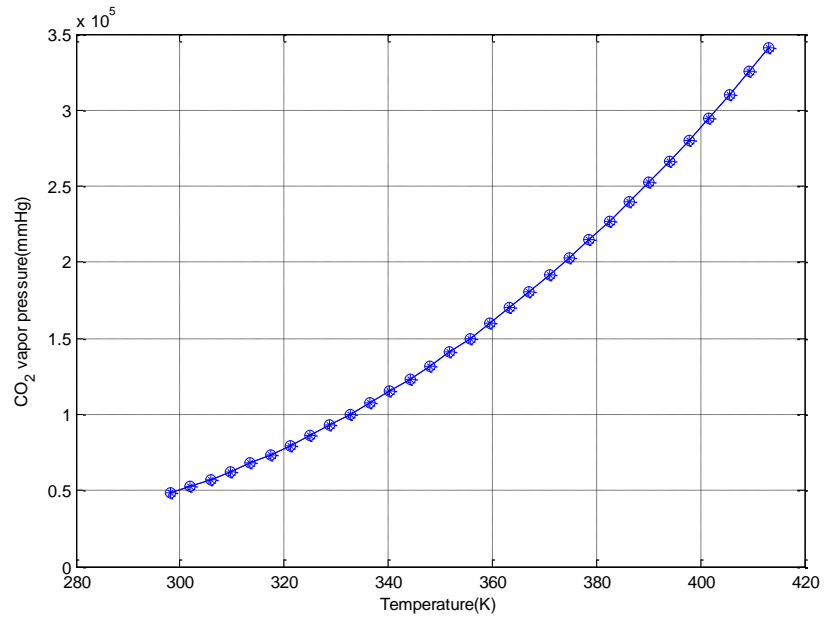| K_2CO_3 Concentration mole/Kg H_2O	min T [K]	Saturation index (SI)	Max T [K]	Saturation index (SI)
1	< 298.15	< 1	> 413.15	< 1
2	< 298.15	< 1	> 413.15	< 1
3	< 298.15	< 1	> 413.15	< 1
4	315.15	1.02	> 413.15	< 1
5	344.15	1.04	> 413.15	< 1
6	373.15	1.01	> 413.15	< 1
7	403.15	1.02	> 413.15	< 1

Figure 4-30 Temperature effects on H_2O pressure

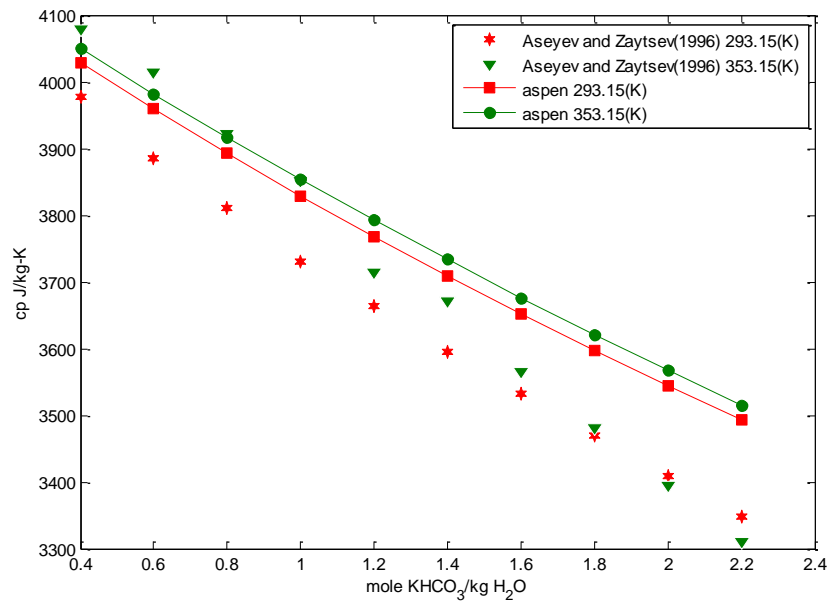Figure 4-31 Temperature effects on CO_2 pressure

Figure 4-32 Heat capacity of bicarbonate system compared with Aseyev (1998)
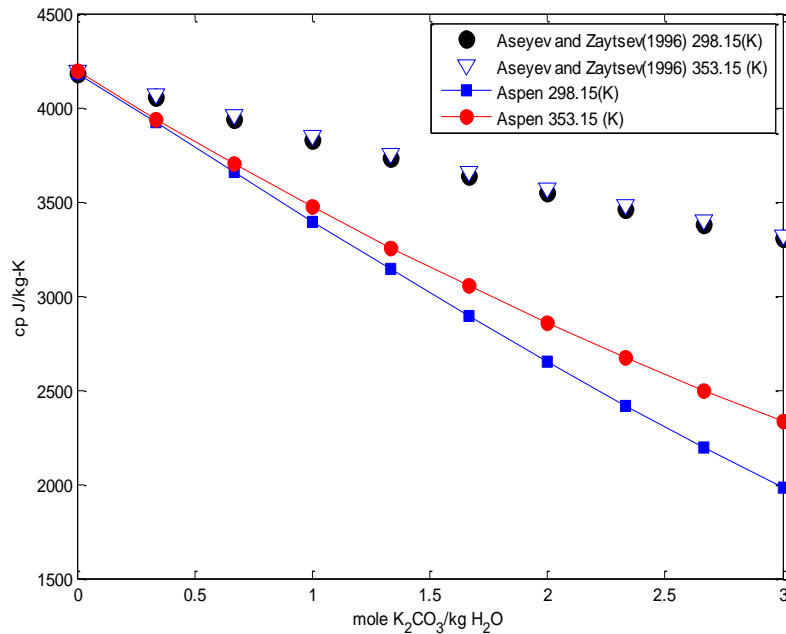
Figure 4-33 Heat capacity of carbonate system compared with Aseyev (1998)

4.2.8 Summary

The findings from this study can be summarized as follows:

1) For the ideal process, the precipitation occurs at temperature higher than the boiling temperature.

2) The reduction of CO_2 rate in the NG stream leads to increase K_2CO_3 concentration in the solvent.

3) The possibilities of the precipitation started at concentrations greater than 3 mole K_2CO_3/ kg H_2O for both pressures 1 and 2 bar.

4) The temperature affects positively on the solvent solubility until the boiling temperature.

5) The process operation at pressure of 2 bar gives solubility range wider than the pressure 1 bar and also increase the boiling temperature by 18 K.

6) The saturation conditions for 30wt% potassium carbonate solution have been estimated at temperature of 287.15K with relative error of +4 K.

7) For mixture system, the saturation temperature was estimated to be 405.15 K for all concentration ratios at pressure 1 bar.

8) For K_2CO_3 in binary system, the saturation temperature was estimated to

76

be 313.15 K for the concentrations less than 3m.

9) For $KHCO_3$ in binary system, the simulation detected the saturation point at temperature 405.15 K for concentrations greater than 4m.

Chapter 5

Conclusion and future work

5.1   Conclusions

Based on the study of potassium carbonate and bicarbonate solution, this research found that the effective parameters that can control the stability of the solvent during the absorption process. The effective parameters can be classified as two types:

1) Process conditions as external parameters consisting of the temperature, pressure, and chemical conversion.

2) Solvent chemical composition and physical properties, such as concentration, freezing point and boiling point.

The study was conducted on the basis of possible deviations of the operating conditions from the designed operating conditions in order to investigate the phenomenon of carbonate and bicarbonate solutes crystallization.

The temperature affect positively on the potassium carbonate and bicarbonate solubility. The observation of solution solubility detects saturation points at temperatures higher than the solution boiling point for 30 wt% K_2CO_3 standard solution. The literature data that were used for model validation represented the stable temperature of the solution in the liquid phase solubility at the range between 283.15 K and 366.48 K. The simulation study of the current work observed the above condition at the range between 287.15 K and 362.15 K with the error of ±4 K.

For all the estimated properties of carbonate and bicarbonate solutions, the increases of the pressure in process leads to an increase in the range of solution stability temperature higher than 362.15 K depending on the solute concentration. The

increase of the operation pressure from 1 bar to 2 bar has increased the mixture solution (carbonate/bicarbonate) boiling temperature with mean temperature $\Delta T_{mean} = 18$ K. This gives a wider range of solvent stability in liquid phase and this influence was also effect on the solvent transport thermodynamics.

Based on the chemical conversion that occurs when CO_2 reacted with K_2CO_3 solution, theoretically, K_2CO_3 should totally be converted to $KHCO_3$ solution and transfer to the regeneration unit. Nevertheless all the plant data have shown that the solution contains a ratio of carbonate/bicarbonate. This indicates that there are technical problems responsible for the efficiency drop. The possible reasons that could have lead to concentration increases for carbonate or bicarbonate can be summarized as follows:

1) Addition a new solution to increase efficiency.

2) Losses of water content from the solvent.

3) Technical problems occur in the units.

4) Temperature drops in heat exchanger units.

Certainly the concentration of solutes is the main factor in the process of crystallization, as well as temperature and pressure. The summary of the study presents the freezing and boiling temperatures for different concentrations of carbonate, bicarbonate and mixture solution at two different pressures of 1 bar and 2 bars. The study also concludes that the solution crystallization can possibly occur at temperatures lower than 313.15 K, pressure 1 bar for concentrations higher than 3 mole K_2CO_3/Kg H_2O. For bicarbonate solution, the solution was unsaturated at the lower temperature and at high temperatures it converts to carbonate solution after CO_2 liberation process.

The findings of the 30 wt% K_2CO_3 were validated with the available literature data for water activity coefficient, viscosity and specific gravity. Hence, the comparison showed a good agreement with the literature data.

5.2 Future work

Further study of processes which affect by the solution composition is required in order to gain more understanding of Benfield's system. The following steps represent the most important future studies:

1) Development of Benfield's process control system. In order to determine the actual concentration of the solution in each unit to avoid the increasing of the solution concentration. Furthermore, to adapt the temperature and pressure according to the freezing and boiling conditions.

2) Modeling the fouling dynamics for Benfield's reboiler system to investigate the precipitation of potassium carbonate solution according to the operation run time.

References

Abdel-Aal,H.K., M.Aggour and M.A. Fahim.(2003). Petroleum and Gas Field Processing, Marcel Dekker,Inc, New York. Basel.

Abovsky, V., Y. Liu and S. Watanasiri. (1998). "Representation of Nonideality in Concentrated Electrolyte Solutions using the Electrolyte NRTL Model with Concentration-Dependence Parameters." Fluid Phase Equilibria, **150-151**: 277-286.

Alley, W. M. (1993). Regional Ground-Water Quality, John Wiley and Sons, New York.

Aresta, M. (2003). Carbon Dioxide Recovery and Utilization, Springer, New York.

AspenTech. (1989). Physical Properties Data Reference Manual. Élan Computer Group, Inc, California.

Barthel, J., K. Hartmut and K. Werner. (1998). Physical Chemistry of Electrolyte Solutions. Springer, New York.

Butler, J. N. (1998). Ionic Equilibrium; solubility and pH Calculations. John Wiley & Sons, Inc, Toronto.

Chen, C. C. (1980). Computer Simulation of Chemical Process with Electrolytes. PhD Thesis, Department of Chemical Engineering. Massachusetts Institute of Technology, Cambridge, U.S.A.

Cullinane, J. T and T. R. Gary. (2004). "Carbon Dioxide Absorption with Aqueous Potassium Carbonate Promoted by Piperazine." Chemical Engineering Science, **59**: 3619-3630.

Du, C., Z. Shili, L. Huiquan, and Z. Yi. (2006). "Solid-Liquid Equilibria of $K_2CO_3+K_2CrO_4+H_2O$ System." Journal of Chemical Engineering Data **51**: 104-106.

Field, J.H., G.E. Johnson, H.E. Benson and J.S. Tosh (1960). Removing Hydrogen Sulphate by Hot Potassium Carbonate Absorption, United States Department of the Interior

Fei, Y., H.K. Zou, G.W. Chu, L. Shao and J.Fengchen. (2009). "Modeling and Experimental studies on Absorption of CO_2 by Benfield Solution in Rotating Packed Bed." Chemical Engineering Journal **145**: 377-384.

Georgios, M.K. and R. Gani. (2004). Computer Aided Property Estimation for Process and Product Design: Computers Aided Chemical Engineering, Elsevier, Amsterdam.

Gerd, M. and F. Deutsche. (2004). Thermodynamic Properties of Complex Fluid Mixtures, John Wiley & Sons, Bonn.

Haghtalab, A. and J. H. Vera. (1988). "A Nonrandom Factor Model for the Excess Gibbs Energy of Electrolyte Solutions." AIChE Journal, **34**(5): 803-813.

Haghtalab,A and P. Kiana (2009). "Electrolyte-UNIQUAC-NRF model for the correlation of the mean activity coefficient of electrolyte solutions." Fluid Phase Equilibria, Elsevier, **281**:163–171

Hilliard, M. (2004). Thermodynamics of Aqueous Piperazine/Potassium Carbonate/Carbon Dioxide Characterized by the Electrolyte NRTL Model within Aspen Plus ®, University of Texas, Austin, USA.

Hilliard, M. and T.R. Gary. (2005). " Thermodynamics of aqueous Piperazine/Potassium Carbonate/Carbon Dioxide Cterized by the Electrolyte Non-Random Two-Liquid Model in Aspen Plus." Greenhouse Gas Control Technologies, **7**: 1975-1978

Hilliard, M. (2008). A Predictive Thermodynamic Modeling for an Aqueous Blend Potassium Carbonate, Piperazine, and Methanol amine for Carbone Dioxide Capture from Flue Gas. **PhD** Thesis,Chemical Engineering Department, University of Texas, Austin, USA.

Ian, M.C. Tomislav, H. Klaus, K. Nikola, and K. Kozo. (2007). Quantities, Units and Symboles in physical Chemistry, IPAQ, Blackwell Science Ltd. USA

Ikoku, C.U. (1992). Natural Gas Production Engineering. John Willey and Sons, Inc, New York.

Job, G. and F. Hermann. (2006). "Chemical Potential- A Quantity in Search of Recognition." Eur.J.Phys **27**: 353-371.

Kathryn. S., et al., (2009). "Recent Developments in Solvent Absorption Technologies at the CO_2 CRC in Australia." Energy Procedia, 1(1): 1549–1555.

Kidnay, J. and R.P. William. (2006). Fundamentals of Natural Gas Processing, CRC press Tayler and Francis group, USA.

Kohl, L. and R.B. Neilsen. (1997). Gas Purification Handbook. Texas Gulf Publishing

Company, Auston, USA.

Larson, T.E. and A.M. Buswell. (1942)." Calcium Carbonate Saturation Index and Alkalinity Interperation."Journal of American Water Works Association,**34** (11).

Liang,S. L, S.l. Sun and C.l. Lin. (2008). "Predictions of thermodynamic properties of aqueous single-electrolyte solutions with the two-ionic-parameter activity coefficient model." Fluid Phase Equilibria, Elsevier, **264**:45–54

Margaret, R. (2007). An Introduction to Aqueous Electrolyte, John Wiley & Sons, Chichester,UK.

Moggia, E. and B. Bianco. (2007). "Mean Activity Coefficient of Electrolyte Solutions." J. Phys. Chem, **111**: 3183-3191.

Mokhatab, S., A.P. William., and S.G. James. (2006). Hand book of Natural Gas Transmission and Processing, Gulf Professional Publishing, Elsevier. Inc, Burlington, USA.

Orbey, H. and S.I. Sandler. (1998). Modeling Vapor-Liquid Equilibria: Cubic Equations of State and Their Mixing Rules, Cambridge University Press, UK.

Perry, R. and D.W. Green. (1999). Perry's Chemical Engineers' Handbook, McGraw-Hill, New York, USA.

UOP. (2000). "Benfield process", http://www.uop.com/objects/99%20Benfield.pdf

Rahimpor, M.R. and A.Z. Kashkooli. (2004). "Enhanced Carbon Dioxide Removal by Promoted Hot Potassium Carbonate in Split-Flow Absorber." Chemical Engineering and Processing, **43**: 857-865.

Robert, N.M. and J.M. Campbell. (1982). Gas Conditioning and Processing, Campbell Petroleum Series, USA.

Sang. W.P, N. H. Heo., J.S. Kim and D.S. Suh (1997). "Facilitated Transport of Carbon Dioxide Trough an Immobilized Liquid Membrane of $K_2CO_3/KHCO_3$ Aqueous solution." Korean Journal of Chemical Engineering, **14(5)**: 312-320.

Sepideh. M.M, V. Taghikhani and C. Ghotbi (2007). "A new Model in Correlating the Activity Coefficients of Aqueous Electrolyte Solutions with Ion Pair Formation" Fluid Phase Equilibria, Elsevier, **261**: 313–319.

Sergio, G. and P.W. David. (1988). Na+/H+ Exchange, CRC Press, Florida, USA.

Thomsen, K. (1997). Electrolytes: Model Parameters and Process Simulation. **PhD** Thesis, Department of Chemical Engineering, Technical University of Denmark.

Thomsen, K. (2008). Electrolyte Solutions: Thermodynamics, Crystallization, Separation methods, Course Notes, Technical University of Denmark.

Walker, R.D. (1970). A Study of Gas Solubilities and Transport Properties in Fuel Cell Electrolytes. Engineering and Industrial Experiment station, Gainesville, Florida, USA.

Zaytsey, I.D. and G.G. Aseyev. (1992). Properties of Aqueous Solutions of Electrolytes, CRC, Florida, USA.
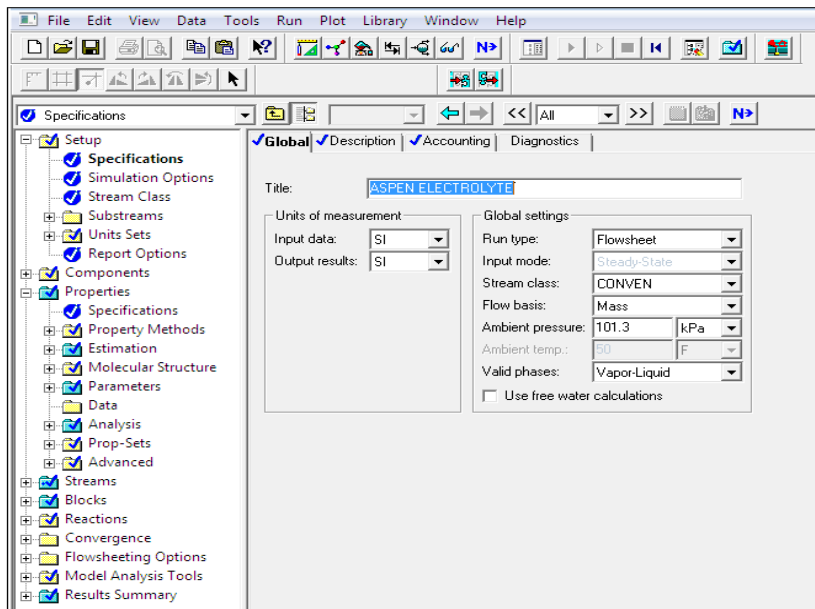
Appendix-A

Aspen Plus interface windows

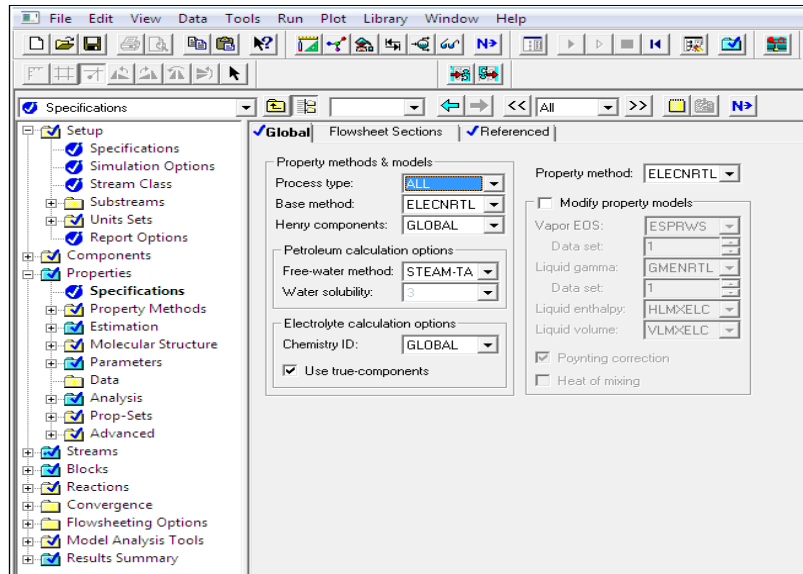Figure A 1: Aspen plus electrolyte setup spcification

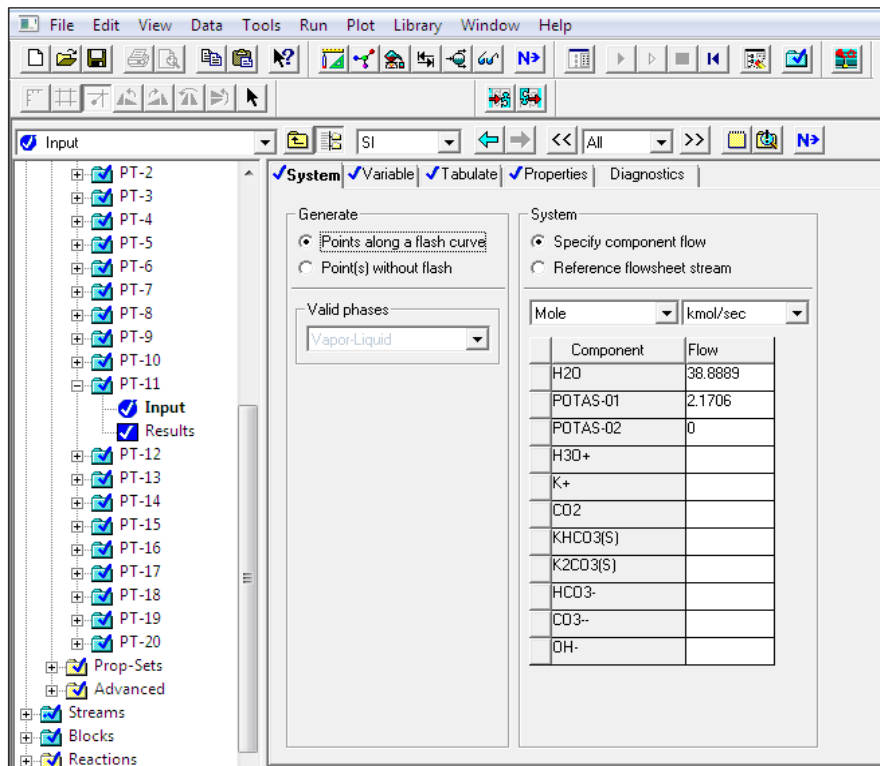Figure A 2: Aspen plus electrolyte properties spicifications
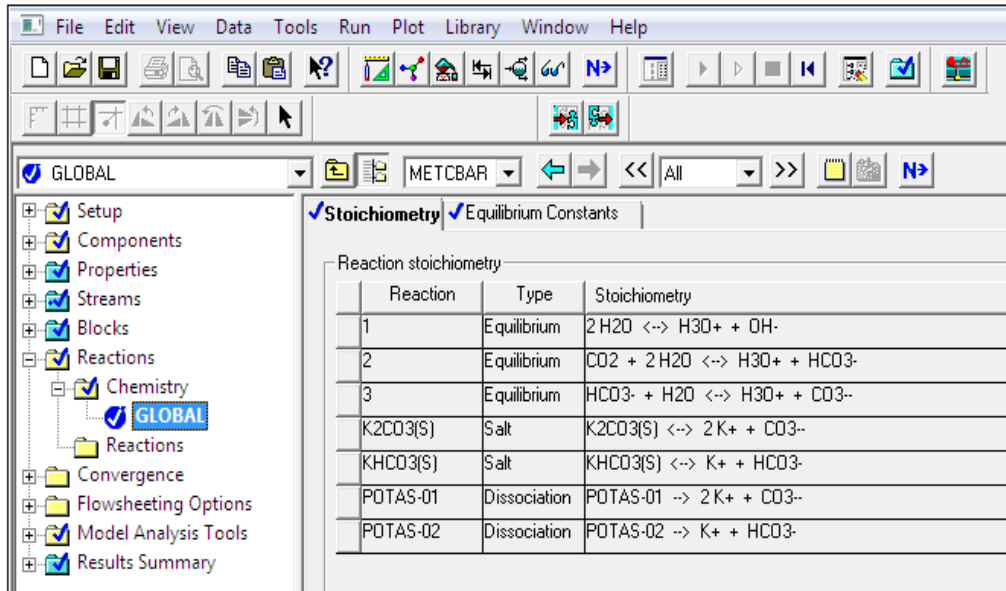

Figure A 3: Aspen plus data analysis input window

Figure A 4: Aspen plus electrolyte reaction chemistry generation

Figure A 5: Aspen plus electrolyte stream results sample

Electrolyte thermodynamic data

A.1 Benfield's system literature graphs
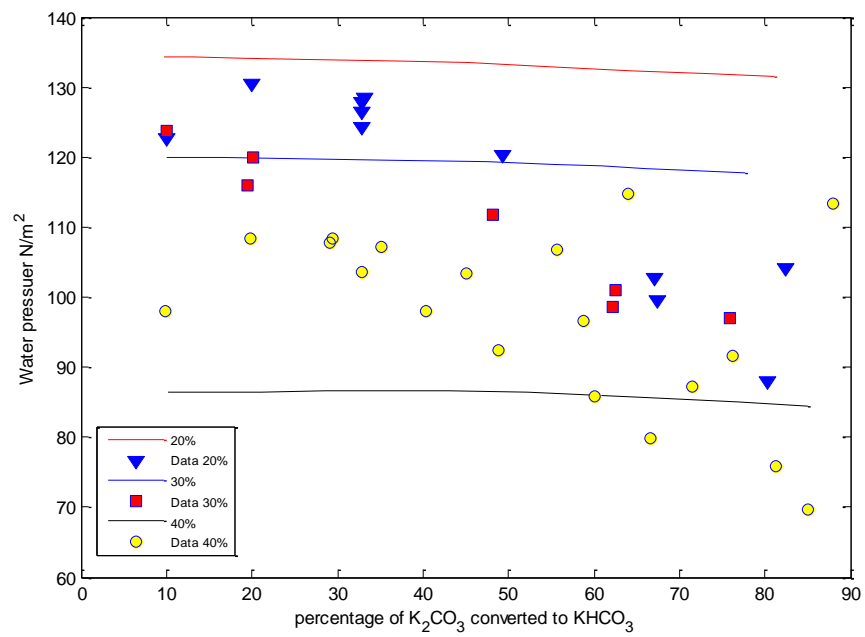
Figure B 1: water pressure changes with K_2CO_3 conversion (Kohl 1997)
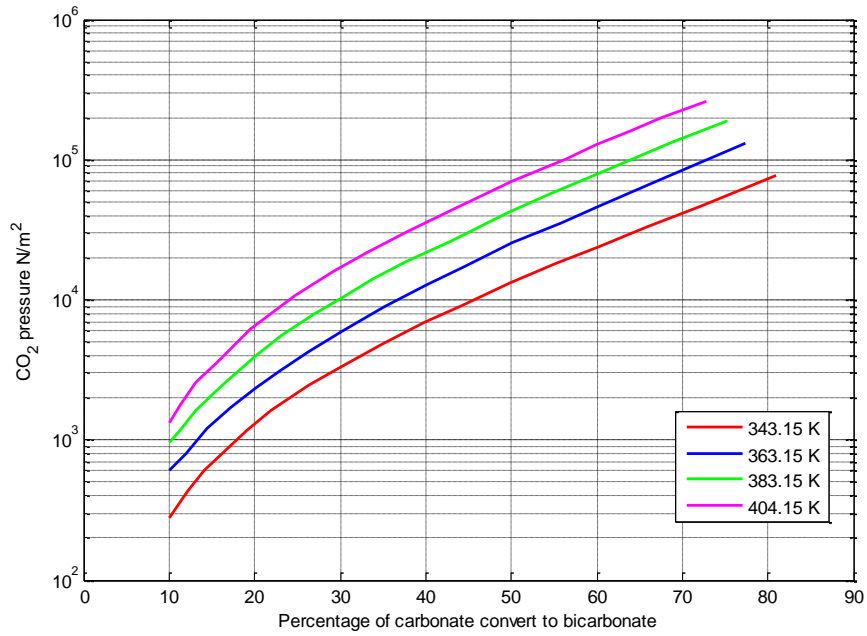
Figure B 2: CO_2 pressure changes with percentage of carbonate converted to bicarbonate (Kohl 1997)
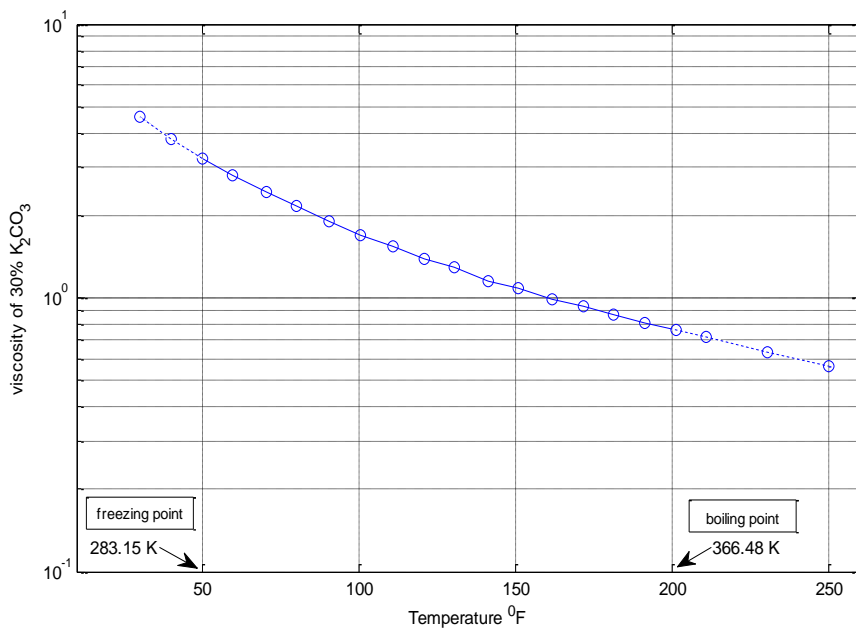
Figure B 3: Effects of temperature on viscosity of 30% (Kohl 1997)
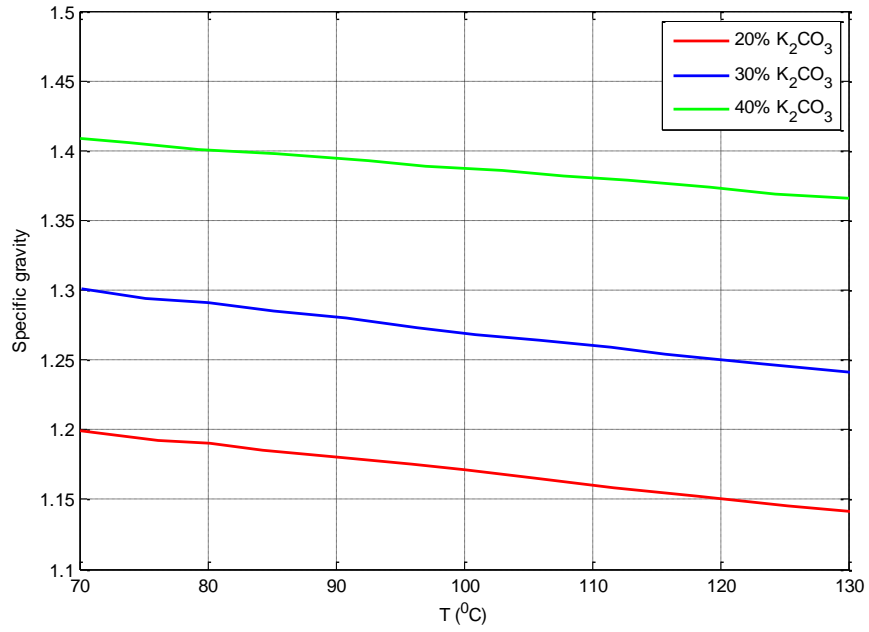
Figure B 4: Specific gravity of 20%, 30%, and 40% K_2CO_3 (Kohl 1997)

Figure B 5: Effects of temperature and percentage of carbonate converted to bicarbonate on carbonate and bicarbonate solubility (Kohl 1997)
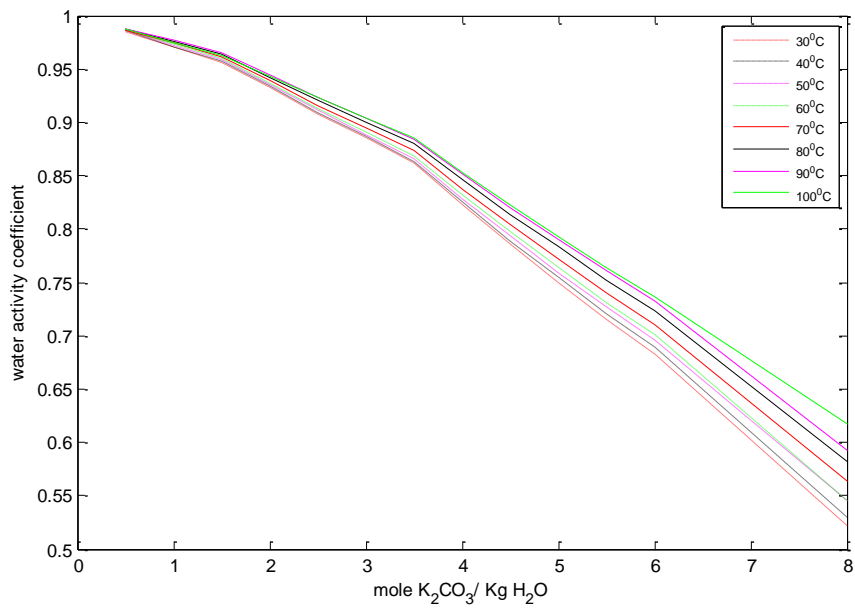
Figure B 6: Effects on carbonate concentration on water activity (Walker 1970)
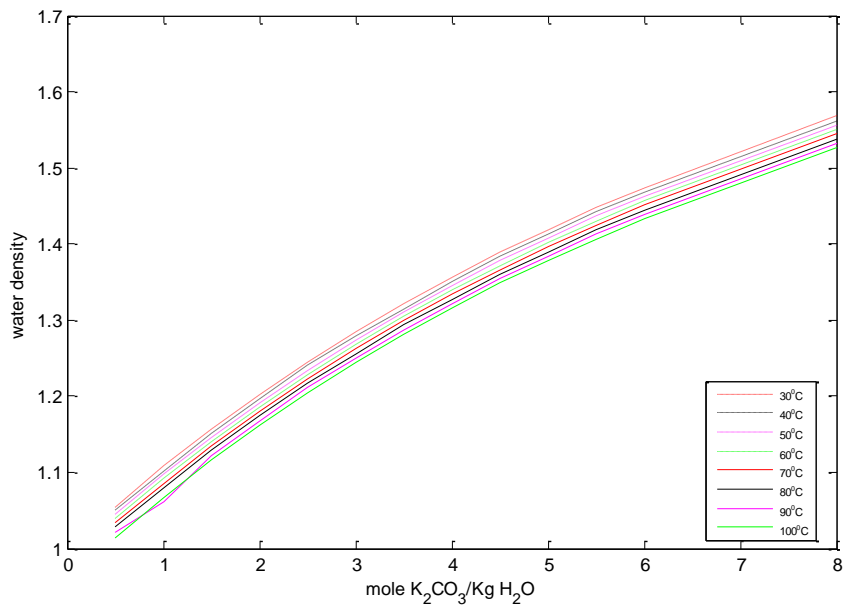
Figure B 7: Effects on carbonate concentration on water density (Walker 1970)

Table B 1 water activity and density for carbonate solution at temperature 30^0C (Walker, 1970)

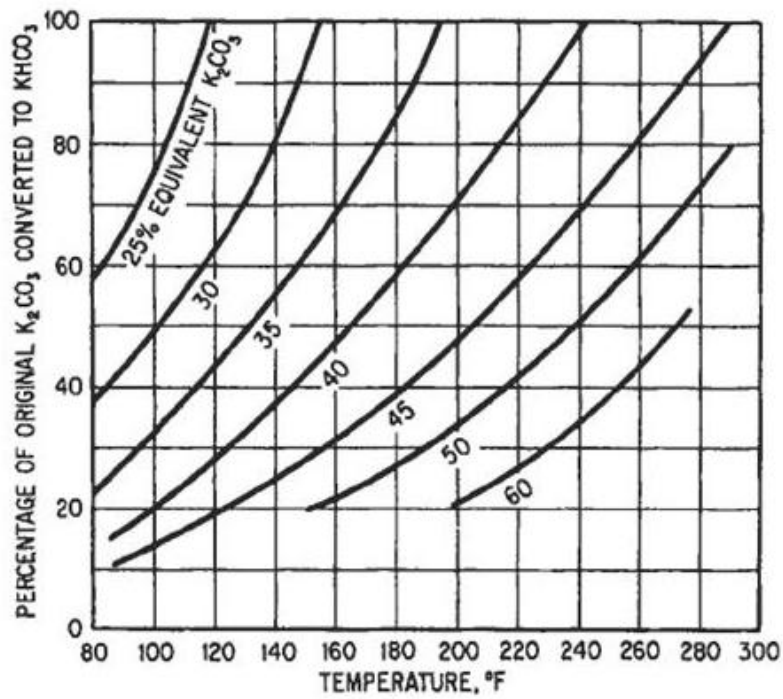| molality	mole%	wt%	molarity	water activity	density
0.5	0.0089	6.46	0.493	0.9846	1.0536
1	0.0177	12.14	0.974	0.9700	1.1085
1.5	0.0263	17.17	1.437	0.9563	1.1563
2	0.0348	21.65	1.884	0.9325	1.2023
2.5	0.0431	25.68	2.314	0.9081	1.2452
3	0.0513	29.31	2.725	0.8855	1.2849
3.5	0.0593	32.6	3.117	0.862	1.3212
4	0.0672	35.6	3.494	0.8228	1.3565
4.5	0.075	38.34	3.853	0.7856	1.3889
5	0.0826	40.86	4.196	0.7496	1.4191
5.5	0.0902	43.19	4.524	0.7155	1.4478
6	0.0975	45.33	4.836	0.6826	1.4744
8	0.126	52.51	5.957	0.5216	1.5681

Table B 2 water activity and density for carbonate solution at temperature 40^0C (Walker, 1970)

molality	mole%	wt%	molarity	water activity	density
0.5	0.0089	6.46	0.493	0.9858	1.05
1	0.0177	12.14	0.974	0.9711	1.1026
1.5	0.0263	17.17	1.437	0.9573	1.1517
2	0.0348	21.65	1.884	0.9335	1.5973
2.5	0.0431	25.68	2.314	0.9093	1.2401
3	0.0513	29.31	2.725	0.8864	1.2796
3.5	0.0593	32.6	3.117	0.8636	1.315
4	0.0672	35.6	3.494	0.8255	1.3511
4.5	0.075	38.34	3.853	0.7889	1.3833
5	0.0826	40.86	4.196	0.7542	1.4135
5.5	0.0902	43.19	4.524	0.7205	1.4421
6	0.0975	45.33	4.836	0.6892	1.4686
8	0.126	52.51	5.957	0.5291	1.5621

Table B 3 water activity and density for carbonate solution at temperature 50^0C (Walker, 1970)

molality	mole%	wt%	molarity	water activity	density
0.5	0.0089	6.46	0.493	0.9863	1.045
1	0.0177	12.14	0.974	0.9724	1.0973
1.5	0.0263	17.17	1.437	0.9586	1.1462
2	0.0348	21.65	1.884	0.9349	1.1917
2.5	0.0431	25.68	2.314	0.9114	1.2344
3	0.0513	29.31	2.725	0.8885	1.2739
3.5	0.0593	32.6	3.117	0.8659	1.3101
4	0.0672	35.6	3.494	0.8284	1.3452
4.5	0.075	38.34	3.853	0.7939	1.3775
5	0.0826	40.86	4.196	0.7591	1.407
5.5	0.0902	43.19	4.524	0.7267	1.4363
6	0.0975	45.33	4.836	0.6952	1.4628
8	0.126	52.51	5.957	0.5455	1.5563

Table B 4 water activity and density for carbonate solution at temperature 60^0C (Walker, 1970)

molality	mole%	wt%	molarity	water activity	density
0.5	0.0089	6.46	0.493	0.9860	1.0400
1	0.0177	12.14	0.974	0.9730	1.0920
1.5	0.0263	17.17	1.437	0.9596	1.1407
2	0.0348	21.65	1.884	0.9368	1.1862
2.5	0.0431	25.68	2.314	0.9134	1.2287
3	0.0513	29.31	2.725	0.891	1.2683
3.5	0.0593	32.60	3.117	0.8687	1.3052
4	0.0672	35.60	3.494	0.8322	1.3394
4.5	0.075	38.34	3.853	0.798	1.3717
5	0.0826	40.86	4.196	0.7637	1.4018
5.5	0.0902	43.19	4.524	0.7316	1.4305
6	0.0975	45.33	4.836	0.7012	1.4570
8	0.1260	52.51	5.957	0.5456	1.5505

Table B 5 water activity and density for carbonate solution at temperature 70^0C (Walker, 1970)

molality	mole%	wt%	molarity	water activity	density
0.5	0.0089	6.46	0.493	0.9865	1.0341
1	0.0177	12.14	0.974	0.9744	1.0861
1.5	0.0263	17.17	1.437	0.9615	1.1347
2	0.0348	21.65	1.884	0.9389	1.1802
2.5	0.0431	25.68	2.314	0.9162	1.2228
3	0.0513	29.31	2.725	0.8948	1.2623
3.5	0.0593	32.6	3.117	0.8733	1.2993
4	0.0672	35.6	3.494	0.8375	1.3337
4.5	0.075	38.34	3.853	0.8043	1.3658
5	0.0826	40.86	4.196	0.7713	1.3959
5.5	0.0902	43.19	4.524	0.7406	1.4246
6	0.0975	45.33	4.836	0.7105	1.451
8	0.126	52.51	5.957	0.5637	1.5444

Table B 6 water activity and density for carbonate solution at temperature 80^0C (Walker, 1970)

molality	mol%	wt%	molarity	water activity	density
0.5	0.0089	6.46	0.493	0.9880	1.0281
1	0.0177	12.14	0.974	0.9753	1.0800
1.5	0.0263	17.17	1.437	0.9634	1.1287
2	0.0348	21.65	1.884	0.9422	1.1742
2.5	0.0431	25.68	2.314	0.9203	1.2168
3	0.0513	29.31	2.725	0.9001	1.2563
3.5	0.0593	32.6	3.117	0.8796	1.2934
4	0.0672	35.6	3.494	0.8467	1.3276
4.5	0.075	38.34	3.853	0.8139	1.3599
5	0.0826	40.86	4.196	0.7829	1.3900
5.5	0.0902	43.19	4.524	0.7523	1.4186
6	0.0975	45.33	4.836	0.7238	1.4450
8	0.126	52.51	5.957	0.5822	1.5383

Table B 7 water activity and density for carbonate solution at temperature 90^0C (Walker, 1970)

molality	mole%	wt%	molarity	water activity	density
0.5	0.0089	6.46	0.493	0.9881	1.0218
1	0.0177	12.14	0.974	0.9772	1.0611
1.5	0.0263	17.17	1.437	0.9649	1.1227
2	0.0348	21.65	1.884	0.944	1.1683
2.5	0.0431	25.68	2.314	0.9232	1.2109
3	0.0513	29.31	2.725	0.9037	1.2504
3.5	0.0593	32.60	3.117	0.8837	1.2875
4	0.0672	35.60	3.494	0.8510	1.3217
4.5	0.0750	38.34	3.853	0.8204	1.3540
5	0.0826	40.86	4.196	0.7901	1.3841
5.5	0.0902	43.19	4.524	0.7615	1.4127
6	0.0975	45.33	4.836	0.7329	1.4391
8	0.1260	52.51	5.957	0.5923	1.5322

Table B 8 water activity and density for carbonate solution at temperature 100^0C (Walker, 1970)

molality	mole%	wt%	molarity	water activity	density
0.5	0.0089	6.46	0.493	0.9877	1.0140
1	0.0177	12.14	0.974	0.9749	1.0677
1.5	0.0263	17.17	1.437	0.963	1.1167
2	0.0348	21.65	1.884	0.9428	1.1623
2.5	0.0431	25.68	2.314	0.9233	1.2050
3	0.0513	29.31	2.725	0.9043	1.2445
3.5	0.0593	32.6	3.117	0.8853	1.2816
4	0.0672	35.6	3.494	0.8533	1.3159
4.5	0.075	38.34	3.853	0.8225	1.3482
5	0.0826	40.86	4.196	0.7929	1.3783
5.5	0.0902	43.19	4.524	0.7643	1.4068
6	0.0975	45.33	4.836	0.7364	1.4332
8	0.126	52.51	5.957	0.6169	1.5262